

THE UNIVERSITY OF HULL

The Characterisation of Family-13 Kinesins in *Trypanosoma brucei*

being a Thesis submitted for the Degree of Doctor of Philosophy

in the University of Hull

by

Chan Kuan Yoow, B.Sc. (Hons.)

May 2008

Table of contents

TABLE OF CONTENTS	I
ACKNOWLEDGEMENTS	III
ABBREVIATIONS	IV
ABSTRACT	VI
1 GENERAL INTRODUCTION	1
1.1 TRYPANOSOMA BRUCEI CAUSES AFRICAN SLEEPING SICKNESS AND NAGANA	1
1.2 ANTIGENIC VARIATION AND VARIABLE SURFACE GLYCOPROTEIN	4
1.3 GENOME ORGANISATION OF TRYPANOSOMA BRUCEI AND MITOSIS	5
1.4 CHROMOSOME SEGREGATION IN TRYPANOSOMA BRUCEI	10
1.5 THE KINESIN MOTOR PROTEINS	12
1.6 KINESIN FUNCTIONS IN INTRACELLULAR TRANSPORT AND MITOSIS	18
1.7 PROJECT AIMS	22
2 PHYLOGENETIC ANALYSIS OF THE KINESIN SUPERFAMILY IN TRYPANOSOMA BRUCEI	23
2.1 ABSTRACT	23
2.2 INTRODUCTION	24
2.3 MATERIALS AND METHODS	27
2.3.1 Trypanosome kinesin sequence retrieval	27
2.3.2 Phylogenetic analysis and classification of trypanosome kinesins	29
2.4 RESULTS	30
2.4.1 Phylogenetic analysis	30
2.4.2 Identification of putative mitotic kinesins in trypanosomes	33
2.4.3 Trypanosome Kinesin-13 proteins	34
2.5 DISCUSSION	39
3 THE BIOLOGICAL CHARACTERISATION OF THE KINESIN-13 FAMILY IN TRYPANOSOMA BRUCEI	42
3.1 ABSTRACT	42
3.2 INTRODUCTION	43
3.3 MATERIALS AND METHODS	45
3.3.1 Trypanosome cell lines, in vitro culture and transfection conditions	45
3.3.2 Generation of kinesin RNA interference (RNAi) cell lines; 29-13/p2T7-TbKif2, 29-13/p2T7-TbKif8, 29-13/p2T7-TbKif9, 29-13/p2T7-TbKif15, 29-13/p2T7-TbKif27 and 29-13/p2T7-TbKif45	46
3.3.3 Production polyclonal antibody of TbKif2, TbKif8, TbKif9, TbKif15, TbKif27 and TbKif45 ..	49
3.3.4 Immunofluorescence microscopy	52
3.3.5 Mitotracker staining for immunofluorescence microscopy	53
3.3.6 SDS-polyacrylamide gel electrophoresis and Western blotting	54
3.3.7 Fluorescence-activated cell sorting (FACS) analysis	55
3.3.8 Detergent extraction and ATP treatment	55
3.3.9 Cloning of TbKif2, TbKif8, TbKif9, TbKif45 and construction of the 449/TbKif2myc, 449/TbKif8myc, 449/TbKif9myc and 449/TbKif45myc cell lines	56
3.3.10 Conditional double knockout of TbKif2	58
3.3.11 Screening for conditional double knockout of TbKif2	60
3.3.12 Flagellar measurements	61
3.3.13 Production of cDNA for reverse transcriptase (RT) PCR	61
3.4 RESULTS	62
3.4.1 TbKif2myc is localised to the distal tip of the trypanosome flagellum	62
3.4.2 TbKif2 is not required for cell viability in procyclic forms	65

3.4.3	<i>TbKif2myc expression resulted in flagellum shortening and TbKif2 expression was not detected in procyclic or bloodstream forms using Western blots</i>	69
3.4.4	<i>TbKif8myc is localised to the cell body</i>	72
3.4.5	<i>TbKif8 expression was not detected in procyclic and bloodstream forms but RNAi targeting TbKif8 resulted in a mild growth defect</i>	75
3.4.6	<i>TbKif9 is localised to the flagellum of both procyclic and bloodstream cells</i>	76
3.4.7	<i>TbKif9 detergent solubility is ATP dependent</i>	78
3.4.8	<i>Depletion of TbKif9 through RNAi had no observable effect in procyclic strain 29-13 cells</i> ..	80
3.4.9	<i>Anti-TbKif9 is able to detect ectopically tagged TbKif9myc</i>	82
3.4.10	<i>TbKif15 is associated to the mitochondrion in procyclic and bloodstream cells</i>	84
3.4.11	<i>TbKif27 localises to the cell body in procyclic cells</i>	88
3.4.12	<i>Depletion of TbKif27 via RNA interference resulted in a growth defect in procyclic strain 29-13 cells</i>	91
3.4.13	<i>TbKif45 is detergent-insoluble but anti-TbKif45 failed to detect native TbKif45 during immunofluorescence microscopy</i>	94
3.4.14	<i>TbKif45M was localised to the nucleus</i>	96
3.4.15	<i>Overexpression of TbKif45M resulted in karyokinesis arrest</i>	99
3.4.16	<i>TbKif45 depletion through RNAi in procyclic strain 29-13 cells resulted in a mild growth defect</i>	102
3.5	DISCUSSION.....	104
3.5.1	<i>TbKif2 and TbKif9 - kinesins localised to the flagellum</i>	107
3.5.2	<i>TbKif8 and TbKif27 - kinesins localised to the cell body</i>	111
3.5.3	<i>TbKif15, a kinesin associated with the mitochondrion</i>	112
3.5.4	<i>TbKif45, a kinesin localised to the nucleus</i>	113
3.5.5	<i>Functional diversity of the Kinesin-13 family</i>	115
4	REFERENCES	117
5	SUPPLEMENTARY DATA	131
6	APPENDIX	136

Acknowledgements

Throughout the entire project I have experienced many setbacks and problems which I would not have been able to overcome without the help from many individuals. I would like to express my gratitude to them.

I would like to thank Dr. Klaus Ersfeld, my supervisor, for providing me with valuable guidance, advice and being patient with me throughout the entire project.

Cath Wadforth for being the mother of the lab and helping out using her technical expertise.

Dr. Frank Voncken for his advice, helpful insights and for providing the various constructs used throughout my project.

Dr. David Lunt for his guidance in the phylogenetic tree construction.

My colleagues in the lab, Dr. Claudia, Mohamed, Priscilla and Wen for all their help and for making lab life more interesting.

Professor Deborah Smith and Dr. Helen Price for providing the antibodies used in some of my experiments.

Finally I would like to express my appreciation to my family, especially my parents for their encouragement and support throughout.

Abbreviations

ACT	Actin
ADP	Adenosine diphosphate
ATP	Adenosine triphosphate
Bleo	Phleomycin
bp	Base pair
BSA	Bovine serum albumin
BSD	Blasticidin
<i>C.reinhardtii</i>	<i>Chlamydomonas reinhardtii</i>
CCD	Charge-coupled device
cDNA	Complementary DNA
CHO	Chinese Hamster Ovary
DAPI	4',6-diamidino-2-phenylindole
DNA	Deoxyribonucleic acid
Dox	Doxycycline
dsRNA	Double stranded RNA
<i>E. coli</i>	<i>Escherichia coli</i>
FACS	Fluorescence-activated cell sorting
FITC	Fluorescein isothiocyanate
GFP	Green fluorescence protein
HYG	Hygromycin
IC	Intermediate sized chromosome
IFT	Intraflagellar transport
IPTG	Isopropyl β -D-1-thiogalactopyranoside
Kin-C	C-terminus kinesin
Kin-I	Internal motor domain kinesin
Kin-N	N-terminus kinesin
<i>L. major</i>	<i>Leishmania major</i>
LB	Luria Bertani
MBC	Megabased sized chromosome

MC	Minichromosome
MCAK	Mitotic centromere associated kinesin
MOTC	Microtubule organising centre
mRNA	Messenger RNA
Neo	Neomycine
OD	Optical density
ORF	Open reading frame
Parp	Procyclin promoter
PBS	Phosphate buffer saline
pI	Isoelectric point
PVP	Polyvinylpyrrolidone
RNA	Ribonucleic acid
RNAi	RNA interference
RPM	Revolutions per minute
RT-PCR	Reverse transcriptase PCR
SDM-79	Semi-defined medium 79
SDS	Sodium dodecyl sulfate
<i>T. brucei</i>	<i>Trypanosoma brucei</i>
<i>T. cruzi</i>	<i>Trypanosoma cruzi</i>
TbKif	<i>Trypanosoma brucei</i> kinesin superfamily
Tet	Tetracycline
Tet OP	Tetracycline operator
TetR	Tetracycline repressor
UTR	Untranslated region
VSG	Variable surface glycoprotein
X-gal	5-bromo-4-chloro-3-indolyl- beta-D-galactopyranoside
ZPFM	Zimmerman postfusion medium

Abstract

Kinesins are motor proteins involved in the movement of organelles and sub-organelles along microtubule tracks within the cell. Phylogenetic analysis of the 46 kinesin genes coded by the *Trypanosoma brucei* genome resulted in the grouping of seven kinesin sequences into the Kinesin-13 family. Members of this family have been characterised in a number of model organisms and, unlike most kinesins, do not exhibit microtubule processivity and are capable of depolymerising microtubules. They play important roles in bipolar spindle assembly and chromosome segregation. Of the six *T. brucei* Kinesin-13 proteins that were characterised during this study, only one was found to have a nuclear localisation, while the rest were found localised to the mitochondrion, cell body or flagellum. Attempts to probe the function of these kinesins using RNAi resulted in a reduction of cell growth in three of the six kinesins studied, but no gross changes in cellular morphology were observed. The distinct localisation of five Kinesin-13 family members outside the nucleus suggests that the functional diversity of the Kinesin-13 family is larger than previously thought.

1 General introduction

1.1 *Trypanosoma brucei* causes African sleeping sickness and Nagana

Trypanosoma brucei (Figure 1.1) or the African Trypanosome is a protozoan parasite capable of infecting a wide range of mammals including humans. In humans, trypanosomes cause African sleeping sickness that, if left untreated, results in coma and ultimately death. In a study made in 2005, it is estimated that approximately 50,000 - 70,000 new infections occur in Africa every year (<http://www.who.int/mediacentre/factsheets/fs259/en/index.html>). The majority of these cases are confined to rural areas or areas of conflict, resulting in the majority of infections left undiagnosed or untreated. Trypanosomes also infect domesticated animals including cattle causing the wasting disease Nagana.

Both diseases are found only in Sub-Saharan Africa where its natural vector the Tsetse fly is prevalent. The trypanosome parasite is described to possess a digenetic life cycle where it alternates between its mammalian and insect host in order to complete its life cycle (Figure 1.2). In order to survive within two distinctly different hosts, the trypanosome exhibits a life cycle which involves complex physiological and morphological adaptations (Matthews, 2005). Among the different stages of the trypanosome life cycle, the procyclic and bloodstream forms are the most extensively studied as both forms are easily cultured *in vitro*. The procyclic form of the trypanosome is found in the midgut of the tsetse fly while the bloodstream form is from the bloodstream of its mammalian host.

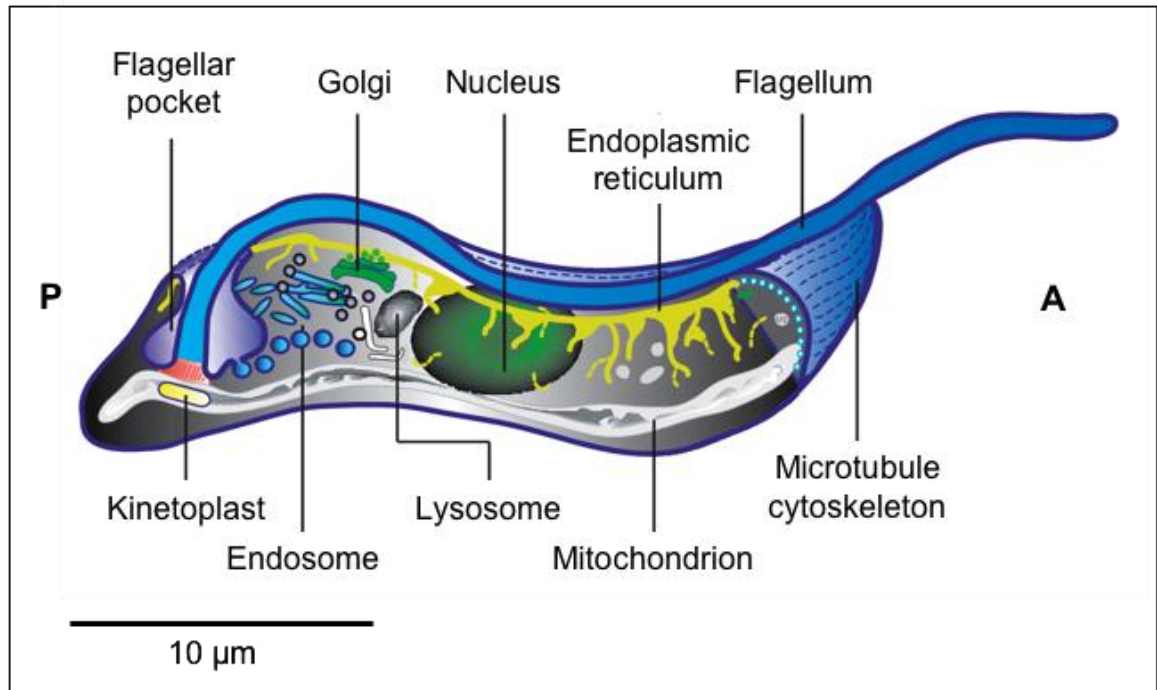


Figure 1.1: A simple representation of the trypanosome structural features. (A) Marks the side which, generally is regarded as the anterior of the parasite and (P) the posterior. At the anterior end of the cell body the subpellicular microtubule corset which runs parallel to each other along the long axis of the cell is partly illustrated. The kinetoplast represents the genome of the mitochondrion of the trypanosome. This image was adapted from Overath and Engstler, 2004.

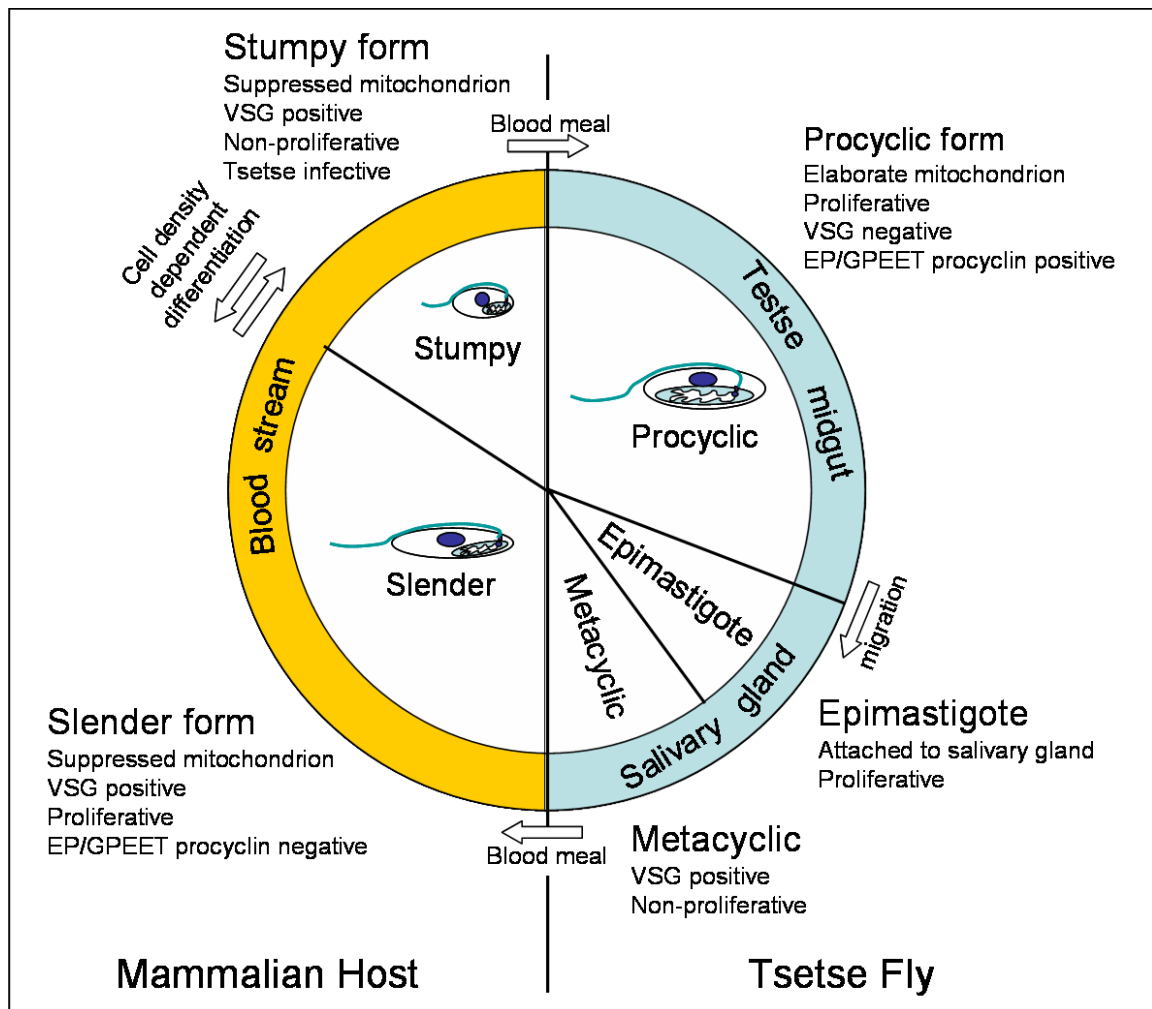


Figure 1.2: The life cycle of *Trypanosoma brucei*. The tsetse fly is infected when it takes a blood meal from a mammal infected with the trypanosome parasite. The trypanosome is capable of proliferating within the midgut of the tsetse fly in the procyclic form and eventually differentiates to epimastigotes when it migrates to the salivary glands of the tsetse fly. In the salivary gland, these epimastigotes transform into the mammalian infective metacyclic trypomastigotes. These metacyclic trypomastigotes are introduced to a new mammalian host when the infected tsetse fly takes a blood meal. When in its mammalian host, the trypanosome exists as a heterogeneous population of slender and stumpy forms (Matthews et al., 2004). The slender form is able to actively proliferate while the non-proliferative stumpy form is tsetse fly infective.

1.2 **Antigenic variation and variable surface glycoprotein**

Trypanosoma brucei is an extracellular parasite as it lives exclusively in the intercellular space and bloodstream of its mammalian host. This results in the parasite being exposed to the complement and antibody-based immune system of its mammalian host, which is potentially fatal to the parasite.

In order to avoid the immune system of its mammalian host, the trypanosome expresses a Variable Surface Glycoprotein (VSG) coat which acts as a physical barrier to the complement immune system from recognising its invariant surface proteins. This VSG coat however is capable of being recognised by the adaptive antibody based immune system which eventually results in the clearance of the parasite from the blood stream of its host. However, a small fraction of the trypanosome population is able to escape detection by periodically changing its VSG coat to an immunologically different VSG coat in a process called antigenic variation (Barry, 1997; Donelson, 2003; Pays et al., 2004). The *T. brucei* genome codes for more than 1000 VSG genes/pseudogenes (Berriman et al., 2005; Van der Ploeg et al., 1982) and it also has approximately 20 telomeric VSG expression sites, responsible for the expression of a variety of expression site associated genes including VSG genes (Berriman et al., 2002; Donelson, 2003). These VSG expression sites are described as mono-allelic as only one VSG expression site is transcriptionally active at a time.

The trypanosome expresses only one VSG gene during antigenic variation, the expression of this VSG gene is changed randomly at a rate of approximately once every 100 cell doublings (Turner, 1997; Turner and Barry, 1989). The switching of active VSG genes can occur through *in situ* switching between different VSG expression sites or through homologous recombination resulting in the change of the VSG gene within the active expression site (McCulloch, 2004; Taylor and Rudenko, 2006). The survival of the trypanosome depends on its ability to express immunologically distinct VSG coats during the course of an infection which could potentially last for several years. In order to generate a large variety of immunologically distinct VSG coats, the trypanosome maintains a large repertoire of VSG genes/pseudogenes and employs genetic recombination in generating novel VSG genes (Barry and McCulloch, 2001; Taylor and Rudenko, 2006). This is reflected on the genome organisation of the trypanosome.

1.3 Genome organisation of *Trypanosoma brucei* and mitosis

The nuclear genome of the trypanosome consists of three chromosome types originally classified by their sizes (Figure 1.3). There are 11 pairs of large (1 to >6Mbp) megabase sized chromosomes (MBCs), a variable number (1 to 5) of intermediate (200 to 900 kb) sized chromosomes (ICs) and a population in the order of approximately 100 minichromosomes (50 to 150 kb, MCs) (Ersfeld et al., 1999; Van der Ploeg et al., 1984; Van der Ploeg et al., 1989). It is estimated that there are more than 1,000 VSG genes in the trypanosome genome representing at least 10% of the total genome content of the trypanosome (Berriman et al., 2005; Van der Ploeg et al., 1982). The majority of these VSG genes are present in the subtelomeric regions in all three classes of chromosomes (Lips et al., 1993; Rudenko et al., 1998; Taylor and Rudenko, 2006; Van der Ploeg et al., 1984). All the VSG expression sites are found in the MBCs and ICs while a significant proportion (~10%) of the silent VSG genes can be found in the MCs (Berriman et al., 2002; Donelson, 2003). While no VSG expression sites are found in the MC population (Wickstead et al., 2004) MCs play an important role as the preferred VSG gene reservoir for antigenic variation during the early stages of mammalian infection (Morrison et al., 2005; Robinson et al., 1999).

In total the *T. brucei* maintains approximately 120 chromosomes of various sizes. Of particular interest is the minichromosomal population in *T. brucei* which represent more than 80% of the total chromosome population. The structure of the minichromosome has been previously studied and it was shown to be made up primarily of telomeric repeats, subtelomeric repeats, internal 177 bp repeats and a single VSG gene at either side in its subtelomeric regions (Wickstead et al., 2004; Zomerdijk et al., 1992). The exact mode of minichromosomal segregation during mitosis is still unknown and uncovering it is a subject interest within our laboratory.

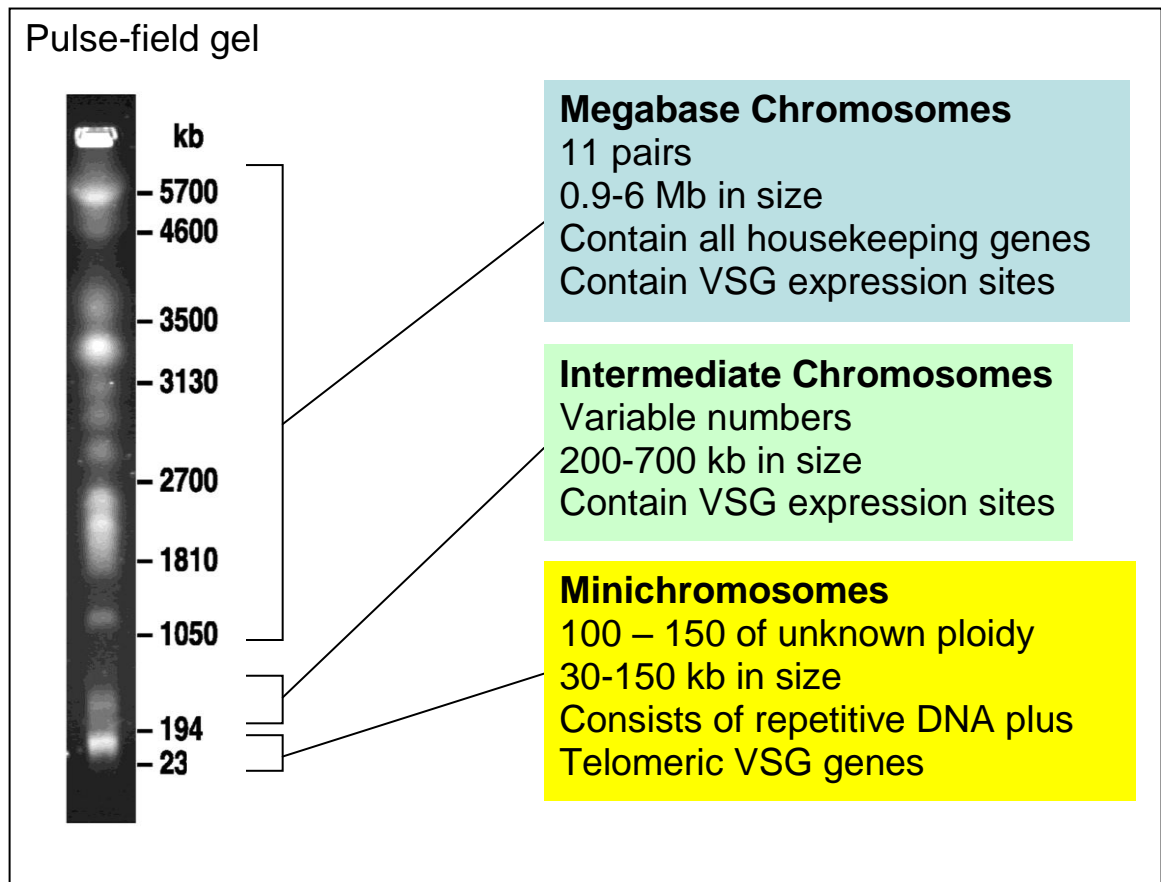


Figure 1.3: Summary of the types of chromosomes in *Trypanosoma brucei*. The pulse field gel electrophoresis image shows the migration pattern of the chromosomes of *T. brucei* strain 427 cells. The gel image was taken from Wickstead et al., 2004.

The trypanosomes exhibit several differences from the metazoan model of mitosis (Figure 1.4). Trypanosomes do not undergo visible chromosome condensation during mitosis (Vickerman and Preston, 1970) and, similar to yeast perform a “closed mitosis” where the mitotic spindle forms within the nucleus without the breakdown of its nuclear envelope. The trypanosome possess several single copy organelles (e.g.: kinetoplast and mitochondrion) which are segregated in a precise order throughout the cell cycle (Gull et al., 1990; McKean, 2003; Sherwin and Gull, 1989a). As in most eukaryotic cells chromosome segregation in trypanosomes is based on the presence of an intact microtubule-spindle apparatus (Ersfeld and Gull, 1997; Ersfeld et al., 1999; Ogbadoyi et al., 2000). Despite the large numbers of minichromosomes (~100) and their relatively small size, minichromosomal segregation occur with high fidelity (Wickstead et al., 2003; Zomerdijk et al., 1992).

The conventional form of chromosome segregation depends on the bipolar attachment of microtubules to either kinetochore of each sister chromatid during mitosis (Figure 1.5). This association plays an important role in chromosome congression during metaphase and the accurate segregation of chromosomes during anaphase (Cimini and Degrossi, 2005). Conventional kinetochore-microtubule based chromosome segregation requires the number of mitotic spindle microtubules present to be at least twice the number of chromosomes being segregated. This is because the two chromatids of each chromosome need to be attached to at least two microtubule filaments from each centrosome/MTOC (microtubule organising centre). However, in most cells this ratio is even higher as most kinetochores harbour binding sites for several microtubule filaments.

The *T. brucei* nucleus has approximately 120 chromosomes. In order to segregate these chromosomes, the mitotic spindle should have least 240 microtubules. However, studies on trypanosome nuclear cross sections using electron microscopy, estimate that the number of microtubules present during mitosis does not exceed 100 which is well below the minimum requirement for conventional kinetochore-microtubule based chromosome segregation (Ogbadoyi et al., 2000). Based on these observations trypanosomes are likely to have evolved alternative/additional methods of chromosome segregation.

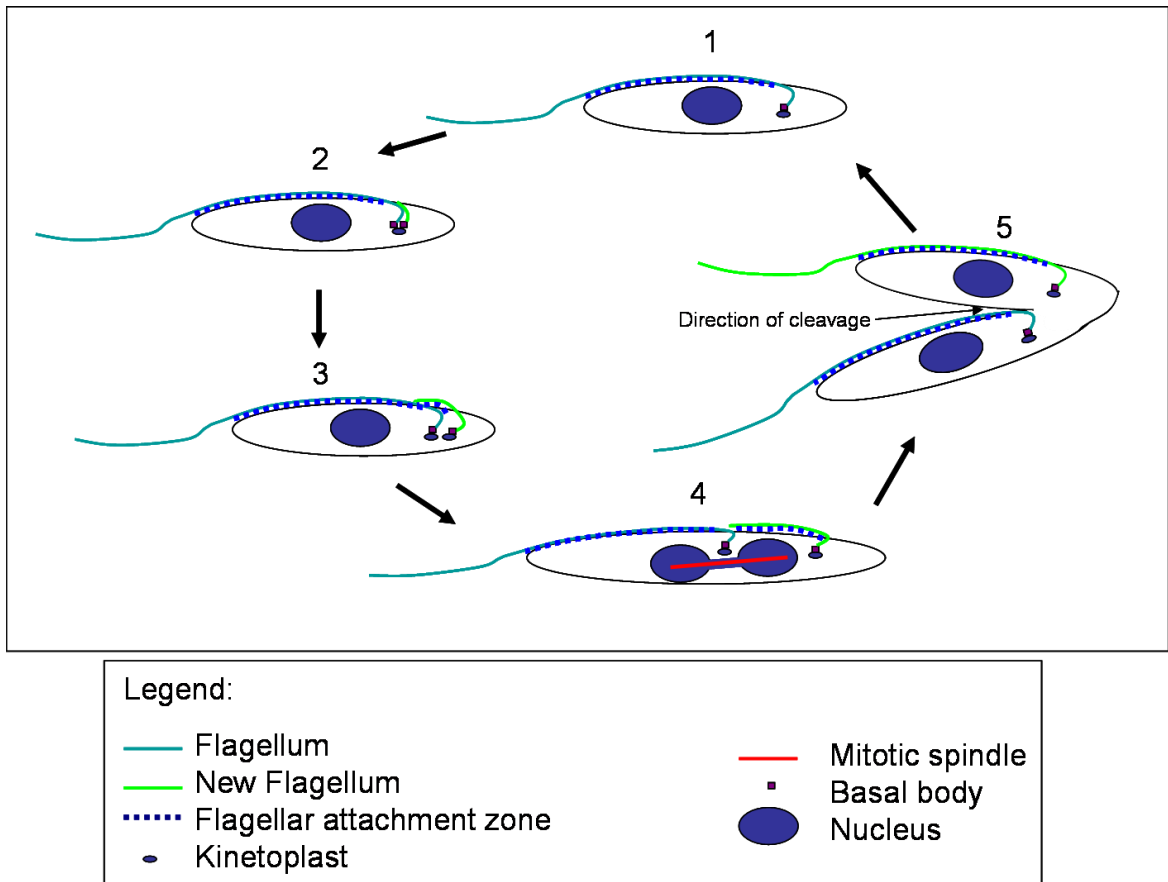


Figure 1.4: The cell cycle of *T. brucei*. One of the earliest observable changes during the cell cycle of the trypanosome is the appearance of two basal bodies and the outgrowth of the daughter flagellum [(1) to (2)]. At (3), segregation of the duplicated basal bodies, flagellum and kinetoplasts occurs. “Closed mitosis” then occurs at stage (4) where the chromosomes within the nucleus are segregated and cell division is completed in stage (5) where the cleavage of the *T. brucei* cell into two sister cells occurs.

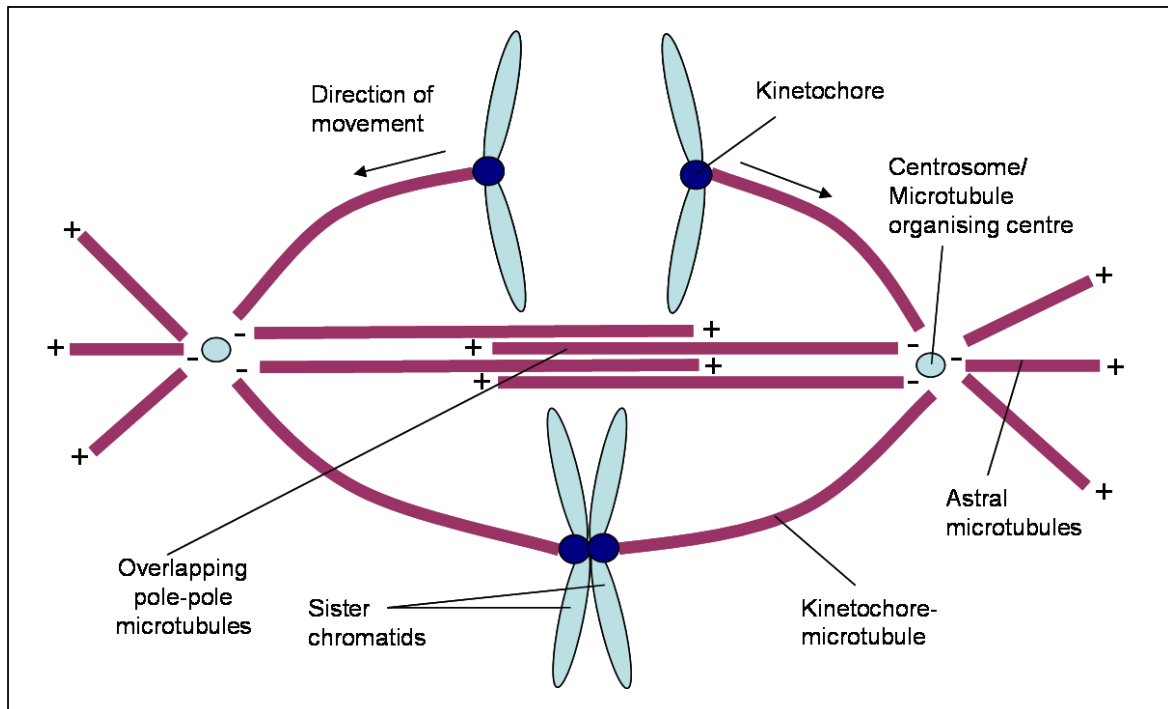


Figure 1.5: A metazoan example of chromosome segregation. Microtubules emanating from the opposing spindle poles can each associate to either kinetochore of each sister chromatid forming a bipolar kinetochore-microtubule attachment or associate with microtubules of opposing poles forming overlapping pole-to-pole microtubule associations. Chromosomes are segregated via tensile forces exerted by the kinetochore-microtubules associations. These forces can be generated via several methods; microtubule depolymerisation at the kinetochore and spindle pole or via spindle elongation due to forces generated by motor proteins at the overlapping pole-to-pole microtubules (Rosenblatt, 2005; Sharp et al., 2000b).

1.4 Chromosome segregation in *Trypanosoma brucei*

Several possible theoretical models have been proposed based on morphological events that occur in trypanosomes during mitosis. One model put forward, suggested that the nuclear envelope may play a role in chromosome segregation by acting as medium for chromosome attachment (Heywood and Weinman, 1978). This mode of chromosome segregation is similar to bacterial cells where their circular chromosomes associate with the cell membrane during chromosome segregation (Ghosh et al., 2006). However, this model is unlikely to occur as it was shown that the chromosomes are segregated in a microtubule dependent manner (Ersfeld and Gull, 1997).

While the exact mode of chromosome segregation remains unknown, several important observations have been made: MCs are mitotically stable (Wickstead et al., 2003; Zomerdijk et al., 1992); MC segregation is microtubule dependent, MCs co-localises with the mitotic spindle and appear to congregate at the metaphase-like plate before migrating to the spindle poles (Ersfeld and Gull, 1997). Furthermore, recent studies have identified centromeric sequences in MBCs (Obado et al., 2007) which, coupled with the observation of kinetochore like structures observed in trypanosome nucleus during mitosis (Ogbadoyi et al., 2000) indicate that at least the MBC population in trypanosomes do segregate conventionally via kinetochore-microtubule interactions. However, given the nature and structural composition of minichromosomes which does not contain any recognisable centromeric sequences (Wickstead et al., 2004), it is likely that the MCs are segregated by an alternative pathway.

Therefore, a new model of minichromosome segregation called the “lateral stacking” model was proposed (Gull et al., 1998). The “lateral stacking” model (Figure 1.6) is a hybrid model where the MBCs and ICs are segregated conventionally while the MCs associate laterally to pole-to-pole microtubules of the mitotic spindle. Forces generated for the segregation of the MCs are produced by minus-end directed motor proteins which would move along the mitotic spindle towards the spindle poles. The advantage of this model is that it allows for the association of multiple MCs to a single pole-to-pole microtubule, giving means for the segregation of the entire trypanosome genome with high fidelity.

While the lateral stacking model does provide a possible mode of chromosome segregation in trypanosomes, there is little direct evidence in support of this model as the molecular machinery involved in chromosome segregation in trypanosomes is unknown. To address this information void, this project was initiated with the express aim of identifying proteins involved in chromosome segregation, in particular the role of kinesin motor proteins in chromosome segregation in *T. brucei*.

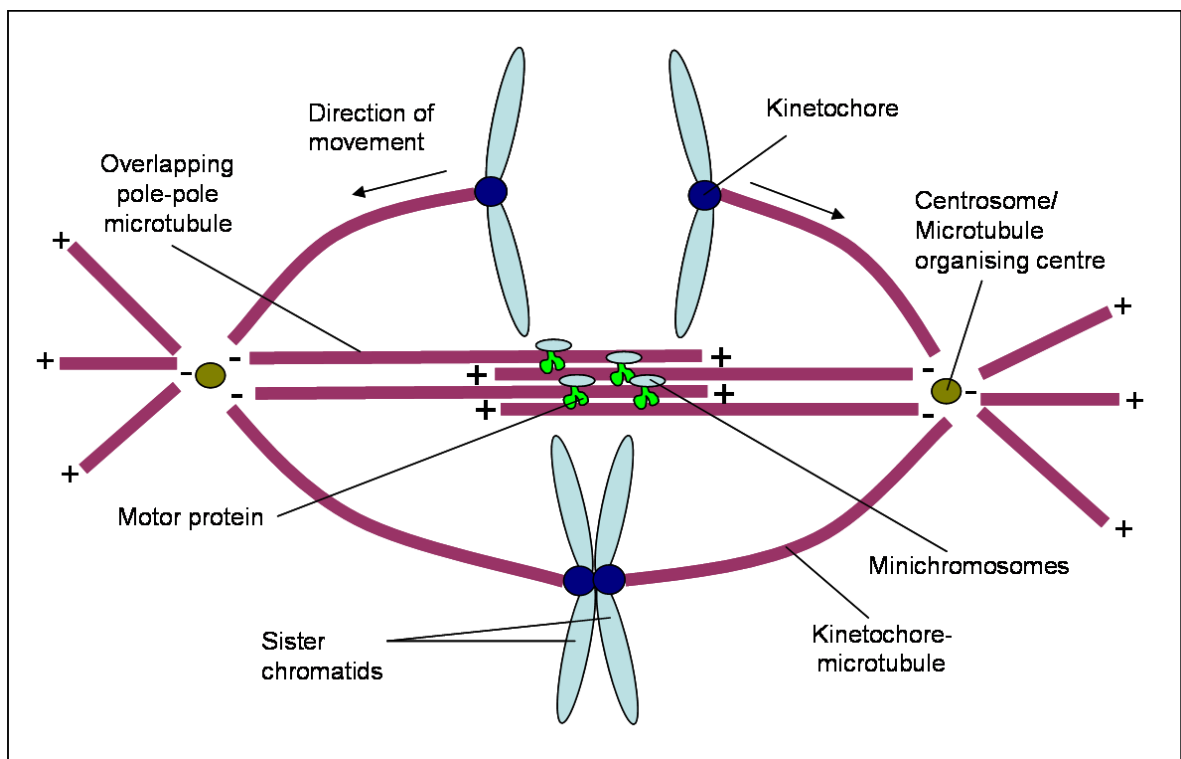


Figure 1.6: Lateral stacking model (Gull et al., 1998) where the large MB chromosomes are segregated conventionally while the smaller MCs are segregated via minus-end directed motor proteins associated to overlapping pole-to-pole microtubules.

1.5 *The kinesin motor proteins*

During mitosis, microtubules of the mitotic spindle play a major role in the accurate segregation of chromosomes (Cimini and Degross, 2005). Essential mediators of chromosome motility along microtubules are two classes of microtubule associated molecular motor proteins known as kinesins (Cassimeris, 2004; Kline-Smith and Walczak, 2004; Wittmann et al., 2001) and dyneins (Banks and Heald, 2001; Karki and Holzbaur, 1999). While the dynein motor proteins are absent in some eukaryotic lineages (Lawrence et al., 2001), the kinesin motor proteins are encoded by the genome of all eukaryotes studied thus far.

Kinesins were first characterised in the axoneme of squids where they play a role in the transport of vesicles (Brady, 1985; Vale et al., 1985). Since then, kinesins have been found in a variety of eukaryotic organisms from the budding yeast *Saccharomyces cerevisiae* (Grishchuk and McIntosh, 2006; Hildebrandt and Hoyt, 2000) to complex multicellular organisms including man (Compton, 2000; Gaglio et al., 1996; Sharp et al., 2000b; Wittmann et al., 2001). More than 600 kinesins have been identified thus far (Miki et al., 2005; Wickstead and Gull, 2006) and kinesins have been found to be involved in a wide variety of microtubule-associated functions.

Kinesins are defined by the presence of a highly conserved globular catalytic core (also known as motor domain) approximately 350 amino acids long, responsible for microtubule binding and translocation of the kinesin along microtubules in the presence of ATP (Hirokawa, 1998; Vale and Fletterick, 1997; Yang et al., 1989). This motor domain can be located at any region of the kinesin polypeptide chain. According to the location of the motor domain, kinesins are divided into three general groups (Figure 1.7). These groups of kinesins are known as; Kin-N where the motor domain is located at the amino-terminus of the kinesin, Kin-C where the motor domain is located within the carboxy-terminus of the kinesin or Kin-I if the kinesin is located internally at the centre of the kinesin polypeptide chain. Kinesins within each group in general share similar characteristics where; Kin-N kinesins move towards the plus-end of microtubules, Kin-C kinesins towards the minus-end of microtubules while Kin-I depolymerise microtubules ends (Hirokawa et al., 1998).

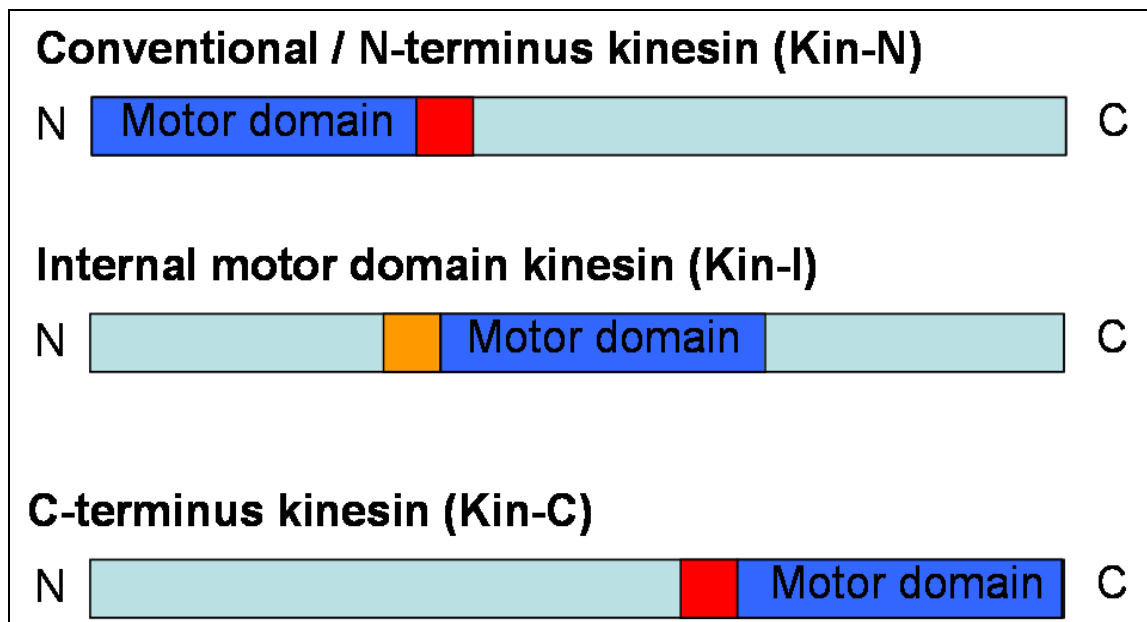


Figure 1.7: A graphical representation of the different classes of kinesins (Hirokawa et al., 1998; Lawrence et al., 2002). Depending on the relative position of the motor domain (dark blue) in the polypeptide chain, the kinesin will either be classified as a Kin-N, Kin-I or Kin-C. The area shaded in red signifies the neck region and the region shaded in light blue corresponds to polypeptide residues that are highly variable in sequence that is sometimes known as the tail or stalk. The neck region in Kin-I is shaded orange as some of the kinesins within this group do not harbour the neck region at the N-terminus of the motor domain.

The kinesin motor domain is usually followed by a divergent “tail/stalk” region located either at the N-terminus and/or C-terminus of the motor domain. The overall protein sequence “tail” generally lacks any sequence conservation and is responsible for various functions like oligomerisation with other kinesins, interacting with other macromolecules or with various organelles (Hirokawa, 1998; Miki et al., 2005; Vale and Fletterick, 1997). Located between the motor domain and the tail of most kinesins is the “neck” region, primarily responsible for the determining the directionality and level of activity of the kinesin (Bathe et al., 2005; Case et al., 1997; Endow and Waligora, 1998). While the neck and tail domains can be divergent in sequence, both domains are often found to be rich in β -sheets and/or coiled-coiled structures (Miki et al., 2005). The coiled-coiled structures in the neck and tail domain are often responsible for the oligomerisation of several kinesin subunits. Additionally, the neck and tail domains may sometimes contain sequence specific motifs which are useful in functional prediction (Miki et al., 2005; Westerholm-Parvinen et al., 2000).

There are several publications featuring the 3D structure study of the kinesin motor protein. However, most of these studies are confined to the kinesin motor domain and the Kin-N/conventional kinesins (Figure 1.8). Kinesins tend form complexes with a variety of proteins including other kinesins (Cole, 1999; Gindhart, 2006; Hirokawa and Takemura, 2004). For example, the conventional/Kin-N kinesins is made up of two different types of polypeptide chains forming a heterotetramer. The polypeptide chain containing the kinesin motor domain is termed the “kinesin heavy chain”. The “kinesin light chain/kinesin associated protein” that does not contain the motor domain, represents the kinesin-associated polypeptide chain. While the rate of identification of the “kinesin heavy chains” in many organisms are progressing rapidly, the discovery of kinesin associated proteins are predominantly confined to members of the conventional kinesins (Gindhart, 2006). This is because not all kinesins possess a kinesin light chain and some kinesins are known to function as monomers, dimers and tetramers (Vale, 2003).

The molecular events that occur when kinesins move along microtubules have also been studied. The current accepted model of kinesin motility in Kin-N type kinesins is described as the “hand-over-hand” model (Figure 1.9) where the kinesin moves along the microtubule track in a bipedal manner (Carter and Cross, 2006; Woehlke and Schliwa,

2000; Yildiz and Selvin, 2005). This model of kinesin movement along microtubules can only occur when the kinesins form dimers. As some kinesins exert their function as monomeric units (Vale, 2003; Yildiz and Selvin, 2005), this model of kinesin motility can only be used in a subset of kinesin proteins.

The microtubule depolymerising ability of Kin-I kinesins has also been studied (Figure 1.10). The molecular model of KinI action on microtubules was constructed primarily based on truncated versions of KinI motor proteins containing only the neck and motor domain. This is because the motor depolymerising activity of KinI is exclusively associated with the neck and motor domain (Maney et al., 2001). It is uncertain if this model is compatible with the full length KinI proteins as they have been shown to form homodimers (Kim and Endow, 2000; Maney et al., 1998).

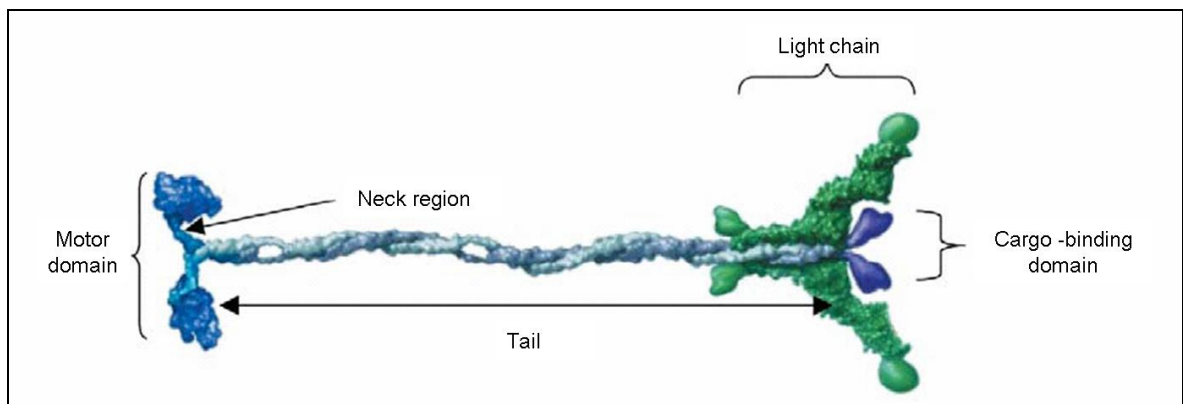


Figure 1.8: A graphical representation of a conventional kinesin, which is a Kin-N type kinesin. The conventional kinesin is a heterotetramer with two kinesin heavy chains (blue) and the two kinesin light chains (green). The kinesin heavy chain (KHC) is the polypeptide chain, which the motor domain resides. The kinesin light chain is responsible for the association with various kinesin associated proteins which play an important role in facilitating the transport of various cargoes (Gindhart, 2006). The image was adapted from (Vale, 2003).

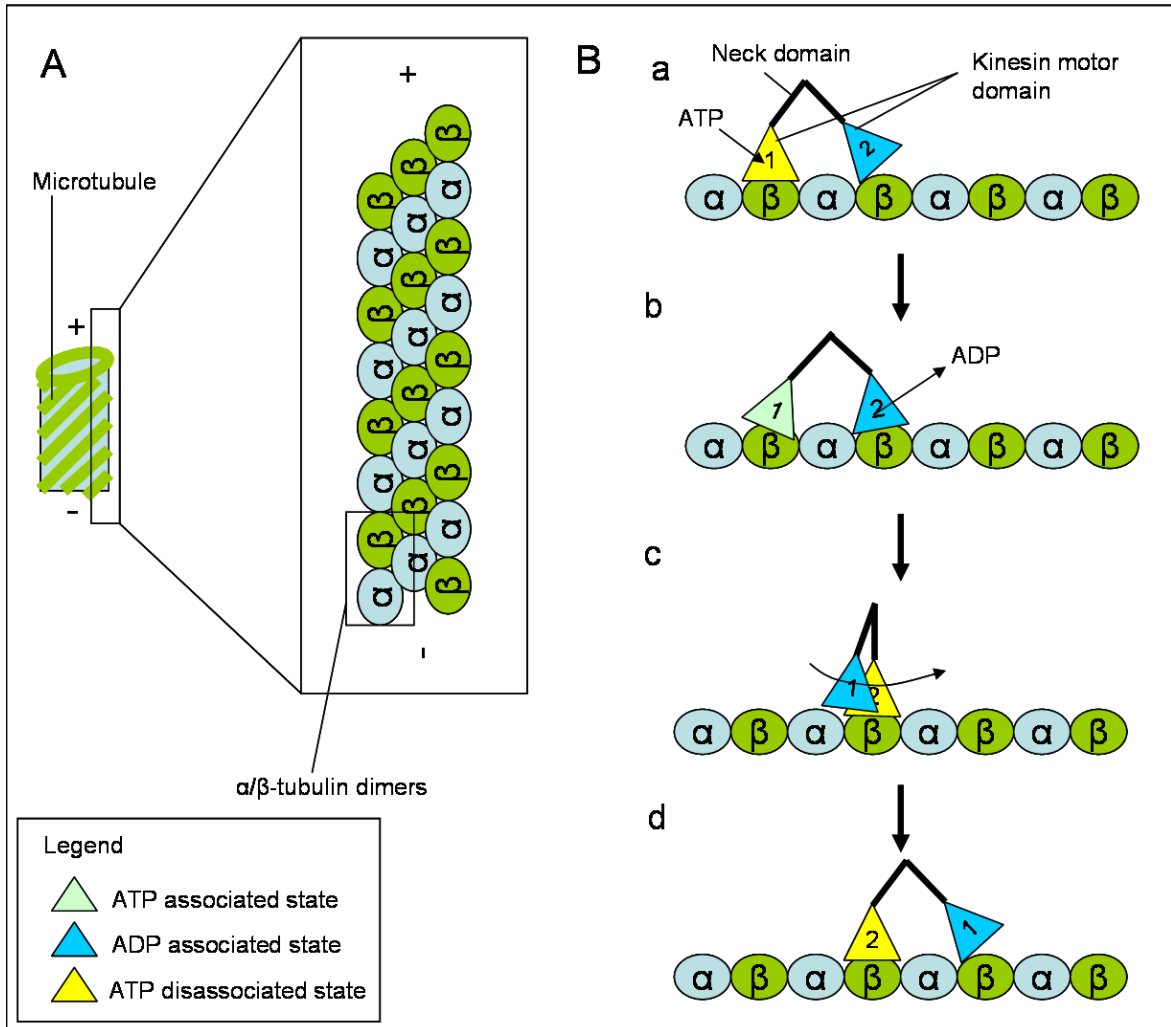


Figure 1.9: Microtubule structure and model of conventional kinesin function (Carter and Cross, 2006; Woehlke and Schliwa, 2000; Yildiz and Selvin, 2005). (A) Microtubules are built from α/β -tubulin dimers stacked in an organised fashion. The end exposing the β -subunit is called the plus-end while the end exposing the α -subunit is called the minus-end. The plus end of the microtubule is usually located at the cell periphery in interphase cells and at the midzone of the mitotic spindle in cells undergoing mitosis. The minus-end is located at the microtubule organising centre. (B) Hand-over-hand model of conventional kinesin movement. The binding of the kinesin motor domain does not require ATP (a). In the ATP unbound state of the motor domain 1, motor domain 2 cannot associate with the microtubules. When ATP associates to the motor domain 1 (b), a conformational change is induced allowing motor domain 2 to associate with the microtubule track. The association of motor domain 2 to the microtubule track results in the release ADP. The hydrolysis of ATP in motor domain 1 (c) would allow motor domain 1 to disassociate from the microtubule and move forward (d).

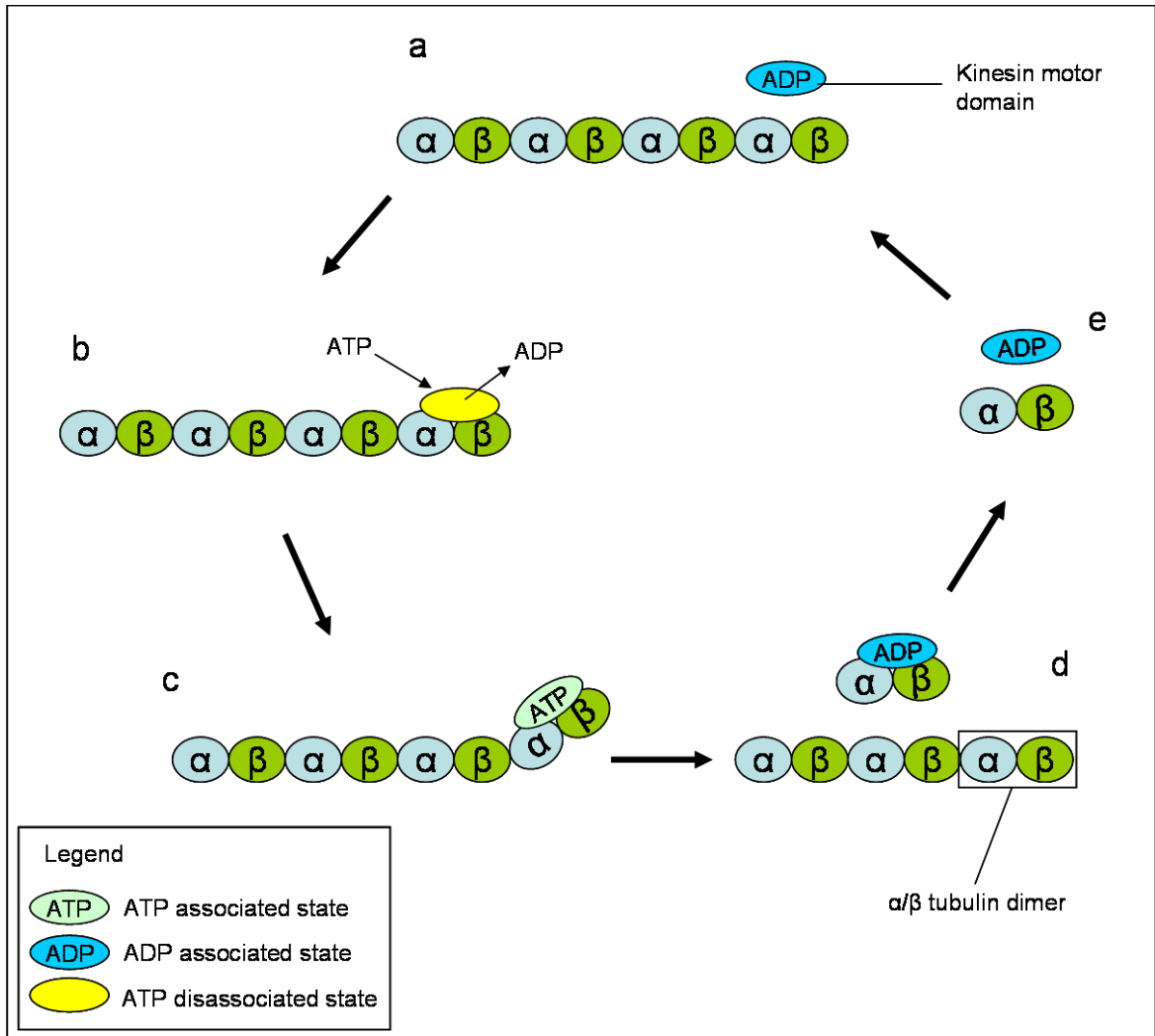


Figure 1.10: The microtubule dependent ATPase cycle of Kin-I kinesins (Moore and Milligan, 2006; Shipley et al., 2004). (a) The motor domain of the KinI contains ADP in its microtubule unbound state. (b) When the motor domain associates to the end of microtubule filament, ADP is released. The release of ADP from the motor domain allows for the entry of ATP. (c) When ATP binds to the motor domain, a conformational shift in the motor domain's structure causes the curling of the microtubule filament (Moore et al., 2003). (d) ATP hydrolysis is stimulated and tubulin dimer associated with the motor domain dissociate from the microtubule filament. (e) ATP hydrolysis weakens the association of the motor domain to the tubulin dimer causing it to disassociate.

1.6 *Kinesin functions in intracellular transport and mitosis*

During mitosis, a multitude of motor proteins are involved in the regulation of the mitotic spindle (Figure 1.11 and Table 1.1). The role of kinesins is not confined to creating the poleward forces required for chromosome segregation. Kinesins are also involved in the formation and maintenance the bipolar spindle, correcting improper microtubule-kinetochore associations and the formation of the cleavage furrow during cytokinesis (Table 1.1). Kinesins on the mitotic spindle work in antagonistic pairs (Cottingham and Hoyt, 1997; Ganem and Compton, 2004; Saunders et al., 1997; Sharp et al., 2000b) where the depletion/overexpression of one of the kinesin pairs will result in aberrant spindle morphology.

Kinesins also perform various microtubule-associated functions in non-dividing cells. During interphase, kinesins play a major role in mediating the transport of various organelles (Hirokawa, 1998; Vale, 2003) (Figure 1.12). In flagellated organisms, kinesins also play a role in intraflagellar transport (Bernstein, 1995; Rosenbaum et al., 1999) and have a role in regulating flagellar motility (Yokoyama et al., 2004).

Thus far, the study of kinesin motor proteins are restricted to relatively few organisms such as mammals and model organisms like *Drosophila*, *Xenopus*, *Saccharomyces*, *Arabidopsis* and *Chlamydomonas*. As more kinesins are characterised from more diverse sources, it is expected that the list of known kinesin functions will expand. In addition, it is important to note that other types of motor proteins like cytoplasmic dyneins do interact with kinesins in mediating the transport of vesicles and organising the mitotic spindle (Banks and Heald, 2001; Hirokawa, 1998).

Due to the essential functions performed by kinesins in cell proliferation and organelle transport, kinesins have become a target for drug development. An example would be Eg5 which is required for the generation of bipolar spindle and the proper segregation of sister chromatids during anaphase (Blangy et al., 1995). As Eg5 does not bear known non-mitotic functions; its inhibition only affects actively proliferating cells. Currently there are several drugs targeting Eg5 undergoing clinical trials being tested as potential anti-cancer drugs (Schmidt and Bastians, 2007).

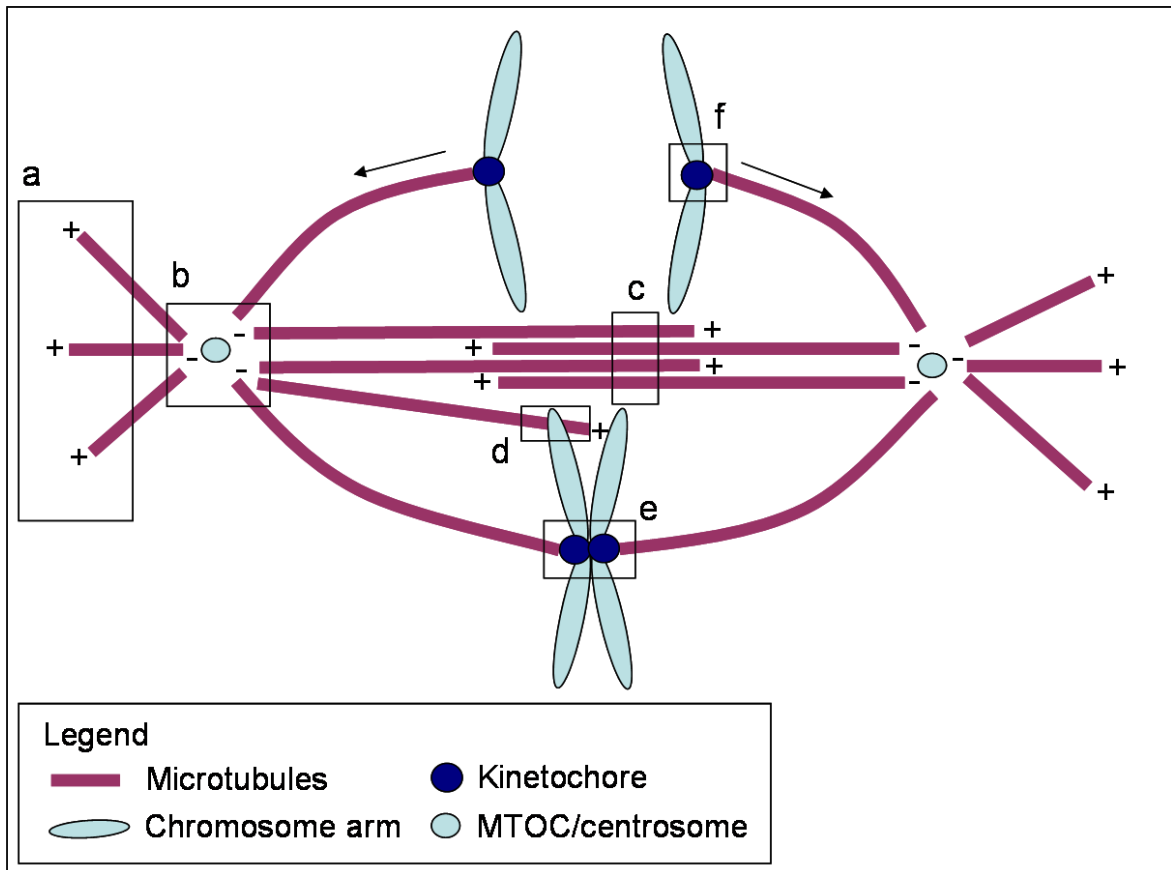


Figure 1.11: The various aspects of the mitotic spindle where several kinesins and dyneins regulate spindle function. (a) Astral microtubules where dyneins are involved in proper spindle positioning. (b) Spindle poles where kinesins are involved in the formation of the bipolar spindle and generate poleward microtubule flux during chromosome segregation. (c) Overlapping pole-to-pole microtubules where kinesins are involved in microtubule sliding, important in spindle length regulation. (d) At the chromosome arms, kinesins are involved in facilitating chromosome motility during congression. (e) At the kinetochore, kinesins facilitate proper kinetochore-microtubule capture and depolymerise microtubules contributing to the poleward movement of chromosomes during anaphase (f). A detailed list of motor protein action on the mitotic spindle is described in Table 1.1.

Table 1.1: A summary of the various functions performed by motor proteins during mitosis.

Localisation in mitotic spindle	Motor protein family/Protein characterised	Function	References
Along overlapping pole-to-pole microtubules/spindle midzone	Kinesin-5/TKRP125, BimC, CIN8 and KIP1	<ul style="list-style-type: none"> • Microtubule bundling • Mitotic spindle elongation • Bipolar spindle formation 	(Asada et al., 1997; Enos and Morris, 1990; Hoyt et al., 1992; Saunders et al., 1997; Saunders et al., 1995; Sawin et al., 1992)
	Kinesin-14/Kar3, ATK1 and Ncd	<ul style="list-style-type: none"> • Microtubule bundling • Mitotic spindle shortening • Bipolar spindle formation 	(Bowser and Reddy, 1997; Chen et al., 2002; Marcus et al., 2003; McDonald et al., 1990; Saunders et al., 1997; Saunders et al., 1995; Sharp et al., 2000c; Vos et al., 2000)
	Kinesin-6/PAV-KLP and Rab6-KIFL	<ul style="list-style-type: none"> • Formation of the cleavage furrow during cytokinesis 	(Adams et al., 1998; Hill et al., 2000)
	Kinesin-8/Kip3, Klp5, Klp6 and Klp67A	<ul style="list-style-type: none"> • Chromosome segregation 	(Gupta et al., 2006; Savoian et al., 2004; West et al., 2002)
Astral microtubules, kinetochore and spindle poles	Cytoplasmic dynein/Dhc1	<ul style="list-style-type: none"> • Spindle pole positioning • Chromosome segregation 	(Banks and Heald, 2001; Gaglio et al., 1997; Karki and Holzbaur, 1999; Lee et al., 1999; Saunders et al., 1995; Sharp et al., 2000a)
Spindle poles	Kinesin-5/Eg5	<ul style="list-style-type: none"> • Bipolar spindle formation 	(Blangy et al., 1995; Gaglio et al., 1996)
	Kinesin-13/Xklp2, DmKlp10A, Kif2a and Kif2b	<ul style="list-style-type: none"> • Bipolar spindle formation and maintenance • Generating poleward microtubule flux for chromosome segregation 	(Boleti et al., 1996; Ganem and Compton, 2004; Goshima and Vale, 2003; Manning et al., 2007; Rogers et al., 2004)
Kinetochore	Kinesin-13/MCAK, DmKlp59C and XKCM1	<ul style="list-style-type: none"> • Regulate proper kinetochore-microtubule association • Mitotic spindle assembly and maintenance • Facilitate chromosome congression 	(Cassimeris and Morabito, 2004; Goshima and Vale, 2003; Kline-Smith et al., 2004; Kline-Smith and Walczak, 2002; Maney et al., 1998; Rogers et al., 2004; Walczak et al., 2002; Walczak et al., 1996; Wordeman and Mitchison, 1995; Wordeman et al., 2007)
	Kinesin-7/CENP-E	<ul style="list-style-type: none"> • Kinetochore microtubule capture • Chromosome congression 	(Kapoor et al., 2006; McEwen et al., 2001; Putkey et al., 2002; Schaar et al., 1997; Weaver et al., 2003; Wood et al., 1997; Yao et al., 1997; Yen et al., 1992; Yucel et al., 2000)
Chromosome arms	Kinesin-4/chromokinesin	<ul style="list-style-type: none"> • Chromosome congression/movement 	(Wang and Adler, 1995)
	Kinesin-10/KID and NOD	<ul style="list-style-type: none"> • Chromosome congression/movement 	(Afshar et al., 1995; Antonio et al., 2000; Funabiki and Murray, 2000; Tokai et al., 1996)

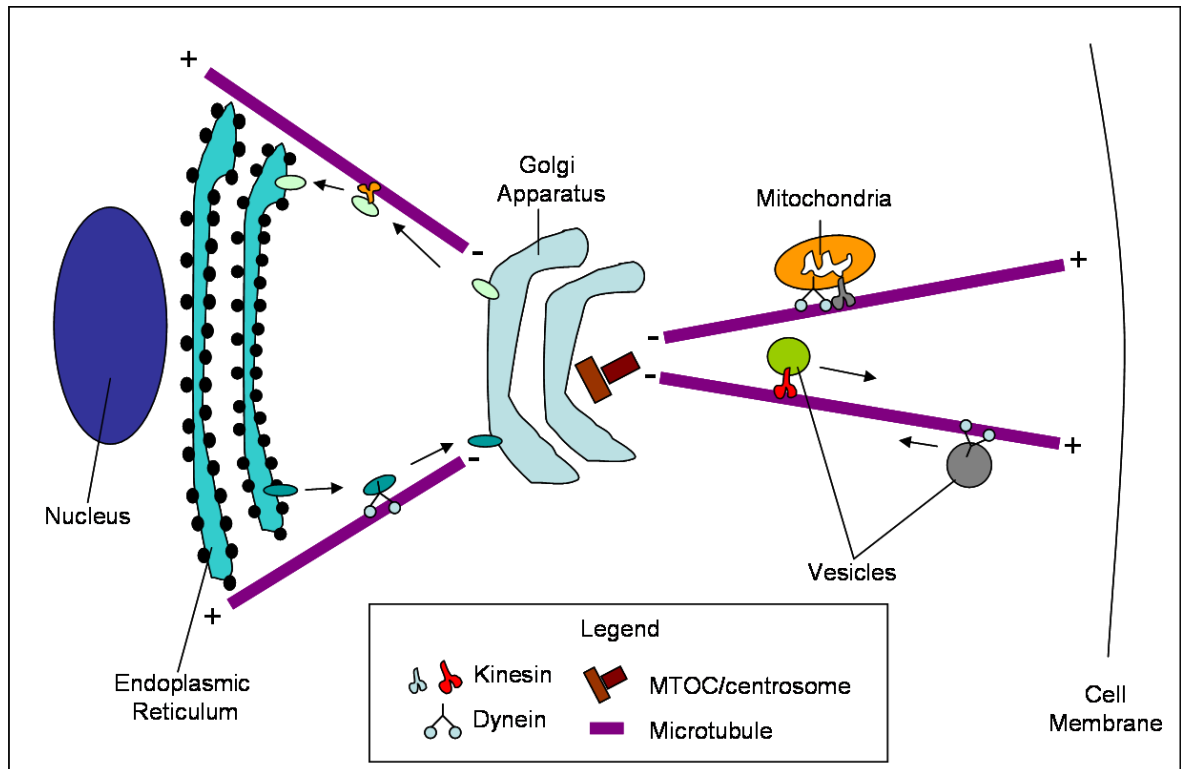


Figure 1.12: The role of motor proteins in organelle transport (Hirokawa, 1998; Vale, 2003). The transport of various organelles to the minus-end of microtubules is mediated by cytoplasmic dyneins and minus-directed (Kin-C) kinesins. The transport of various organelles to the plus-end of microtubules is mediated by plus-end directed (Kin-N) kinesins. Kinesins are known to form multi-protein complexes during intracellular transport. These complexes are regulated via signal transduction pathways in the cells through various kinases (Caviston and Holzbaur, 2006).

1.7 Project aims

The aims of this project are to identify and to functionally characterise kinesin motor proteins involved in the segregation of chromosomes in *Trypanosoma brucei*. The results of this thesis will be divided into two general sections.

The first section describes the identification of kinesin motor proteins likely to have mitotic function. The methods used include:

- a) The construction of a phylogenetic tree based on the motor domains of all trypanosome kinesins and a selection of functionally characterised kinesin from other eukaryotes.
- b) The search of sequences or motifs that may confer specific functions to the corresponding kinesin sequence.

The second section describes the experimental procedures used to probe the function of candidate kinesin sequences which involves:

- a) The production of polyclonal antibodies specific to each of the candidate kinesin sequences, used in immunolocalisation studies and Western blot analysis.
- b) The generation of *T. brucei* cell lines expressing an epitope tagged version of a selected subset of kinesins for immunolocalisation studies.
- c) Protein overexpression experiments to study the function of the kinesin of interest.
- d) The generation of RNAi and conditional double knock out cell lines to study the effect of loss of gene function.

2 Phylogenetic analysis of the kinesin superfamily in *Trypanosoma brucei*

2.1 Abstract

Kinesins are motor proteins involved in microtubule-associated transport of various organelles or sub-organelle assemblies in all eukaryotes. There are currently 14 kinesin families divided according to the phylogenetic relatedness of the kinesin motor domain. The trypanosome genome codes for 46 kinesin genes. Using phylogenetic analysis on the kinesin motor domain, only 14 of the 46 kinesins were classified into the 14 known kinesin families. Of the 14 kinesins sequences, one sequence was found grouped to the Kinesin-1 family, two sequences to the Kinesin-2 family, one sequence to the Kinesin-3 family, one sequence to the Kinesin-9 family, seven sequences to the Kinesin-13 family and two sequences to the Kinesin-14 family. Members of the Kinesin-13 family are microtubule depolymerisers playing a role in mediating the mitotic spindle and in chromosome segregation. Examination of the neck domain and a detailed phylogenetic analysis suggests that the Kinesin-13 family may be comprised of several subfamilies. Furthermore, several protozoan Kinesin-13 family members were found to lack the neck domain suggesting that these “neckless” Kinesin-13 members may constitute a subgroup within the Kinesin-13 family with a potentially unique functionality.

2.2 Introduction

Inside a eukaryotic cell a variety of organelles are constantly transported to various destinations. These movements are achieved through a complex network of microtubules and actin filaments which span the entire cell. On the microtubule tracks, two types of molecular motors, called kinesins and dyneins play a major role in maintaining these microtubule networks and powering the movement of these organelles to their destinations.

Data mining from the trypanosome genome database (<http://www.genedb.org/genedb/tryp/>) has revealed that the trypanosome genome contains 47 kinesin genes. It is likely that a small proportion of these kinesin genes play a role in mitosis, as it has been shown that at least 25% of all kinesins coded in the genome of *Drosophila* (Goshima and Vale, 2003) and man (Zhu et al., 2005) have mitotic functions. As majority of the kinesins coded by the trypanosome genome might not have mitotic functions, a method of identifying kinesin candidates likely to play a role in chromosome segregation is therefore necessary.

Since the discovery of the first kinesin in 1982, more than 600 kinesins have been identified (Goodson et al., 1994; Miki et al., 2005). As more kinesins are characterised, inconsistencies regarding the functional classification according to the location of motor domains have been found. A good example would be the discovery of kinesins with motor domain located at the N-terminus of the polypeptide chain, capable of exhibiting depolymerisation activities similar to Kin-I kinesins (Ogawa et al., 2004; Ovechkina and Wordeman, 2003). To overcome this, kinesins are now classified based on the phylogenetic or ancestral relationship of its motor domain. There are currently 14 kinesin families (Table 2.1) (Lawrence et al., 2004; Miki et al., 2005) where; Kinesin-1 to Kinesin-12 are Kin-N, Kinesin-13 represents Kin-I and Kinesin-14 represents Kin-C. Kinesins within the same family are found likely to share similar characteristics and cellular functions (Goodson et al., 1994; Hirokawa, 1998; Lawrence et al., 2002), meaning that functional prediction based on the kinesin phylogeny should be possible to a certain extent.

Only the motor domain of the kinesin sequences is used in the construction of the phylogenetic trees. Kinesin tails are excluded, as they are extremely divergent, sometimes within the same kinesin family complicating any meaningful interpretations of such

alignments. In addition, some kinesin families contain specific motifs within the motor domain and outside the motor domain which can be used in family classifications (Hertzer et al., 2003; Lawrence et al., 2004; Westerholm-Parvinen et al., 2000).

Table 2.1: Summary of all 14 accepted kinesin families which describe family specific motifs, microtubule motility/action and their known function.

Kinesin family	Family specific motifs	Microtubule action	Functions
Kinesin-1	N/A	Plus-end directed	<ul style="list-style-type: none"> • Organelle transport (Brady et al., 1990) • Nuclear migration in postmitotic cells (Holzinger and Lutz-Meindl, 2002)
Kinesin-2	N/A	Plus-end directed	<ul style="list-style-type: none"> • Organelle transport (Setou et al., 2000) • Intraflagellar transport (Rosenbaum and Witman, 2002; Yamazaki et al., 1995)
Kinesin-3	Forkhead-associated (FHA) domain (Vale, 2003)	Plus-end directed	<ul style="list-style-type: none"> • Organelle transport (Nangaku et al., 1994; Okada et al., 1995)
Kinesin-4	N/A	Plus-end directed	<ul style="list-style-type: none"> • Chromosome congression (Wang and Adler, 1995) • Organelle transport (Sekine et al., 1994)
Kinesin-5	BimC box domain (Miki et al., 2005)	Plus-end directed	<ul style="list-style-type: none"> • Bipolar spindle formation and spindle elongation (Asada et al., 1997; Enos and Morris, 1990; Hoyt et al., 1992; Saunders et al., 1997; Sawin et al., 1992)
Kinesin-6	N/A	Plus-end directed	<ul style="list-style-type: none"> • Cleavage furrow formation during cytokinesis (Adams et al., 1998; Hill et al., 2000) • Microtubule sliding (Nislow et al., 1992)
Kinesin-7	N/A	Plus-end directed	<ul style="list-style-type: none"> • Chromosome congression and kinetochore microtubule capture (Kapoor et al., 2006; Weaver et al., 2003; Wood et al., 1997; Yen et al., 1992) • Nuclear migration (Miller et al., 1998)
Kinesin-8	N/A	Plus-end directed and microtubule depolymeriser	<ul style="list-style-type: none"> • Chromosome segregation (Gupta et al., 2006; Savoian et al., 2004; West et al., 2002) • Mitochondrial transport (Pereira et al., 1997)
Kinesin-9	N/A	N/A	<ul style="list-style-type: none"> • Flagellar motility (Yokoyama et al., 2004)
Kinesin-10	Helix-hairpin-Helix (HhH) motif (Miki et al., 2005)	Plus-end directed	<ul style="list-style-type: none"> • Chromosome congression and movement (Antonio et al., 2000; Funabiki and Murray, 2000; Tokai et al., 1996)
Kinesin-11	N/A	N/A	<ul style="list-style-type: none"> • Signal transduction (Wolf et al., 1998)
Kinesin-12	N/A	N/A	<ul style="list-style-type: none"> • N/A
Kinesin-13	N/A	Microtubule depolymeriser	<ul style="list-style-type: none"> • Bipolar spindle formation (Boleti et al., 1996; Cassimeris and Morabito, 2004; Kline-Smith and Walczak, 2002; Manning et al., 2007) • Chromosome segregation (Rogers et al., 2004) • Proper kinetochore-MT association (Kline-Smith et al., 2004; Manning et al., 2007)
Kinesin-14	N/A	Minus-end directed	<ul style="list-style-type: none"> • Bipolar spindle formation (Chen et al., 2002; Marcus et al., 2003) • Organelle transport (Hanlon et al., 1997; Saito et al., 1997; Xu et al., 2002)

2.3 Materials and Methods

2.3.1 Trypanosome kinesin sequence retrieval

The full-length kinesin genes and corresponding protein sequences were obtained from the *T. brucei* gene database, <http://www.genedb.org/genedb/tryp/>. Data mining from the *T. brucei* gene database resulted in the retrieval of 47 sequences. These genes were identified as kinesins by the presence of a kinesin motor domain predicted by protein databases (Pfam, InterPro, PRINTS, PROSITE and SMART) using the translated protein sequence of the coding strand of these putative gene. A naming scheme was adopted in no particular order for each of the corresponding kinesin genes (Table 2.2). The kinesin genes were named “TbKif###” where “Tb” stands for “*Trypanosoma brucei*”, the acronym “Kif” denotes “Kinesin superfamily” and “###” corresponds to the Arabic numeral from 1 to 47. Of these 47 kinesin sequences, 46 sequences appear to be full length proteins while 1 of these kinesin sequence (TbKif43/Tb927.7.3840) is a kinesin fragment containing only part of the kinesin motor domain which is unlikely to code for a functional protein.

Table 2.2: Table showing the naming scheme adopted for the Trypanosome kinesin genes. (a.a., amino acids)

Assigned Name	Systematic Name	Located in chromosome	Predicted length (a.a.)	First 10 a.a. sequence
TbKif1	Tb927.7.3000	7	1342	MTSQTSAVLV
TbKif2	Tb11.02.2260	11	690	MTSLCPITSS
TbKif3	Tb927.3.2020	3	746	MSNIKVAVRC
TbKif4	Tb11.01.0850	11	669	MQRLAGKRQR
TbKif5	Tb927.7.5650	7	638	MAEKVQVVS
TbKif6	Tb11.01.3990	11	916	MENIRVVVRV
TbKif7	Tb927.3.3390	3	591	MHDSVGTGTR
TbKif8	Tb11.02.0790	11	719	MERQLRELLE
TbKif9	Tb927.4.3910	4	787	MQDEQHEELP
TbKif10	Tb10.70.6990	10	1798	MAIEYPDNGY
TbKif11	Tb927.3.4960	3	1594	MSMHRDLLRI
TbKif12	Tb11.02.0090	11	1572	MSKPRDAEEG
TbKif13	Tb10.61.0990	10	1682	MVRLDPSAST
TbKif14	Tb927.6.4390	6	1111	MSDADVKEGT
TbKif15	Tb09.211.1400	9	482	MPNIPLVAEL
TbKif16	Tb927.5.2410	5	1339	MSKAAVSRPR
TbKif17	Tb927.8.4950	8	1456	MEYKRCNSSR
TbKif18	Tb927.7.6290	7	891	MRSQVRVIIR
TbKif19	Tb927.4.2730	4	803	MTTSLDSTA
TbKif20	Tb927.7.3830	7	1803	MISNIRRAGE
TbKif21	Tb10.61.1750	10	820	MSVEQPEQQI
TbKif22	Tb927.7.7120	7	810	MNGIHLNSTI
TbKif23	Tb927.7.4830	7	516	MEHIGAFLRV
TbKif24	Tb10.70.7260	10	2889	MLHKPCVQVV
TbKif25	Tb927.8.6830	8	1819	MRRGANTTDD
TbKif26	Tb927.1.1350	1	886	MQTSRPSADN
TbKif27	Tb11.02.2970	11	566	MNNSRICVAV
TbKif28	Tb927.3.3400	3	578	MHDSVGTGTR
TbKif29	Tb11.02.0400	11	862	MSIEVHVRIR
TbKif30	Tb09.244.2560	9	681	MADMKKVTVA
TbKif31	Tb927.7.4110	7	894	MSERETTSHS
TbKif32	Tb10.389.1210	10	1132	MMSSSSSAQV
TbKif33	Tb927.8.4840	8	1014	MVNSSALVSV
TbKif34	Tb11.02.4260	11	986	MGGEDNVARR
TbKif35	Tb927.6.1770	6	628	MAKPLSGKAA
TbKif36	Tb927.6.2880	6	1085	MNVRVATAVR
TbKif37	Tb927.8.2630	8	750	MRTNEERDDK
TbKif38	Tb10.61.1020	10	1095	MCDRLNTMSI
TbKif39	Tb11.01.2530	11	617	MQADTFAYAR
TbKif40	Tb927.7.7260	7	1041	MGKSEGIRVF
TbKif41	Tb11.01.5490	11	1115	MGSSVTVCCL
TbKif42	Tb10.389.1270	10	832	MSGIYAISIP
TbKif43	Tb927.7.3840	7	53	MHAFNGYNCS
TbKif44	Tb927.3.2040	3	1072	MNTSACFTGS
TbKif45	Tb09.160.2260	9	691	MAKWEKLVSV
TbKif46	Tb927.5.2090	5	1088	MGKKTNSAAE
TbKif47	Tb927.8.8350	8	786	MQKSIQDEV

2.3.2 Phylogenetic analysis and classification of trypanosome kinesins

The motor domains of the trypanosomes sequences were extracted by submitting these kinesin sequences for analysis using the SMART database, http://smart.embl-heidelberg.de/smart/set_mode.cgi?NORMAL=1 (Letunic et al., 2006; Schultz et al., 1998). The motor domain of these kinesin sequences were aligned against a representative selection of kinesin motor domain sequences which include members from all the kinesin families using Clustal X1.81, <http://bips.u-strasbg.fr/fr/Documentation/ClustalX/> (Thompson et al., 1997). A Neighbour-Joining tree (Saitou and Nei, 1987) was then created using Clustal X1.81 and drawn using MEGA 4, <http://www.megasoftware.net/> (Tamura et al., 2007). Statistical support for the resulting neighbour-joining tree was provided by the use of bootstrap resampling (1,000 replicates) on the alignments used to create the phylogenetic tree in Clustal X1.81. No manual sequence editing was performed on the alignments during the construction of the phylogenetic tree.

2.4 Results

2.4.1 Phylogenetic analysis

A phylogenetic tree was created using the protein sequence alignments of the motor domains of 99 kinesins (Figure 2.1). Of the 99 sequences, 43 were kinesin sequences representative of the 14 established kinesin families. The number of kinesin motor proteins was limited to 99 sequences as larger datasets would take an extremely large amount of time to process. The tree constructed is in agreement with the phylogenetic results from earlier studies (Hirokawa and Takemura, 2004; Kim and Endow, 2000; Kollmar and Glockner, 2003; Lawrence et al., 2002; Miki et al., 2005; Miki et al., 2001; Wickstead and Gull, 2006) as majority of the kinesins from known families do group together, except for LdKIN and ScSMY1p.

ScSMY1p is a kinesin from the yeast *Saccharomyces cerevisiae* and is part of the kinesin-11 family known for its highly divergent catalytic core when compared to other families (Miki et al., 2005). It is likely that due to its highly divergent catalytic core and the use of a small dataset of only three related sequences was insufficient in resolving the phylogeny of ScSMY1p.

LdKIN is a kinesin from the protozoan *Leishmania donovani*. An examination on the protein sequence of LdKIN revealed that LdKIN does not contain the forkhead-associated (FHA) domain C-terminus to its motor domain (Figure 2.2). This FHA domain is characteristic of all kinesin-3 family members (Miki et al., 2005; Vale, 2003). The lack of this FHA domain coupled with the outgrouping of LdKIN in the phylogenetic tree strongly suggests that LdKIN is unlikely to be a member of the kinesin-3 family.

Based on this phylogenetic analysis, only 14 out of 46 trypanosome kinesins grouped with other established kinesin families (Table 2.3). Of the 14 kinesins classified, 12 of the kinesins classifications were in agreement with recent published phylogenetic data (Wickstead and Gull, 2006). In addition, 2 more trypanosome kinesin sequences (TbKif15 and TbKif47), which were not included in a previous analysis (Wickstead and Gull, 2006), were shown to be grouped into the Kinesin-13 family.

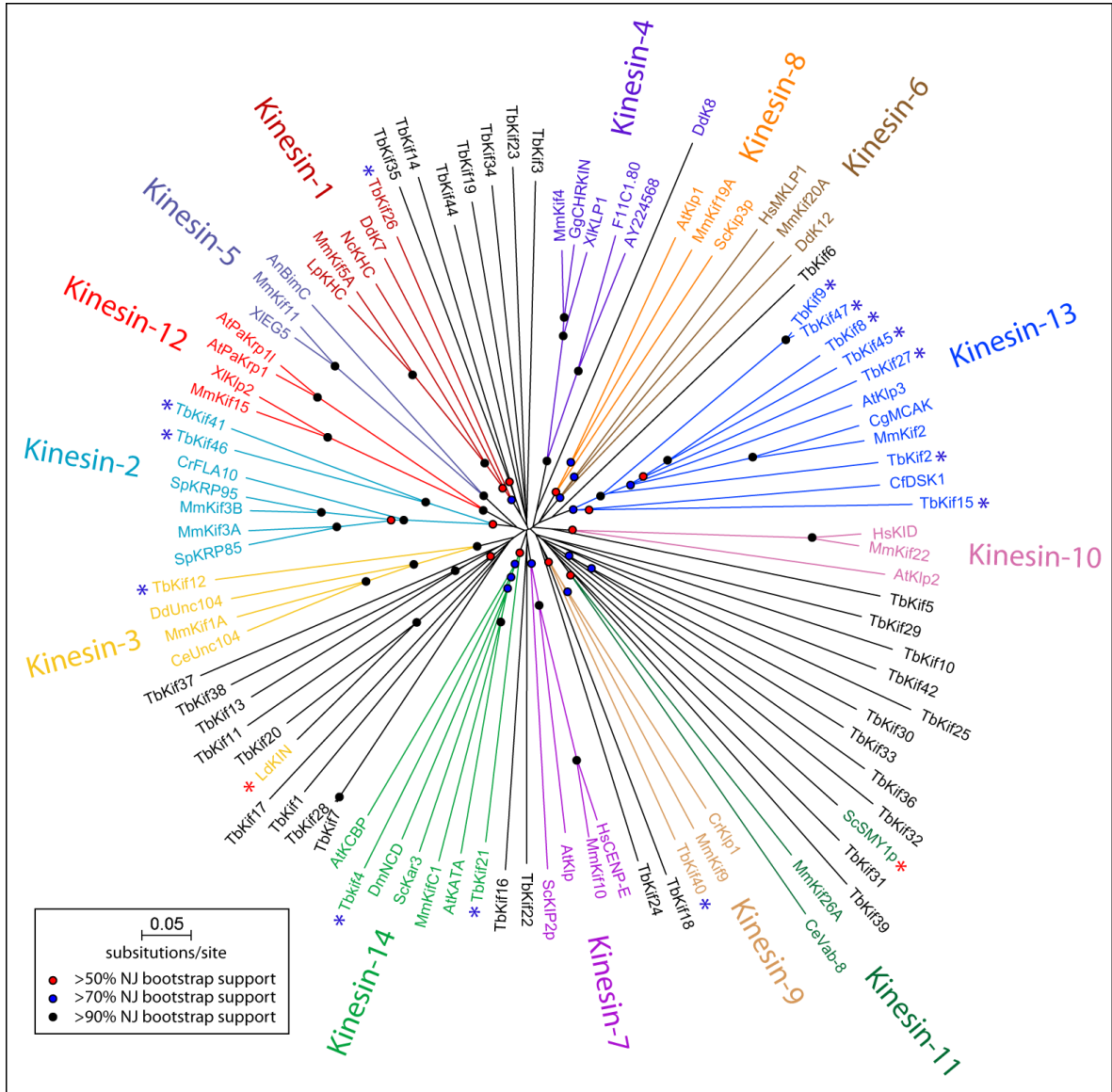


Figure 2.1: Phylogenetic analysis of trypanosome kinesins. An unrooted neighbour-joining tree constructed from the alignment of motor domain kinesin sequences including 46 trypanosome kinesins. The sequences denoted by (*) are trypanosome kinesin sequences that are grouped to known kinesin families, (*) are kinesin sequences that were found not to group within their expected families. The kinesin sequences used in the phylogenetic construction of this are listed in Table S 5.1 and Table 2.2.

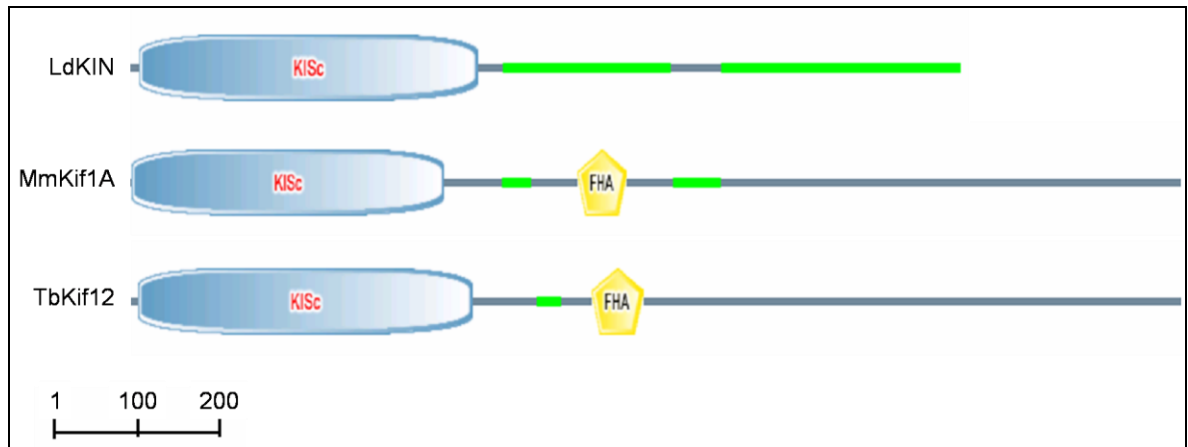


Figure 2.2: Results of a structure and domain analysis from SMART of MmKif1A which is a member of the Kinesin-3 family, TbKif12 which is a trypanosome kinesin classified in the kinesin-3 family and LdKIN, a kinesin likely to be wrongly classified into the kinesin-3 family. The bar represents 200 amino acids in length, (■) represents predicted coil-coil regions and (FHA) is the FHA domain which is found in all kinesin-3 family members.

Table 2.3: A list of trypanosome kinesins identified as members of established kinesin families. The compilation is based on our own analysis and published data. The sequences highlighted in yellow are trypanosome sequences that have been previously classified into their respective kinesin families (Wickstead and Gull, 2006).

Kinesin Family	Kinesin Name
Kinesin-1	TbKif26
Kinesin-2	TbKif41
	TbKif46
Kinesin-3	TbKif12
Kinesin-9	TbKif40
Kinesin-13	TbKif2
	TbKif8
	TbKif9
	TbKif15
	TbKif27
	TbKif45
	TbKif47
Kinesin-14	TbKif4
	TbKif21

2.4.2 Identification of putative mitotic kinesins in trypanosomes

The trypanosome kinesins classified as Kinesin-1, Kinesin-2, Kinesin-3 are unlikely to perform any mitotic functions as members characterised from these families thus far are involved in intracellular and intraflagellar transport of various organelles (Miki et al., 2005; Vale, 2003; Wickstead and Gull, 2006). Only a single member from the Kinesin-9 family have been characterised thus far. CrKlp1, a Kinesin-9 family member from the protozoan *Chlamydomonas reinhardtii*, was localised to the flagellum and found to play a role in flagellar motility (Bernstein et al., 1994; Yokoyama et al., 2004). Based on published data, it is likely that members of the Kinesin-9 family do not harbour any mitotic functions (Bernstein et al., 1994; Miki et al., 2005).

Members of the Kinesin-14 family have been implicated in the retrograde (towards the minus end of microtubules) transport of vesicles and organelles (Miki et al., 2005). However, there are several reports indicating that some members of the Kinesin-14 family in plants and in yeast have mitotic functions (Bowser and Reddy, 1997; Grishchuk and McIntosh, 2006; Meluh and Rose, 1990; Vos et al., 2000). CrKCBP, a protozoan Kinesin-14 member from *Chlamydomonas reinhardtii* was reported to have a cell cycle dependent nuclear localisation (Dymek et al., 2006). CrKCBP localises preferentially to the base of the two flagella during interphase, but during mitosis it localised to the spindle poles suggesting that CrKCBP has multiple functions including mitotic functions. Within this kinesin family, two trypanosome sequences are present, TbKif21 and TbKif4. TbKif21 was previously characterised and is implicated with the normal function and maintenance of acidocalcisomes in procyclic cells (Dutoya et al., 2001). TbKif4 has yet to be functionally characterised and based on previous publications, TbKif4 may harbour mitotic functions.

Members of the Kinesin-13 family are of particular interest as majority of the characterised members of this family were previously shown to have mitotic functions.

2.4.3 Trypanosome Kinesin-13 proteins

Kinesin-13 family members are microtubule depolymerisers (Desai et al., 1999; Hertzler et al., 2003; Maney et al., 2001; Shipley et al., 2004) and they play a major role in the regulation of microtubule dynamics throughout mitosis. Members of the Kinesin-13 family preferentially localise to the spindle poles and kinetochore of chromosomes (Manning et al., 2007; Ohi et al., 2007; Rogers et al., 2004; Wordeman and Mitchison, 1995). Kinesin-13 proteins have been implicated in the segregation of chromosomes (Ganem et al., 2005; Maney et al., 1998; Rogers et al., 2004), regulating spindle bipolarity and assembly (Manning et al., 2007; Ohi et al., 2007; Walczak et al., 1996), and promote proper microtubule-kinetochore attachments during metaphase (Kline-Smith et al., 2004). Protozoan members of this kinesin family have also been previously characterised in *Leishmania major* (Dubessay et al., 2006) and *Giardia intestinalis* (Dawson et al., 2007) where they were shown to have nuclear localisations suggesting that the mitotic functions of Kinesin-13 members are evolutionarily conserved across kingdoms.

Based on the phylogenetic tree constructed (Figure 2.1 and Figure 2.5), The *T. brucei* genome was found to possess seven Kinesin-13 family genes. The motor domain of the trypanosome Kinesin-13 members was examined for the presence of the conserved KEC and KVD motifs which is specific to the Kinesin-13 family (Hertzler et al., 2003; Ogawa et al., 2004) (Figure 2.3). Both the KEC and KVD motifs play an essential role in microtubule binding and depolymerisation in the Kinesin-13 family proteins (Dubessay et al., 2006; Ogawa et al., 2004; Shipley et al., 2004). Protein sequence alignments of the motor domain of trypanosome Kinesin-13 family members were all shown to contain the KEC motif. In contrast, the KVD motif in trypanosome Kinesin-13 family members was observed to have single amino acid substitutions where; the lysine (K) residue was replaced by an arginine (R) residue (in TbKif2, TbKif9 and TbKif47) or the valine (V) residue was replaced by a tyrosine (Y) residue (in TbKif27).

The neck domain of the Kinesin-13 family members was also examined (Figure 2.4). Previous publications have shown that the protein sequence of the Kinesin-13 neck domain is rich in basic residues lysine (L) and arginine (R) (Ogawa et al., 2004). The presence of highly basic sequences in the neck region provides the positive net charge which is

important for Kinesin-13 microtubule depolymerisation activity *in vivo* (Ovechkina et al., 2002). Examination of the neck domain on the trypanosome Kinesin-13 members revealed that TbKif45 does not possess a positively charged neck domain and its (isoelectric point) pI value was calculated to be 4.61. When the neck domain of other Kinesin-13 family members were examined (Figure 2.4 and Figure 2.5), several members from the Kif24 subfamily were also found to exhibit similar low pI values. In addition, some of the trypanosome Kinesin-13 members (TbKif2 and TbKif27) lacked a neck domain (Figure 2.4). This feature was also found on several other Kinesin-13 family members of protozoan origin.

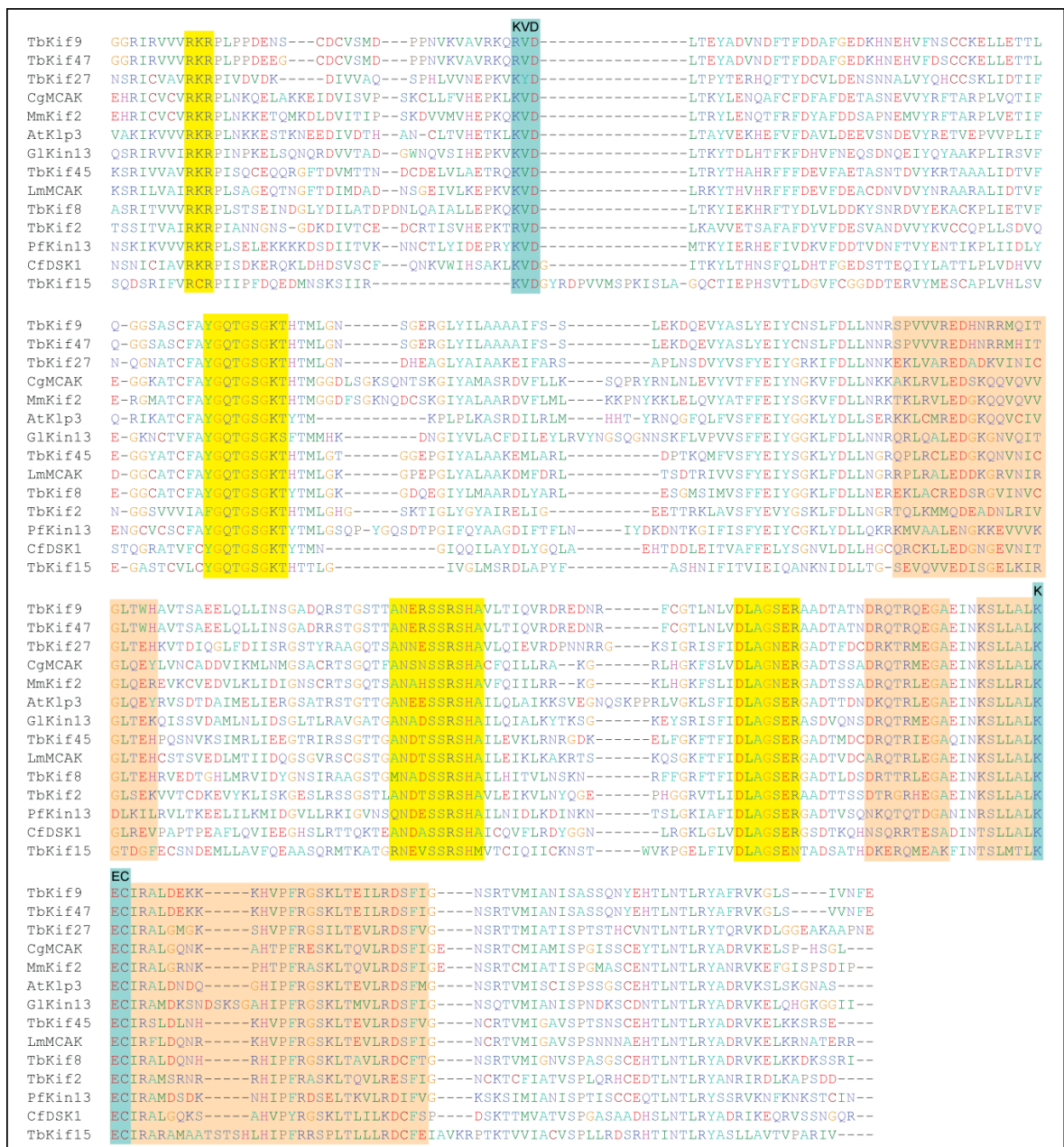


Figure 2.3: Sequence alignment of the motor domain of known and putative Kinesin-13 proteins. The sequences highlighted in yellow are ATP binding motifs and sequences shaded in orange are microtubule binding motifs as described in the papers (Hertzer et al., 2003; Kikkawa et al., 2000). The sequence highlighted in blue are Kinesin-13 family specific motifs. Details of the kinesin sequences used in this alignment can be found in Table S 5.2.

	Neck Domain	Motor Domain	pI
MmKif2A	KKEFGPPSRRRKSNVCVEKLEKLEKRRRLQOQELREKRAQ--DVDATNPNYEMCMIRDFRGS-----LDYRLTADPI--DEHRI ^{CV} CVRRKRLNKK		10.02
CgMCAK	-----ARRKSCIVKEKEMKMKKEKRAQNSEIRIKRAQ--EYDSSFNWEFARMIKEFRVT-----IECHFLTLTDPF--EEHRI ^{CV} CVRRKRLNKK		10.16
FrKif2C	-----FLTSTHIMRSRRTMSQRGLHHLQSK--FGEASRPNQKPYEMIQDFRET-----LEVIPLSSNSV--EPRRI ^{CV} CVRRKRLNKK		10.61
XlXKCM1	-----QGRRKSNIVKEMKMKKKEEQAQNYERRMKAQ--DYDTSVPNWEEFGMIKEFRAT-----MDCHRISMADPA--EEHRI ^{CV} CVRRKRLNKK		10.47
NtTBK10	-----LDTLELLPEFVAGLYDAPSMHHEGRAKSFDD--EQFLANNKQTGRVRLGLESNV-----SKSFADVKEKAS--NVAKIKVVVRN ^E PLNKK		5.64
OsP0006C01.8	-----ELISDFQVPGICM ^Y DGAQKFGYGGGDD--SDFEAPNKQMSKSTVFAESN-----FLKAFPEKEKAA--PVAKIKVVVRN ^E PLNKK		4.33
AtMGL6.9	-----AGLLDLHAMDDTELLSEHVITEPEFEPFMPGSVNK--EFEDDYNLAAARQORQTEAEP-----LGLLEPKSKDENN--SVAKIKVVVRN ^E PLNKK		4.01
DmK1p59D	SQGGNNSQRFSSVREVNRMKEQEKRRRAREQLQEKDALRRNPNW ^E YSVMLRQYRST-----LIFSLRCLDPNGGTQQITV ^{CV} RRKRLNKK		11.63
AgK1p10A	-----SIPKSSCVTVGMMEEENRIKQDMFKVMREKKNALMNQDGGNPNW ^E FINMIREYQST-----IDFRIVQGGSI--DQHQITV ^{CV} RRKRLNKK		9.96
TbKif45	-----LLVPPILPSTSLPPPMEAAATGAVGDSDDILDEKVKERQYTRGTLMLMRTDDSR-----EYKRRKRSRVVAVRRKRLPISQC		4.61
CeKlp7	-----APPIANM ^T SQRAPSPVARVPSPKNVPRSPQQDVQSPNGNFAPFAMIRNYRAQ-----IDYRPLSMFDGV--NENRISV ^{CV} RRKRLNKK		10.26
TbKif8	-----NARMNESQLSGAGRRDPLHVIDDMELSAMKMTNSRPLSRVARASPTAATR-----KPGESGITTKRKASRITVVVRRKRLPST		12.00
GKlin13	-----MSLYEYDGGYEPYVSAQGGSPANGDDYVPTIYHFNAPNPNPRGIPVWRT-----VVPVVDLFLNQIQSRIRVVIRKRLPINPK		4.04
TbKif9	-----RCATSVTRPYOSKQETPCSSRVFPGRASERPIASPSSIAANMDSVTPAAVTEDP-----QADGKQCAIMRTRGGIRVVVRRKRLPFPD		8.51
TbKif47	TRRGASFAFPYPNKPGTPOSRA ^P PRRASARPIASPSPLAAPLHRADSVI ^{PA} AAVAED-----SSADGKQSAVARTGGIRVVVRRKRLPFPD		12.22
EcECU11_0470	-----SLAEKSGAMFGSEETISQKLSICSMPRKNSPKSLIGLDGIDIDGSKLTHGACN---ESLLTSSDTGGLVKEE ^{KIVV} CVRRKRLPFPD		7.25
MmKif24	-----LQKIDELAKVTMKDYSR ^L GVHDMNDRKRLFQLIKIKIMQEE ^D KALG-----IPEHPLQASSIYTKPREFRSGPRRLHFD		9.03
CfDSK1	-----MKIEQMEKERKERRKMTMQRKEARKQEHMKNIEAGNPGD ^V DFIGLVEEWRREQE---NKIGDKSPSPSLFAS ^{TNS} NICIAVRRKRLPISDK		9.91
TbKif15	-----MPNIFLVAELG ^{TK} CAEFORLLNTSEVPEVVKKLRPSMDPKELFTSQDSR-----I ^{FV} RCRPIIPF		8.53
PfKin13	-----MFKKTMQQRQSF ^T KNKVMDBERKKKKKNNSMCI ^{NN} LIGSNMCS ^{EV} YYPQKSVN-----LGNKIKVRSKTMNSKIKVVVRRKRLPSEL		11.19
TbKif27	-----MNSR ^{IC} CVAVRRKRLPVD-----		N/A
TbKif2	-----MTSL ^{CP} ITSSITVAIRKRLPIANN-----		N/A

Figure 2.4: The sequence alignment of the neck domain of several Kinesin-13 family members. The region highlighted in blue is the neck domain while the region highlighted in yellow represents part of the motor domain (Ogawa et al., 2004). The panel on the left represents the calculated isoelectric point (pI) of the neck domain. Details of the kinesin sequences used in this alignment can be found in Table S 5.3.

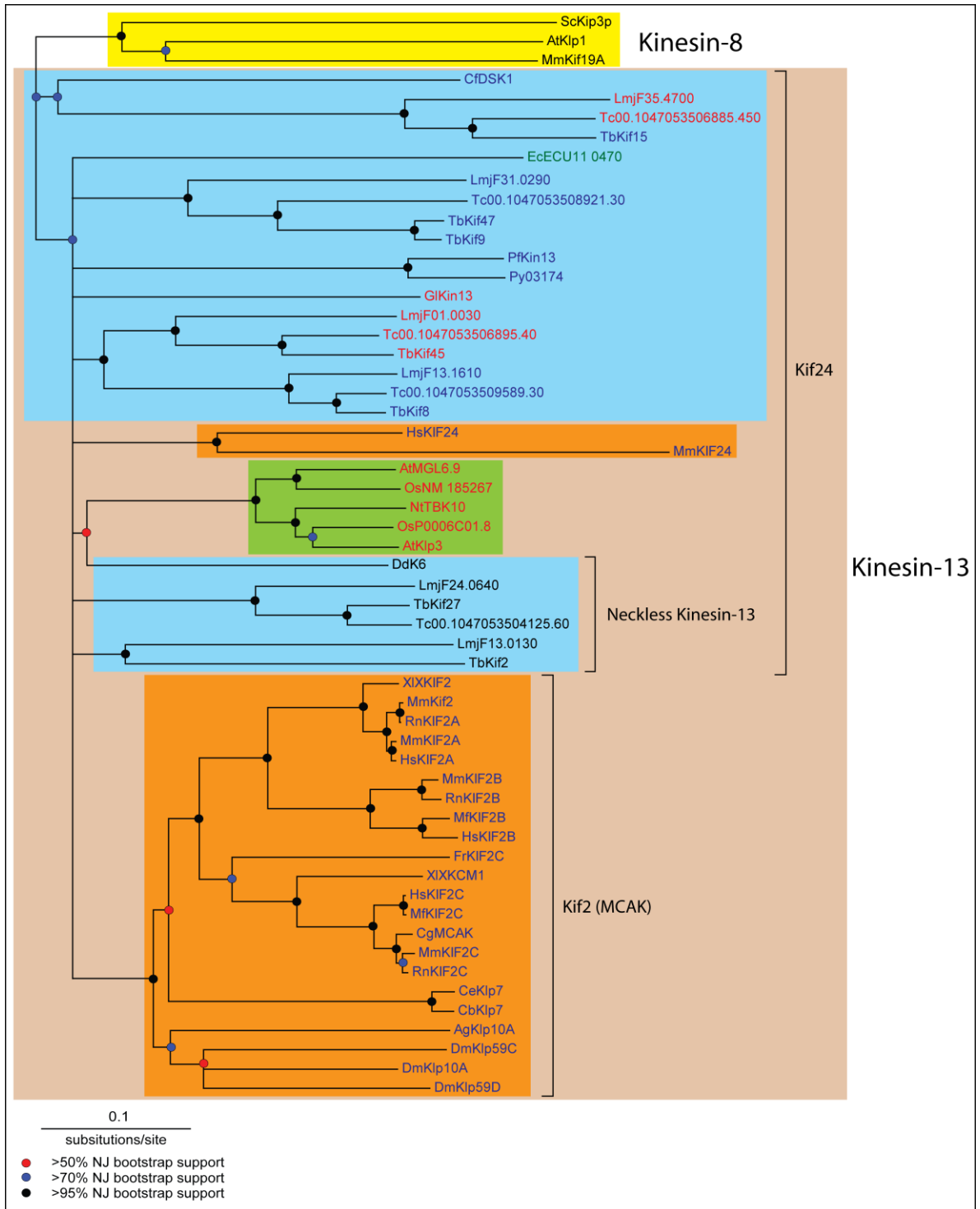


Figure 2.5: A neighbour-joining tree of the Kinesin-13 family proteins. Only nodes which have more than 50% bootstrap support are shown. This tree is arbitrarily rooted by the Kinesin-8 family members ScKip3p, AtKlp1 and MmKif19A (yellow box). According to previous publications, the Kinesin-13 family (brown box) is divided into 2 subclasses; the Kif2 (Mitotic Centromeric Associated Kinesin, MCAK) and the Kif24 subfamily (Miki et al., 2005; Ogawa et al., 2004). The sequences contained in the blue box represent protozoan kinesins, the green box representing plant kinesins while the orange box represents kinesins from the metazoan kingdom. The Kinesin-13 family members were also colour coded according to the isoelectric point (pI) of its neck region. The sequences labelled in blue represents a pI value of more than 8, green represents a pI value of between 6 and 8 and red represents a pI value of below 6. Kinesins where the neck domain is absent are labelled as “neckless Kinesin-13” members. The details of the kinesin sequences used in this phylogenetic tree can be found in Table 2.2 and Table S 5.3.

2.5 Discussion

The search for kinesin sequences likely to contain mitotic functions using phylogenetic analysis has yielded several candidates from two kinesin families; Kinesin-13 (seven kinesin sequences) and Kinesin-14 (one kinesin sequence). Of the two kinesin families, candidates from the Kinesin-13 family appear to be more promising candidates as majority of the kinesins characterised from this family were shown to possess mitotic functions. In addition, a *Leishmania* Kinesin-13 member was shown to have a nuclear localisation (Dubessay et al., 2006); therefore it is likely that its trypanosome homologue would share a similar characteristic. The trypanosome codes for a relatively large number of Kinesin-13 family members when compared with most organisms studied thus far. This includes humans who contain only four Kinesin-13 members (Miki et al., 2005; Miki et al., 2001). This expanded kinesin family in trypanosomes could mean that Kinesin-13 family in trypanosomes may harbour other functions which are yet to be characterised.

Phylogenetic analysis based on motor domain alignments of Kinesin-13 family members from several eukaryotic kingdoms (Figure 2.5) has revealed that there are potentially more than two Kinesin-13 subfamilies. While the Kif2 (MCAK) subfamily was shown to be well supported with high bootstrap values, the phylogenetic relationship of members from the Kif24 subfamily was not well resolved. Furthermore, examination of the Kinesin-13 neck domains of the Kif24 subfamily revealed that, not all Kinesin-13 family members possess a positively charged neck domain. Previous structural studies on the Kinesin-13 family members have shown that while the motor domain is capable of performing microtubule depolymerisation (Shipley et al., 2004), the neck domain is

important for full microtubule depolymerisation activity *in vivo* (Ems-McClung et al., 2007; Hertzler et al., 2003; Maney et al., 2001; Moores et al., 2006; Ogawa et al., 2004; Ovechkina et al., 2002). In addition, the single amino acid substitutions in the KVD motif observed in TbKif2, TbKif9, TbKif47 and TbKif27 could potentially perturb its microtubule depolymerising ability as the KVD motif is essential for microtubule depolymerisation (Ogawa et al., 2004; Shipley et al., 2004). This could mean that some of the Kinesin-13 family members have a functionally different role where efficient microtubule depolymerisation is not essential.

Kinesins are among the largest protein families found in the trypanosome genome (Berriman et al., 2005) and interestingly, the ratio of kinesin to total protein coding genes is the largest of all eukaryotic genomes surveyed thus far (Table 2.4). This may reflect upon the cellular biology of trypanosomes which possess a complex vesicular transport system (Overath and Engstler, 2004) and a microtubule based cytoskeleton (Kohl and Gull, 1998). The absence of trypanosome kinesin members in 8 out of 14 established families indicate that much is still unknown about the kinesins of protozoan origin. This is was illustrated in a recent phylogenetic analysis using complete kinesin repertoires from organisms belonging to several eukaryotic kingdoms resulting in the proposal of three new kinesin families (Wickstead and Gull, 2006). As more kinesins are discovered within the protists kingdom, these ungrouped kinesin sequences may become founding members of novel kinesin families.

Table 2.4: Table showing total amount of non-redundant kinesin encoding genes found in each species, the estimated number of all protein coding genes they have and the ratio of kinesin genes to total number of genes represented in percentage.

Species	Total number of kinesins	Estimated total number of genes	Kinesin to total gene ratio (%)	Reference
<i>Homo Sapiens</i>	45	22,287	0.202	(Miki et al., 2001)
<i>Drosophila melanogaster</i>	25	13,600	0.184	(Goshima and Vale, 2003)
<i>Saccharomyces cerevisiae</i>	6	6,000	0.100	(Hildebrandt and Hoyt, 2000)
<i>Caenorhabditis elegans</i>	21	19,000	0.111	(Siddiqui, 2002)
<i>Arabidopsis thaliana</i>	61	25,498	0.239	(Reddy and Day, 2001)
<i>Trypanosoma brucei</i>	46	8,100	0.568	(Berriman et al., 2005)
<i>Plasmodium falciparum</i>	9	5,300	0.170	(Gardner et al., 2002)
<i>Giardia lamblia</i>	30	6,500	0.462	(Morrison et al., 2007)
<i>Entamoeba histolytica</i>	6	9,938	0.060	(Loftus et al., 2005)

3 The biological characterisation of the Kinesin-13 family in *Trypanosoma brucei*

3.1 Abstract

Members of the Kinesin-13 family are microtubule depolymerisers and most members characterised so far play an important role in mediating the mitotic spindle during mitosis. This report describes the localisation and characterisation of six of the seven *T. brucei* Kinesin-13 family members. Of the six kinesins only one was found to be localised to the nucleus while the rest of the kinesins were localised to cell body, mitochondrion or flagellum. The RNAi induced protein depletion in three of the six kinesins resulted in a mild growth defect although no gross changes in cellular morphology was observed. The discrete localisations observed by the Kinesin-13 family members to various structures in the trypanosome suggest that the functional diversity of this family is greater than previously thought.

3.2 Introduction

The Kinesin-13 family constitutes one of the 14 established kinesin families and exhibits the ability to depolymerise microtubules, a property shared by the Kinesin-8 and part of the Kinesin-14 family (Ovechkina and Wordeman, 2003). However, unlike the Kinesin-8 and Kinesin-14 families, members of the Kinesin-13 family do not exhibit microtubule processivity and preferentially associate to microtubule ends where they promote the destabilisation of the microtubule complex (Desai et al., 1999; Hertzler et al., 2003). It is well established that the Kinesin-13 family harbour mitotic functions where they play an important role in regulating the microtubule turnover of mitotic spindle (Figure 3.1) (Kline-Smith et al., 2004; Maney et al., 1998; Manning et al., 2007; Ohi et al., 2007; Rogers et al., 2004; Walczak et al., 1996; Wordeman and Mitchison, 1995).

However, there have been reports that some members of the Kinesin-13 family do have non-mitotic functions. In mice, it was found that a member of the Kinesin-13 family; MmKIF2A, in addition to its role in mitosis was found to be involved in the proper development of neuronal axons in the brain (Ganem and Compton, 2004; Homma et al., 2003). In the plant *Arabidopsis thaliana*, a Kinesin-13 family member; AtKinesin-13A/AtMGL6.9 was found to be exclusively non-mitotic and it was involved in the organisation of Golgi stacks (Lu et al., 2005; Vanstraelen et al., 2006). These findings suggest that the Kinesin-13 family members are not limited only to mitotic roles.

Based on phylogenetic analysis and family specific motif searches (refer Chapter 2.4.1 and Chapter 2.4.3), seven of the 46 kinesin genes coded by the trypanosome genome were grouped into the Kinesin-13 family. Six of the seven Kinesin-13 genes (*TbKif2*, *TbKif8*, *TbKif9*, *TbKif15* and *TbKif45*) were targeted for further analysis. In this study, *TbKif47* was not included as this gene was only later identified as member of the Kinesin-13 family and added into the database.

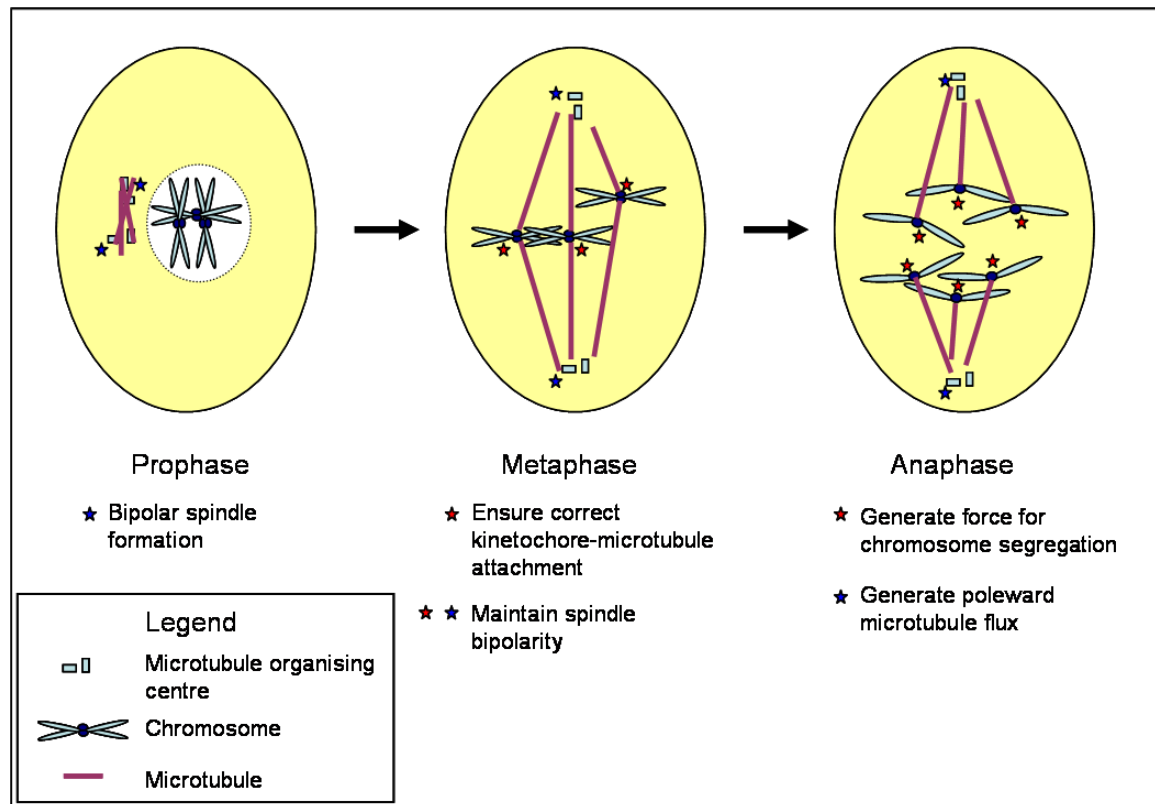


Figure 3.1: A summary of known Kinesin-13 functions during mitosis (Kline-Smith et al., 2004; Maney et al., 1998; Manning et al., 2007; Ohi et al., 2007; Rogers et al., 2004; Walczak et al., 1996; Wordeman and Mitchison, 1995). The blue star marks the microtubule ends located at the microtubule organising centre while the red star marks the kinetochore. Members of the Kinesin-13 family have been shown to associate to both locations of the mitotic spindle throughout the various stages of mitosis.

3.3 Materials and methods

3.3.1 Trypanosome cell lines, *in vitro* culture and transfection conditions

The *Trypanosoma brucei* bloodstream form strain 442 were grown in HMI-9 medium at 37 °C, 5% CO₂ (Hirumi and Hirumi, 1989). Procyclic strains 427, 449 and 29-13 were all maintained in a semi-defined medium (SDM-79), at 28 °C (Brun and Schonenberger, 1979). Several antibiotics were used in the maintenance and selection of cell lines. The following are the antibiotics and concentrations typically used unless specified otherwise: hygromycin (HYG, 50 µg ml⁻¹), G418 (NEO, 15 µg ml⁻¹), phleomycin (Bleo, 5 µg ml⁻¹) and blasticidin (BSD, 20 µg ml⁻¹). 449 expresses a Tet repressor (*TetR*) gene which was maintained with the use of 0.5 µg ml⁻¹ of phleomycin (Biebinger et al., 1997). The 29-13 cell line contains both the T7 RNA polymerase and *TetR* genes which were maintained with hygromycin and G418 (Wirtz et al., 1999).

Transfection on procyclic strains were done as described in (Beverley and Clayton, 1993). Cells growing to mid log phase was harvested and washed twice in ZPFM buffer [132 mM NaCl, 8 mM KCl, 8 mM Na₂HPO₄, 1.5 KH₂PO₄, 1.5 mM Mg(CH₃COO)₂, 90 µM Ca(CH₃COO)₂, pH 7.3]. The cells were then resuspended in ZPFM buffer to a final cell concentration of 4 × 10⁷ cells ml⁻¹. Using 10 µg of linearised plasmid DNA, 500 µl of the resuspended cells was electroporated using an Electro Square Porator (BTX ECM830) with the following settings (1700 V, 3 × 100 µS pulse length, with 200 ms intervals). After a recovery period of 1 minute on ice, the electroporation was repeated once. Cells were allowed to recuperate overnight in SDM-79 at 28 °C before being diluted to a concentration of 5 × 10⁵ cells ml⁻¹ with SDM containing appropriate antibiotics. The cells were subsequently plated into a 24-wells plate and sealed with parafilm before being incubated at 28 °C.

3.3.2 Generation of kinesin RNA interference (RNAi) cell lines; 29-13/p2T7-*TbKif2*, 29-13/p2T7-*TbKif8*, 29-13/p2T7-*TbKif9*, 29-13/p2T7-*TbKif15*, 29-13/p2T7-*TbKif27* and 29-13/p2T7-*TbKif45*

The kinesin RNAi constructs were made using the vector p2T7-177 (LaCount et al., 2000; Wickstead et al., 2002) to allow for tetracycline inducible production of double-stranded RNA (dsRNA) from opposing T7 promoters within the vector (Figure 3.2). DNA fragments specific to each of six targeted kinesin genes were amplified via standard PCR using the primer pairs specified in Table 3.1 and genomic DNA from strain 427 as template. These DNA fragments were initially cloned into pGEM-T Easy (Promega, cat #A1360) using the protocol provided by the manufacturer. 2 μ l of the resulting ligation mix was then transformed into competent *E. coli* XL1-Blue cells (Stratagene, cat #200249) for amplification. The preparation of the chemically competent *E. coli* cells and the transformation were done according to the method described (Inoue et al., 1990). Transformed cells were plated onto Luria-Bertani (LB, Bacto Tryptone, 10 g; Bacto Yeast extract, 5 g; NaCl, 10 g; in 1 L ddH₂O) agarose plates (1.5% agarose w/v) containing ampicillin (100 μ g/ml) to select for transformants. IPTG and X-gal were added to the agarose plates in order to select for positive clones via blue/white screening as described in the manual of pGEM-T Easy (Promega, cat #A1360). After overnight incubation at 37 °C, positive colonies were selected and plasmid DNA was harvested using alkaline lysis as described (Sambrook, 1989). The purified plasmids were then digested using the restriction enzymes HindIII and BamHI and separated on an agarose gel. The DNA band containing the digested fragment of interest was excised from the gel and cleaned using a PCR cleanup gel extraction kit, NucleoSpin Extract II (Macherey-Nagel, cat #740609). The purified DNA fragment was ligated into the HindIII and BamHI digested plasmid vector p2T7-177. The plasmid was subsequently purified from a 50 ml overnight *E. coli* culture in LB using the NucleoBond PC100 columns (Macherey-Nagel, cat #740573).

The procyclic *Trypanosoma brucei* strain 29-13 was used in the construction of the RNAi cell lines. Selection of stable transfectants was done using the antibiotic phleomycin (5 μ g ml⁻¹) and production of dsRNA was induced by the addition of 1 μ g ml⁻¹ doxycycline (from 1 mg ml⁻¹ doxycycline stock in ethanol). To quantify the effect of RNAi induction on the growth rate of the various RNAi cell lines, a standard procedure was adopted. The cells

counted and were diluted to a density 1×10^6 cells ml^{-1} before being split equally into two flasks. One flask was kept as a control while doxycycline was added to the second flask. Both cultures were counted 3 times using a CASY Cell counter + Analyzer System (Scharfe System) every 24 hours and its average used to construct a growth curve. The cells were diluted to 1×10^6 cells ml^{-1} with fresh medium every 2 days.

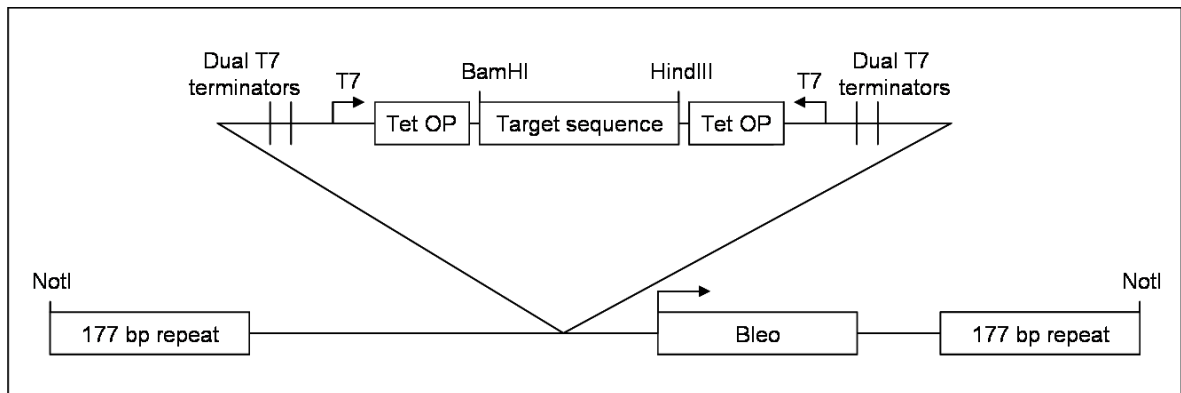


Figure 3.2: The basic features of the vector p2T7-177 in its linearised form, after NotI digestion. This vector integrates to the transcriptionally silent 177 bp repeat region of the minichromosomal population in the trypanosomes (Wickstead et al., 2002). A phleomycin resistance gene (Bleo) is present for selection of transfected *T. brucei* cells. The transcription of the target sequence into double stranded RNA (dsRNA) was induced using an exogenously expressed T7 RNA polymerase and a pair of T7 promoters flanking opposite sides of the target sequence. These T7 promoters are under the control of the Tetracycline operator (Tet OP).

Table 3.1: Forward and reverse primer sequences for the corresponding *T. brucei* kinesin genes used in the construction of the RNAi expression vectors. The design of the primers was done using the programme RNAit from <http://trypanofan.path.cam.ac.uk/software/RNAit.html>. To avoid any potential cross-interference resulting from unspecific RNA interference, DNA sequences coding for protein sequences outside the motor domain was specified for the creation of the RNAi constructs. The sequences underlined in the forward primer correspond to the BamHI restriction site and in the reverse primer, the HindIII restriction site. Both restriction sites were introduced to the primers to allow the cloning of the PCR fragments into the p2T7-177 RNAi expression construct. The primers were obtained from MWG biotech Inc.

Kinesin gene	Primer type	DNA sequence (5' to 3')
<i>TbKif2</i>	Forward	<u>GGATCC</u> ATCTCTAGTGCGCTGTCCGT
	Reverse	AAGCTT <u>CAAGTGGCCCTAAGGGTTTT</u>
<i>TbKif8</i>	Forward	<u>GGATCC</u> AATTCAGGGGTTTGTCGATG
	Reverse	AAGCTT <u>TTTGCATGCCTTCTCGTACAC</u>
<i>TbKif9</i>	Forward	<u>GGATCC</u> GGATTTGTCGCGTGATATCC
	Reverse	AAGCTT <u>TTTATCCTCACCGAAAGCGTC</u>
<i>TbKif15</i>	Forward	<u>GGATCC</u> GTTTCAACGCTTGCTCAACA
	Reverse	AAGCTT <u>TCGAGAGTTACGCTGTGTGG</u>
<i>TbKif27</i>	Forward	<u>GGATCC</u> GAGCGGATACCTTTGACTGC
	Reverse	AAGCTT <u>TTCTTCTTCTCACGGAGCAT</u>
<i>TbKif45</i>	Forward	<u>GGATCC</u> CAGCACTCGCTTGGGCA
	Reverse	AAGCTT <u>TGTCAGTATTGCTCGCCGTTT</u>

3.3.3 Production polyclonal antibody of TbKif2, TbKif8, TbKif9, TbKif15, TbKif27 and TbKif45

The construction of the protein expression vectors was done using the pTrcHisC vector (Invitrogen, cat #V360-20, Figure 3.3). The pTrcHisC vector adds a polyhistidine tag at the N-terminus of the inserted gene fragment. This polyhistidine tag binds specifically to divalent cations which were used in subsequent purification steps. Standard PCR using proof reading AccuSure Taq polymerase (Bioline, cat #BIO-25029) was performed using the primer pairs specified in Table 3.2 and genomic DNA from strain 427 as a template to amplify of segments of DNA coding for regions specific to each of the six kinesins (Table S 5.4). After digestion with BamHI and EcoRI restriction enzymes, the PCR fragments were directly cloned into the pTrcHisC vector. DNA sequencing using primers 100 bp upstream (5'-AAGAGGTATATATTAATGTATCGA-3') from the point of insertion of the PCR fragment was done to verify the correct reading frame of the expression construct before it was used in protein expression experiments. These constructs were then used for the expression of the recombinant kinesin fragments in *E. coli* BL21 cell line (Novagen, cat #69386-3). The transformation was performed as described in chapter 3.3.2.

Transformed BL21 cells were grown in 350 ml batches of prewarmed (37 °C) LB medium containing 100 µg ml⁻¹ ampicilin in 3 litre Erlenmeyer flasks. The culture was incubated at 37 °C with vigorous shaking (~300 RPM) until its optical density at 600 nm (OD₆₀₀) is 0.5 - 0.6. Isopropyl-β-D-thiogalactopyranoside (IPTG) was then added into the culture to a final concentration of 1 mM to induce the production of recombinant proteins and left to incubate for 4 hours at 37 °C with shaking. The cells were harvested by centrifugation and resuspended in 80 ml of ice-cold lysis buffer (50 mM NaH₂PO₄, 300 mM NaCl, 10 mM imidazole, pH adjusted to 8.0 using NaOH). The cells were lysed by two passages at 1000 kPsi through a French pressure cell and the resulting lysate was centrifuged for at 14,000 g for 10 minutes at 4 °C to separate the soluble from the insoluble fraction of the cell lysate. For recombinant proteins located in the soluble fraction, the resulting supernatant from centrifugation was collected for purification. For recombinant proteins located in the insoluble fraction, the supernatant was discarded and the pellet

resuspended in 30 ml of denaturing lysis buffer (6M guanidine.HCl, 50 mM NaH₂PO₄, 300 mM NaCl, 10 mM imidazole, pH 8.0) to solubilise the recombinant protein which was then centrifuged (20,000 g for 10 min at 4 °C) to remove any insoluble particles.

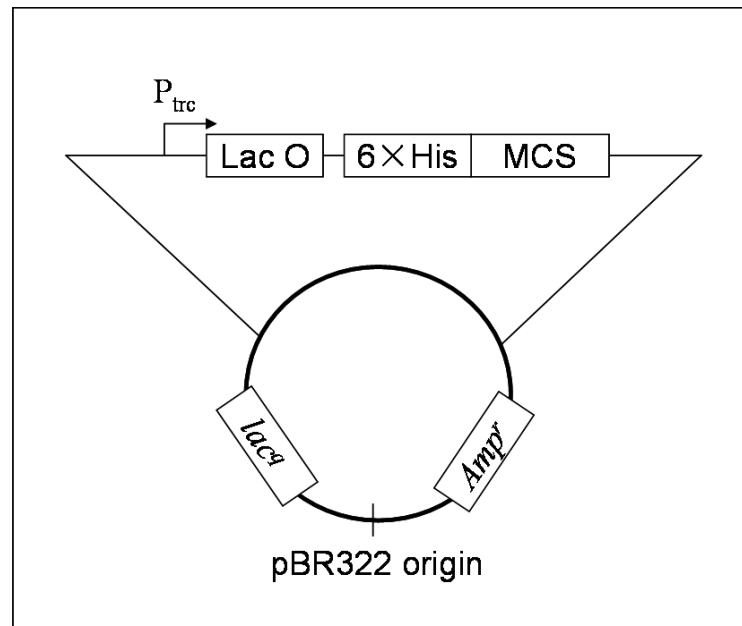


Figure 3.3: The basic features of the pTrcHisC expression vector (Invitrogen, cat #V360-20). This vector contains the ampicillin resistance gene (*Amp^r*) which will be used for the selection of transformed *E. coli* cells, a *lac^q* gene which encodes and overexpresses the Lac repressor protein and a pBR322 origin which confers a low plasmid copy number in the *E. coli* cell. The expression of the recombinant protein is induced by the *trc* promoter (P_{trc}) which is under the control of the Lac operator (Lac O). This allows for the control of the expression of the recombinant protein with the use of IPTG (isopropyl-β-D-thiogalactopyranoside). The pTrcHisC vector contains a multiple cloning site (MCS) which is used in the cloning of DNA fragments into the expression vector. The recombinant proteins expressed in the pTrcHisC vector will include a polyhistidine (6 × His) tag at the N-terminus of the recombinant protein. This polyhistidine tag binds specifically to divalent cations (e.g. Co²⁺ and Ni²⁺) which used in the subsequent purification of these recombinant proteins.

Table 3.2: Forward and reverse primer sequences for the corresponding *T. brucei* kinesin genes used in the construction of the protein expression vectors. The sequences underlined in the forward primer correspond to the BamHI restriction site and in the reverse primer, the EcoRI restriction site. Both restriction sites were introduced to the primers to allow the cloning of the PCR fragments into the pTrcHisC expression construct. The primers were obtained from MWG biotech Inc.

Kinesin gene	Primer type	DNA sequence (5' to 3')
<i>TbKif2</i>	Forward	C <u>GGGATCCC</u> GACACGATGTCCGCACTGTAG
	Reverse	GGAAT <u>TCCGCTTT</u> GAAGCCTTAGTGGTGCC
<i>TbKif8</i>	Forward	C <u>GGGATCCC</u> GCGGTCCTCCAGTCATCTTTC
	Reverse	GGAAT <u>TCCGCGGTTT</u> AGCAACTGCCTTA
<i>TbKif9</i>	Forward	C <u>GGGATCCC</u> GATGAGCGGTGTGCCGTCAAGAAC
	Reverse	GGAAT <u>TCCGAATTGCTT</u> GCCCCTTACAGT
<i>TbKif15</i>	Forward	C <u>GGGATCCC</u> GACGATCCAAATGGGTTTGACAG
	Reverse	GGAAT <u>TCCGCGTAGCACAC</u> CGGGGCAAT
<i>TbKif27</i>	Forward	C <u>GGGATCCC</u> GTGAAACTATTCGAGGCACC
	Reverse	GGAAT <u>TCCCTGGAAGAGTT</u> CAGGGTGCAAG
<i>TbKif45</i>	Forward	C <u>GGGATCCC</u> GAAACAGACATCACCAGCTGCC
	Reverse	GGAAT <u>TCCGCTCGAGACGCT</u> GACAAAGT

The purification of the recombinant proteins both from the soluble and insoluble fraction of was done by using metal affinity resins obtained from BD Biosciences (BD Talon, cat #635503). The purification of the recombinant proteins for both native and denaturing conditions were done as described in the protocol provided by the manufacturer (Protocol #PT1320-1). The recombinant proteins were subsequently eluted in elution buffer [50 mM NaH₂PO₄, 300 mM NaCl, 250 mM imidazole, pH 8.0, (with 6 M guanidine.HCl if performed under denaturing conditions)]. The purified proteins were then dialysed against a MES buffer (50 mM MES buffer, pH 6.0, 0.1% SDS) or TBS buffer (20 mM Tris, 150 mM NaCl, 2 M Urea, pH 7.6) if the protein was purified under denaturing conditions. The resulting dialysed protein solution was then concentrated by sprinkling high molecular weight substances [Polyvinylpyrrolidone (PVP), M_r 40,000] over the dialysis tube after dialysis. The purified proteins were concentrated to a concentration between 600 µg ml⁻¹ to 1000 µg ml⁻¹ as determined by a Bicinchoninic Acid Protein Assay Kit (Sigma, cat #BCA-1 and #B9643). The purified proteins were used to raise rabbit polyclonal antibodies (Yorkshire Biosciences).

Western blot analysis using the generated polyclonal antisera revealed that there were several cross-reacting protein bands in procyclic trypanosome cells (Appendix 6.1). The polyclonal antibodies were therefore subsequently affinity-purified using the purified recombinant kinesin protein fragments. The recombinant kinesin protein fragments were coupled to CNBr-activated Sepharose 4B (Amersham Biosciences, cat #17-043-01) as described by the manufacturer. The coupled beads were washed 5 × with PBS containing 500 mM NaCl before being incubated with the polyclonal antibodies at room temperature for 1 hour. The beads were then washed 3 × with PBS containing 500 mM NaCl before elution using a low pH glycine buffer (100 mM glycine-HCl, 100 mM NaCl, pH 2.5). The elute was collected in 10 × 0.5 ml fractions which were neutralised to pH 7 using 1 M Tris-HCl, pH 9. The fractions containing significant proportions of antibodies were dialysed against PBS containing 0.01% azide and stored at 4°C or frozen at -80 °C.

The dilutions used for these purified antibodies during Western blotting and immunofluorescence were determined experimentally. Unless specified, the purified antibodies were diluted 1:25 for immunofluorescence and 1:1,000 in Western blots.

3.3.4 Immunofluorescence microscopy

The entire procedure was performed at room temperature. Trypanosome cells were fixed in suspension with 3.6% formaldehyde in PBS (NaCl, 137 mM; KCl, 3 mM; Na₂HPO₄, 16 mM, KH₂PO₄, 3mM; pH 7.4) for 15 minutes. The cells were then washed twice in PBS before being allowed to settle to poly-L-lysine coated slides. Cells attached to the poly-L-lysine coated slides were permeabilised with 0.1% Nonidet P-40 in PBS for 20 minutes before being blocked with blocking solution (PBS containing 0.1% Triton-X100, 2% BSA and 0.01% Azide). Primary antibodies diluted in blocking solution were then applied to the cells. Depending on the primary antibody, either an anti-mouse fluorescein isothiocyanate (FITC)-conjugated secondary antibodies (Dako, cat #F0216, 1:50 dilution) or an anti-rabbit FITC-conjugated secondary antibody (Sigma, cat #F1262, 1:100 dilution) diluted in blocking solution was used. The primary and secondary antibody incubations were performed at room temperature for 1 hour. After each antibody incubation, 3 × 5 minute washes of PBS, 0.1% Triton-X100 were performed. The cells were mounted in

Vectashield containing 1.5 µg/ml of 4',6-diamidino-2-phenylindole (DAPI, Vector Laboratories, cat #H-1200). The cells were examined using an epifluorescence Olympus IX71 microscope. Images were captured using a CCD-camera (F-View, Soft Imaging System) and visualised and saved in Cell-D software package (Olympus). Images were then processed and pseudo-coloured in Adobe Photoshop.

For double labelling experiments, the cells were treated as described above with a second additional primary antibody treatment performed. A second secondary antibody treatment was also performed with a cyanine based fluorescent dye (Cy3)-conjugated anti-mouse antibody (Zymed, cat #81-6515, 1:150 dilution). For cytoskeleton preparations, live trypanosome cells were resuspended in PBS and allowed to attach to poly-L-lysine coated slides for 5 minutes. The attached cells were treated with ice cold PEM (0.1 M PIPES, 2 mM EGTA, 1 mM MgSO₄, pH 6.9) buffer containing 0.1% NP40 for 30 seconds before being fixed with 3.6% formaldehyde in PBS for 15 minutes. After fixation, the cytoskeleton preparations were washed twice with PBS and blocked with blocking solution before proceeding with antibody incubations as described above.

3.3.5 Mitotracker staining for immunofluorescence microscopy

Trypanosome procyclic cells were incubated with pre-warmed SDM79 medium containing 0.5 µM Mito Tracker Red CMXRos (Invitrogen, cat# M7512) at 28 °C for 10 minutes (from 1 mM stock in DMSO). The cells were harvested via centrifugation and washed with pre-warmed SDM79 twice to remove unincorporated dye. The cells were then incubated in pre-warmed culture medium for another 30 minutes to allow the incorporation of the Mito Tracker dye from the cytosol into the mitochondria. The cells were fixed with 3.6% formaldehyde in PBS and the cells processed in a similar fashion as described in the immunofluorescence microscopy section.

3.3.6 SDS-polyacrylamide gel electrophoresis and Western blotting

Unless specified, the entire process was done on room temperature on a 10 × 10 cm gel and each lane was loaded with 2×10^6 cell of either procyclic or bloodstream form trypanosomes. The cell samples were first washed once with PBS before being dissolved in hot (95 °C) 1 × SDS PAGE loading buffer (0.045 M Tris-Cl, pH 6.8, 10% glycerol, 1% SDS, 0.02% bromophenolblue, 2.5% β-mercaptoethanol). The samples were then loaded onto a 10% Tris/Glycine (25 mM Tris, 250 mM glycine, 0.1% SDS) SDS-Polyacrylamide gel for protein separation. After separation, the gel is either stained with Coomassie stain [0.2 % (w/v) Coomassie Brilliant Blue R250, 50% (v/v) methanol, 10% (v/v) Acetic acid] or transferred to a nitrocellulose membrane in NuPage buffer [500 mM Bicine, 500 mM Bis-Tris, 20.5 mM EDTA, 10% (v/v) Methanol] for 1 hour at 30 V. The membranes were blocked in 7 % milk (w/v) diluted in Tris-buffered Saline containing 0.1% Tween-20 (TBS-T) for 30 minutes at room temperature with gentle shaking. All antibody incubations were done in 7 % (w/v) milk TBS-T. The membrane was first incubated with primary antibody for 1 hour. This was followed by 3 × 15 minute washes with TBS-T before proceeding with the incubation using an appropriate corresponding anti-rabbit (ZyMax, 1:20,000 dilution, cat #81-6120) or anti-mouse (Sigma, 1:80,000 dilution, cat #A-9044) peroxidase-conjugated antibody for 1 hour. The membrane was then washed 3 × 15 minutes in TBS-T and processed using the Western Lighting Plus chemiluminescence reagent (PerkinElmer, cat #NEL 104). The chemiluminescence signals were detected by exposing the cling film wrapped blots to light sensitive film (Amersham, cat #28906837) for 1 to 10 minutes.

3.3.7 Fluorescence-activated cell sorting (FACS) analysis

Unless specified, the process was done at room temperature. 2×10^7 cells were used in each analysis. The cells were harvested via centrifugation at 1500 g for 5 minutes and washed once in PBS. The cells were then treated with 200 μ l of ice cold 0.5% formaldehyde diluted in PBS for 5 minutes before being fixed with the addition of ice cold 70 % (v/v) ethanol. After fixation overnight at 4 °C, the cells were pelleted by centrifugation and resuspended in 1 ml of staining solution (PBS with 0.2 mg ml⁻¹ RNase A, 50 μ g ml⁻¹ propidium iodide). The cells were incubated at 37 °C for 30 minutes and analysed by a FACS Calibur flow cytometer (Becton Dickson). For the analysis of DNA content/cell cycle, the signal of the FL3-A channel (propidium iodide fluorescence) was recorded against cell number. A total of 20,000 cells were counted for each treatment and analysed using CellQuest software (Becton Dickson).

3.3.8 Detergent extraction and ATP treatment

Kinesins were previously shown to bind to microtubules in the absence of ATP or presence of the non-hydrolysable analogue of ATP, AMPPNP (Cole et al., 1992; Gerald et al., 2007; Hertzler et al., 2006). This affinity to microtubules by kinesins can be reversed with the addition of ATP to the extraction solution.

Cells were prepared as described (Gerald et al., 2007). 2×10^7 trypanosome strain 427 cells were washed twice in PEM (0.1 M PIPES, 2 mM EGTA, 1 mM MgSO₄, pH 6.9) buffer. The cells were then extracted with NP40/PEM (PEM with 1 % (v/v) Nonidet P-40, 50 μ g ml⁻¹ PMSF, protease inhibitor cocktail Sigma, cat #P8340); with or without 10 mM MgATP. The cells were extracted with 1 ml of either NP40/PEM buffers on ice for 1 minute or 16 minutes before being centrifuged at 3500 g for 4 minutes at 4 °C. The supernatant was then precipitated using chloroform-methanol. Both pellet and precipitated supernatant was resuspended in 100 μ l of 1 \times SDS PAGE loading buffer. 10 μ l of each sample corresponding to 2×10^6 cells was loaded onto gels for Western blotting.

3.3.9 Cloning of *TbKif2*, *TbKif8*, *TbKif9*, *TbKif45* and construction of the 449/*TbKif2myc*, 449/*TbKif8myc*, 449/*TbKif9myc* and 449/*TbKif45myc* cell lines

The construction of the conditionally expressed ectopic myc tagged *TbKif2myc*, *TbKif8myc*, *TbKif9myc* and *TbKif45myc* kinesins were done using one of the 2 different tetracycline inducible expression plasmids pHD1484 (Colasante et al., 2006) or P2674 (Kelly et al., 2007). Both the P2674 and pHD1484 vector (Figure 3.4) contain a hygromycin resistance gene (*HYG*) for drug selection. The expression of the gene of interested is under the control of a tetracycline-inducible procyclin promoter. When the genes of interested were cloned into either expression plasmids, a double-myc (pHD1484) or triple-myc (P2674) tag will be introduced to the carboxy terminus of the expressed protein (Colasante et al., 2006; Kelly et al., 2007). The entire open reading frames (ORF) for each of the four kinesin genes were amplified using proof reading AccuSure Taq polymerase (Bioline, cat #BIO-25029) on genomic DNA from trypanosome strain 427 as a template with primers listed in Table 3.3. The PCR fragments were subsequently cloned into their respective expression plasmids using appropriate restriction enzymes. Both constructs were transfected into the procyclic strain 449 cells yielding the 449/*TbKif2myc*, 449/*TbKif8myc*, 449/*TbKif9myc*, 449/*TbKif45myc* cell lines. The selection of stable transfectants was done with hygromycin. The recombinant myc tagged kinesin production was induced by the addition of 1 $\mu\text{g ml}^{-1}$ of tetracycline.

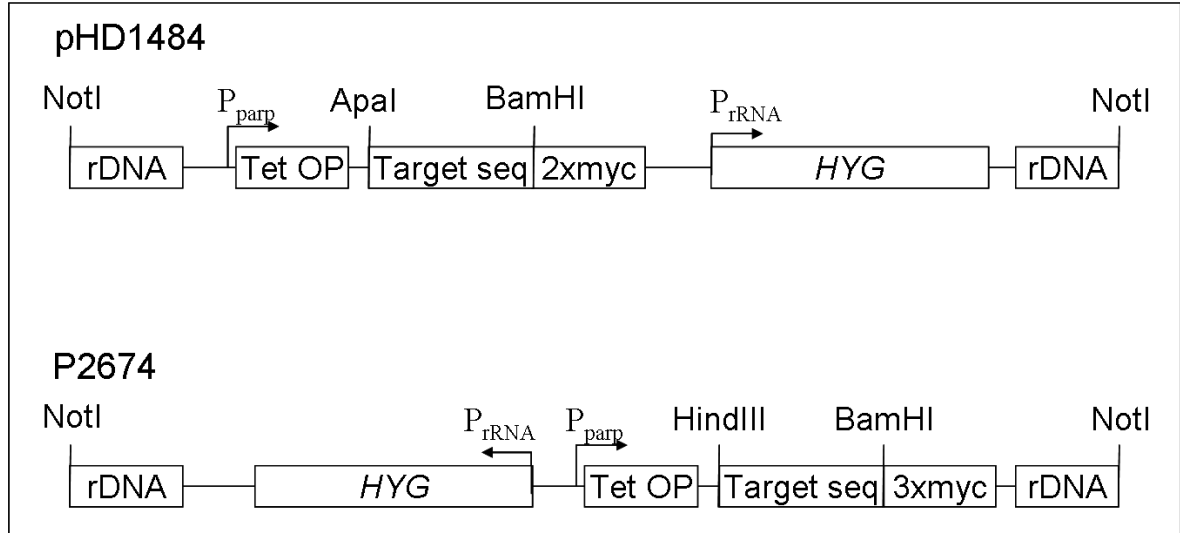


Figure 3.4: The basic features of the myc epitope tagged vectors pHD1484 (Colasante et al., 2006) and P2674 (Kelly et al., 2007). Both vectors target the non-transcribed space between ribosomal RNA genes (rDNA) for stable integration into the trypanosome genome. A hygromycin resistance gene (*HYG*) powered by an rRNA promoter (P_{rRNA}) was used for selection of transfected cells in trypanosomes. The symbols (P_{parp}) represent the procyclic acidic repetitive protein (procyclin) promoter and (Tet OP) represents the binding site for the tetracycline repressor protein.

Table 3.3: The forward and reverse primer sequences used in the cloning of each corresponding *T. brucei* kinesin genes. The resulting PCR fragments were cloned into the respective myc-tagging construct and were subsequently transfected into trypanosome procyclic strain 449 cells. The underlined sequence GGGCCC (ApaI), GGATCC (BamHI) and AAGCTT (HindIII) corresponds to the restriction sites used to clone the PCR fragments to their respective vector constructs. The sequence highlighted in blue corresponds to a stop codon inserted into the primer to prevent a read through frame starting 75 bp upstream from HindIII cloning site potentially interfering with the expression of *TbKif45myc* in the P2674 expression construct. The start codons are indicated in bold.

Kinesin gene	Construct	Primer type	Sequence (5' to 3')
<i>TbKif2</i>	pHD1484	Forward	ACGGGCCCAGGGC ATG ACCTCACTCTGTCC
		Reverse	CGGGATCCCACGCTTTCAAGTTCATGAAGCTTTG
<i>TbKif8</i>	pHD1484	Forward	ACGGGCCCAGGAA ATG GAGCGACAGCTTCG
		Reverse	CGGGATCCCCGGCGTTGCCGAGACTCC
<i>TbKif9</i>	pHD1484	Forward	GGGCCC ATG CAGGACGAACAGCATGAGG
		Reverse	GGATCCATTCGGTTGCTGCTGCACCGG
<i>TbKif45</i>	P2674	Forward	TGATGAAAGCTT TAG GAAAGG ATG GCGAAGTGGGAATTAAG
		Reverse	TGATCAGGATCCAATCCCGTTTTGCTCGAGACGCT

3.3.10 Conditional double knockout of *TbKif2*

The method used in the creation of the conditional double knockout of $\Delta TbKif2$ /*TbKif2myc* was performed in a similar fashion as described (Colasante et al., 2006). The cell line 442/*TbKif2myc* was used for the subsequent deletion of both endogenous copies of *TbKif2*. Both *TbKif2* alleles were replaced via homologous recombination using two different antibiotic resistance cassettes, *BSD* and *NEO* (Figure 3.5). The *TbKif2* 5' UTR and 3' UTR inserted to the 5' and 3' regions flanking the *BSD* and *NEO* resistance cassettes were amplified via standard PCR on genomic DNA from strain 427 using the primers specified in Table 3.4. The PCR fragments were subsequently cloned to the *BSD* and *NEO* resistance cassettes using the restriction sites *ApaI*, *BamHI*, *SacI* and *SpeI*.

The antibiotic tetracycline was added ($1 \mu\text{g ml}^{-1}$) to the culture medium before the deletion of the second *TbKif2* allele to induce the expression of myc tagged *TbKif2myc*.

Table 3.4: The forward and reverse primer sequences used in the construction of the *BSD* and *NEO* resistance cassettes. The sequences underlined represents the restriction sites *ApaI* (GGCCC), *BamHI* (GGATCC), *SacI* (GAGCTC) and *SpeI* (ACTAGT) that were used for the construction of the knock out cassettes.

UTR region	Primer type	Size	Sequence (5' to 3')
5'	Forward	444	<u>GAGCTC</u> TGATGTTTGTGGCTCGTTTGTGCC
	Reverse		ACTAGTACAGCCACCAGCTGTCGTACC
3'	Forward	358	<u>GGATCC</u> ATCACATGCCTCAGTGCGCAC
	Reverse		<u>GGGCCC</u> ATGCACAGTTGCATACTCGTAACAC

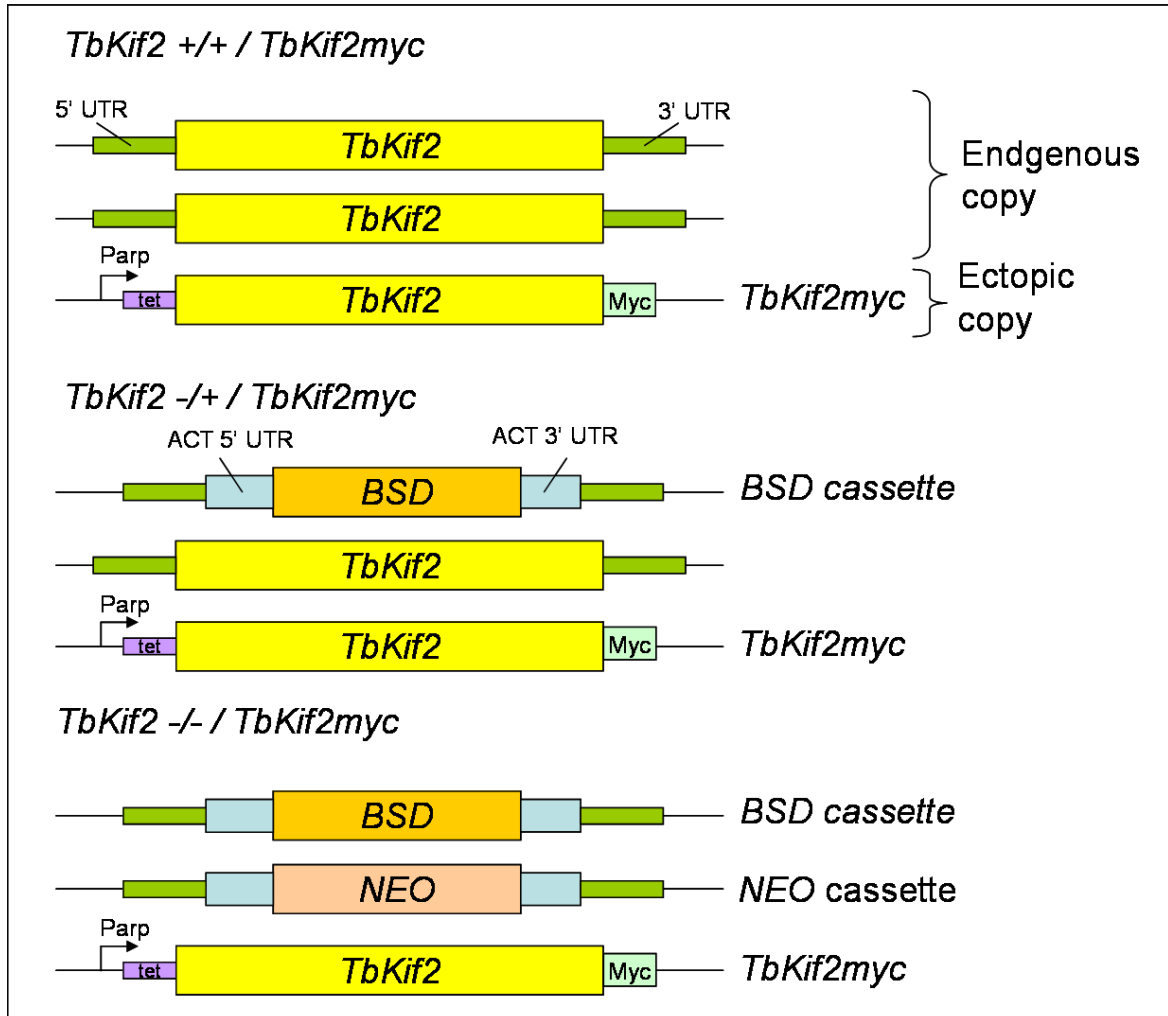


Figure 3.5: A schematic representation of the strategy used in the creation of the conditional knock out of *TbKif2*. *TbKif2myc* represents the inducible rescue copy expressing the myc tagged version of *TbKif2*. The 5' and 3' UTR regions (green) were used to target the resistance cassettes to each of the endogenous *TbKif2* genes. The abbreviations used were *NEO*, neomycin resistance cassette; *BSD*, blasticidin resistance cassette; *ACT*, actin; *tet*, tet operator; *Parp*, procyclin promoter and *Myc*, myc tag.

3.3.11 Screening for conditional double knockout of *TbKif2*

The isolation of genomic DNA was performed using a standard phenol/chloroform extraction in the presence of LiCl and Triton-X100 (Medina-Acosta and Cross, 1993). To identify clones with endogenous copies of the *TbKif2* genes deleted, two different methods of analysis were used. An initial standard PCR reaction was performed using the forward 5' UTR primer of *TbKif2* and reverse 3' UTR primer of *TbKif2*. This method exploits the difference in length of the PCR product between the knockout construct and the endogenous *TbKif2* gene. Positive clones were then further analysed via Southern blotting. 10 µg of genomic DNA from each clone was digested with appropriate restriction enzymes before being separated on a 0.8% agarose gel. The dsDNA was denatured in denaturing buffer (0.4 M NaOH, 1.5 M NaCl) for 15 minutes and capillary transferred to a positively charged nylon membrane (Roche, cat #1417240) for 12 hours in denaturing buffer. The nylon membrane was neutralised in 0.5 M Tris-HCl pH 7.0 for 5 minutes before being washed briefly in 2 × SCC and processed as described by the Gene Images random prime labelling module manual (Amersham, cat #RPN 3540). The blot was probed using fluorescein-labelled probes targeting the 5' UTR region of *Tbkif2* made using the same kit. Probe detection was done via chemiluminescence using the Gene Images CDP-Star detection module (Amersham, cat #3510). The chemiluminescence signals were detected by exposing the cling film wrapped blots to light sensitive film (Amersham, cat #28906837) for 1 hour.

3.3.12 Flagellar measurements

Live trypanosome cells freshly harvested was resuspended in PBS and allowed to attach to poly-L-lysine coated slides for 5 minutes. The attached cells were treated with ice cold PBS containing 0.1% NP40 for 30 seconds before being fixed immediately with 3.6% formaldehyde in PBS at room temperature for 15 minutes. The cells were then labelled with an mouse anti-parafagellar rod (PFR) antibody, L2C4 (Kohl et al., 1999) and processed as described in the immunofluorescence microscopy section. The cells were examined under an Olympus IX71 microscope. Images were captured using a CCD-camera (F-View soft imaging system) and measurements were made using the measuring tool of the Cell* software package (Olympus). Statistical analysis was performed in Excel or SPSS.

3.3.13 Production of cDNA for reverse transcriptase (RT) PCR

The total RNA extracts of the bloodstream and procyclic form of *T. brucei* cells were obtained using the RNeasy Mini Kit (QIAGEN, cat #74104). The RNA extract was further cleaned using an on-column DNase digestion kit (QIAGEN, cat #79254). The resulting purified total RNA was used in the production of cDNA using QIAGEN Omniscript RT Kit (cat #205110). The production of cDNA was done as suggested by the manufacturer using oligo dT₁₈-primers to the final concentration of 10 pMol/μl. All the components used for cDNA production was provided by the kit except for the dT₁₈-primers which was obtained from MWG biotech Inc. The resulting cDNA was used as substrate in a standard PCR with appropriate primers.

3.4 Results

3.4.1 TbKif2myc is localised to the distal tip of the trypanosome flagellum

To determine whether *TbKif2* was expressed in the procyclic and bloodstream stages of the *T. brucei brucei*, RT-PCR was performed on the cDNA produced from total RNA extracts of both 427 (procyclic) and 442 (bloodstream) cell lines. The results of the RT-PCR showed that the mRNA of *TbKif2* was transcribed at approximately equal levels in both procyclic and bloodstream forms (Figure 3.6).

To investigate the specificity of the affinity-purified polyclonal anti-TbKif2, a Western blot using the whole cell lysate of strain 427 cells was performed. The Western blots did not produce any identifiable signals (results not shown). In addition, immunofluorescence microscopy using anti-TbKif2 on formaldehyde fixed cells did not produce any discernable signals (results not shown). Because the purified anti-TbKif2 did not produce any results, trypanosome cell lines expressing an exogenous copy of the *TbKif2* gene fused with a myc tag (*TbKif2myc*) was created.

Western blots using anti-myc performed on cells expressing *TbKif2myc* resulted in the detection of a single band slightly larger than 75 kD in size which corresponds to the expected size of *TbKif2myc* of 77 kD (Figure 3.7A). When immunolocalisation studies using anti-myc were performed, *TbKif2myc* was observed to exclusively localise to the distal tip of the flagellum (Figure 3.7B). It was also observed that during mitosis, *TbKif2myc* was found to be more abundant in the new outgrowing flagellum when compared to the mature flagellum.

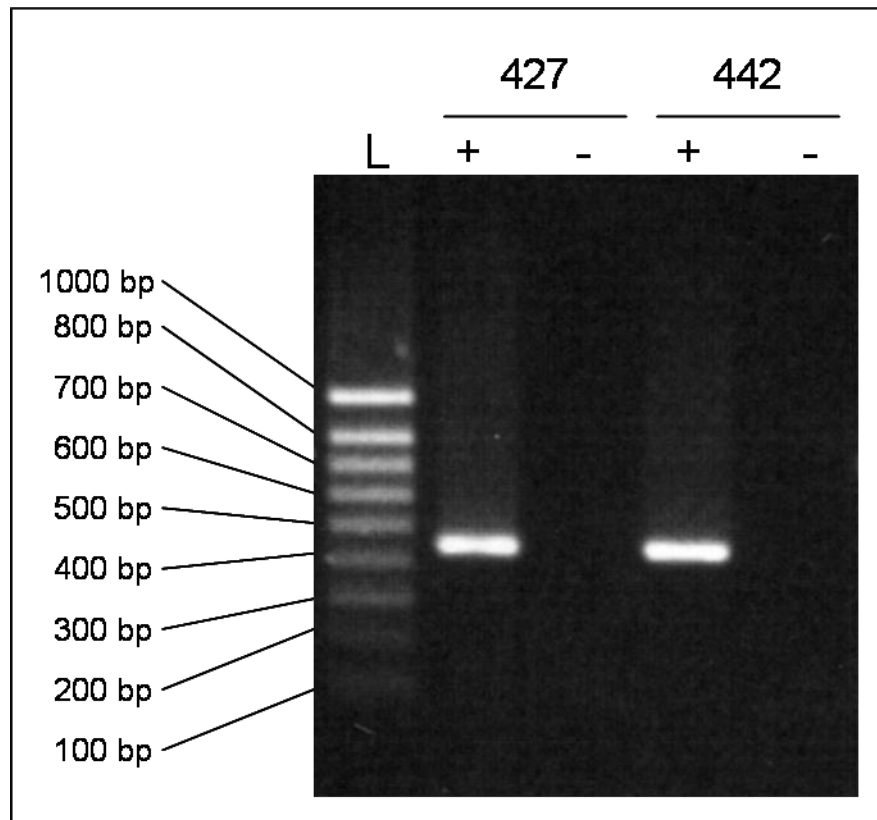


Figure 3.6: The RT-PCR results showing *TbKif2* is expressed in both the procyclic (427) form and bloodstream (442) form of trypanosomes. Lane (L) indicates the DNA ladder with its corresponding length annotated, (+) indicates the results of the RT-PCR experiment using primers specific to *TbKif2*, (-) indicates the negative control (- reverse transcriptase enzyme).

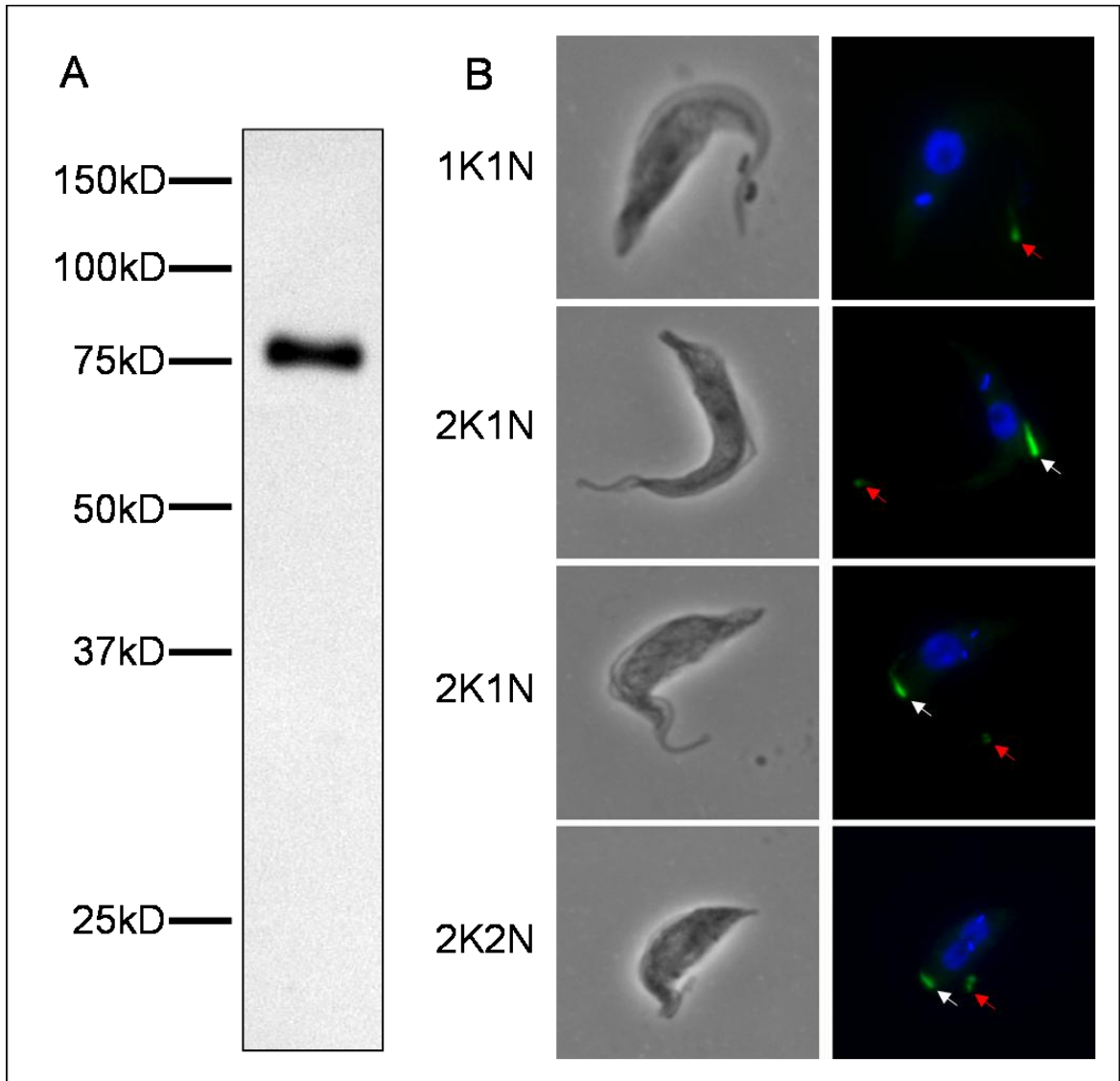


Figure 3.7: The expression of TbKif2myc in procyclic trypanosome cells. (A) A Western blot using anti-myc antibodies on the whole cell lysate of trypanosome cells expressing TbKif2myc. (B) Images of procyclic cells (1,000 times magnification) expressing TbKif2myc viewed in phase contrast (left) and fluorescence microscopy (right). The cells were fixed in formaldehyde and stained with anti-myc. The nucleus and kinetoplast is stained in blue while TbKif2myc is stained in green. The red arrow marks the localisation of TbKif2myc in the mature flagellum and the white arrow marks the localisation of TbKif2myc in new flagellum in dividing cells.

3.4.2 *TbKif2* is not required for cell viability in procyclic forms

To study the function of *TbKif2* in trypanosomes, RNAi was performed on procyclic strain 29-13 cells using the RNAi vector p2T7-*TbKif2*. It was observed that the induction of the p2T7-*TbKif2* vector in trypanosomes resulted in a severe growth defect after 2 days of induction (Figure 3.8A). This was in contrast with the published results where RNAi targeting *TbKif2* in trypanosome procyclic cells was reported to have no impact on *in vitro* cell growth (Blaineau et al., 2007).

In order to address this discrepancy, a procyclic cell line with a double knockout of *TbKif2* and a single tetracycline inducible copy of *TbKif2myc* was created (Figure 3.9). To deplete the *TbKif2myc* protein in the *TbKif2* conditional knockout (Δ *TbKif2/TbKif2myc*) cell line, tetracycline was removed from the culture medium. It was observed that the removal of tetracycline reduced the protein levels of *TbKif2myc* to undetectable levels (by Western blot and immunofluorescence) within 24 hours and it remained undetectable throughout the experiment which lasted for 10 day (Figure 3.10A and Figure 3.10C). RT-PCR on RNA isolated from knockout cell lines two days after tetracycline removal (Figure 3.10B) yielded no detectable *TbKif2* mRNA indicating that the transcription of *TbKif2myc* was suppressed. The removal of *TbKif2myc* did not have any effect on the growth of Δ *TbKif2/TbKif2myc* (Figure 3.8B). In addition, comparisons between live *TbKif2* knockout cells with or without the expression of *TbKif2myc* indicated there were no gross changes in its cellular morphology or motility.

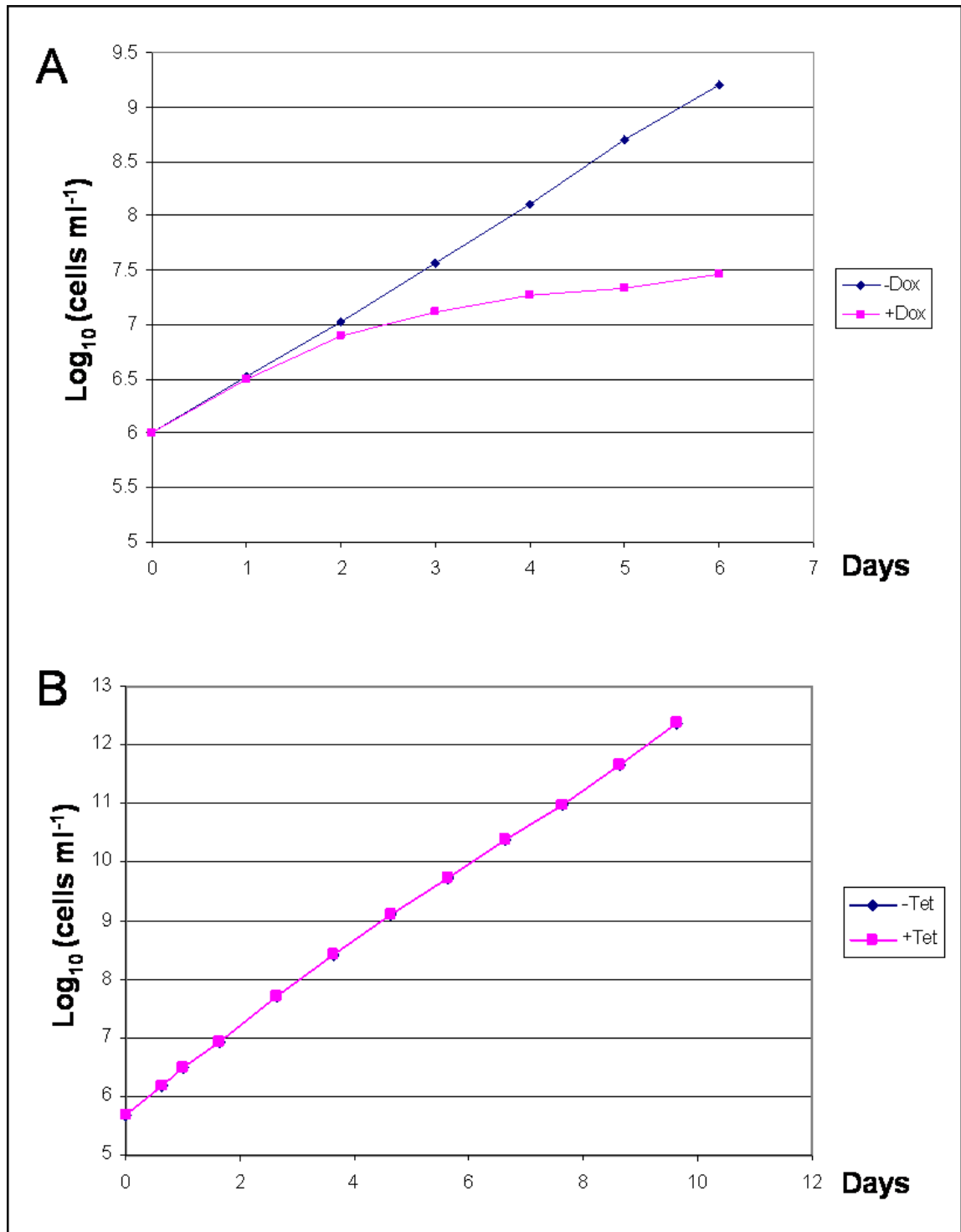


Figure 3.8: Growth curves (A) RNAi on 29-13/p2T7-*TbKif2* cells. The cells were diluted to a density 1×10^6 cells ml⁻¹ and counted every 24 hours in the presence or absence of doxycycline (Dox; $1 \mu\text{g ml}^{-1}$). The cells were diluted to 1×10^6 cells ml⁻¹ with fresh medium and doxycycline when required every 2 days. (B) Conditional knockout cell line $\Delta T b K i f 2 / T b K i f 2 m y c$. The cells were grown for 10 days with (+) or without (-) tetracycline (Tet, $1 \mu\text{g ml}^{-1}$). The cells were washed with SDM medium before being diluted down to a density of 5×10^5 cells ml⁻¹ with fresh medium. Every 2 days, the cultures were diluted to a density of 1×10^6 cells ml⁻¹ with fresh medium.

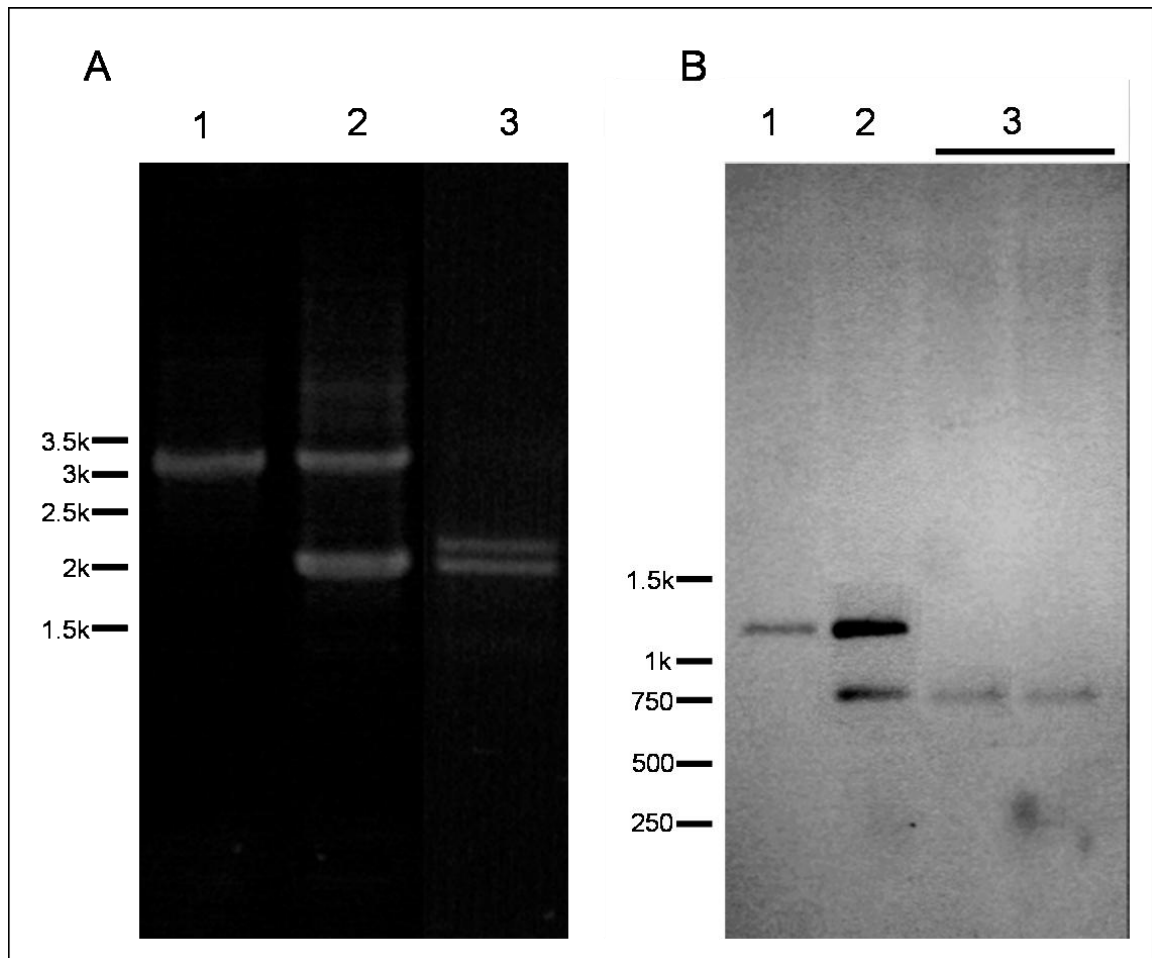


Figure 3.9: Creation of the conditional knockout $\Delta TbKif2/TbKif2myc$ cell line. (A) PCR results on genomic DNA obtained from wild-type 449 (1), $\Delta TbKif2::BSD/TbKif2/TbKif2myc$ (2) and $\Delta TbKif2/TbKif2myc$ (3). The forward 5'UTR and reverse 3'UTR was used in the PCR reaction. The band of approximately 3 kb in size represents the native *TbKif2* gene while the bands of approximately 2 kb represents the *BSD* and *NEO* resistance cassette used to replace the native *TbKif2* gene. (B) Southern blot analysis of the genomic DNA of wild-type 449 (1), $\Delta TbKif2::BSD/TbKif2/TbKif2myc$ (2) and $\Delta TbKif2/TbKif2myc$ (3). The genomic DNA was digested with *XhoI* / *HindIII* and probed using the 5'UTR of *TbKif2*. The deletion of the native *TbKif2* gene will result in the shift from ~1100 kb to ~700 kb.

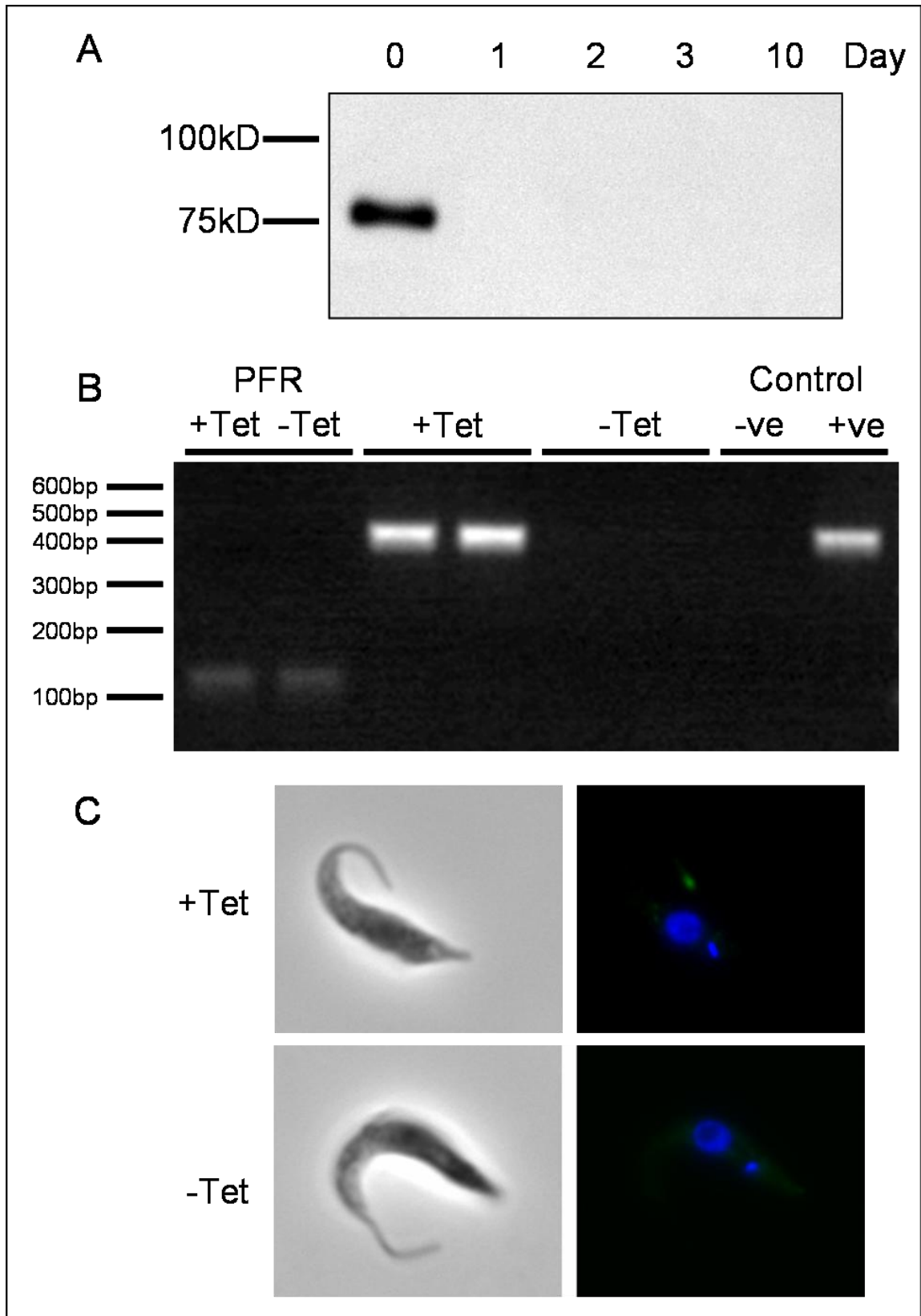


Figure 3.10: The depletion of TbKif2myc from conditional knockout $\Delta TbKif2/TbKif2myc$ cells. (A) Western blot analysis of $\Delta TbKif2/TbKif2myc$ cells grown for 10 days after removal of tetracycline. Samples for Western blotting were taken at every 24 hour interval for 10 days. Only samples from day 0, 1, 2, 3, and 10 were shown. (B) RT-PCR analysis of RNA extracts from $\Delta TbKif2/TbKif2myc$ cells grown with (+Tet) or without (-Tet) tetracycline for 2 days. The primers primer pairs used in the creation of the p2T7-*TbKif2* RNAi vector was used to detect the presence of *TbKif2myc* cDNA. The primers specific for the paraflagellar rod gene (*PFR*) was used as a loading control. The +ve and -ve control are PCR reactions with the presence (+ve) or absence (-ve) of genomic DNA (C) Immunofluorescence microscopy of procyclic $\Delta TbKif2/TbKif2myc$ cells (1,000 times magnification) grown with (+Tet) or without (-Tet) tetracycline for 2 days. The image on the left represents the phase contrast image and the left corresponds to the fluorescence image. The anti-myc antibody was used in the detection of TbKif2myc which is stained in green. The DAPI staining of the nucleus and kinetoplast is shown in blue.

3.4.3 TbKif2myc expression resulted in flagellum shortening and TbKif2 expression was not detected in procyclic or bloodstream forms using Western blots

It was previously reported in *Leishmania major* that LmjKIN13-2, a homologue to TbKif2 play a role in regulating the length of the flagellum (Blaineau et al., 2007). To determine if TbKif2 shares similar functions to LmjKIN13-2 in trypanosomes, measurements of the flagellum was compared between wild-type 449 cells and knockout $\Delta TbKif2/TbKif2myc$ cells with or without the expression of TbKif2myc (Figure 3.11). It was observed that there were no significant changes ($p = 0.77$) in the length between wild-type 449 cells when compared with knockout *TbKif2* cells where TbKif2myc expression was suppressed. This was in contrast with previously published results where it was shown that RNAi directed against *TbKif2* in procyclic cells resulted in flagellum lengthening (Blaineau et al., 2007). However, there was a significant reduction in flagellum length from $21.46 \pm 2.98 \mu\text{m}$ to $18.26 \pm 3.34 \mu\text{m}$ ($p < 0.01$), when TbKif2myc expression was induced in the knockout *TbKif2* cells.

Previously purified antibodies raised against wild-type TbKif2 were tested against $\Delta TbKif2/TbKif2myc$ cells expressing TbKif2myc (Figure 3.12). It was observed that the purified TbKif2 antibody was able to detect TbKif2myc when used in immunofluorescence and in Western blots. This indicated that the inability of the anti-TbKif2 antibody to detect the endogenous protein in wild-type cells was not due to epitope-masking or superficial problems, but be explained by the protein level of endogenous TbKif2 in procyclic form and bloodstream form which was below the detection threshold of anti-TbKif2. The

inability of anti-TbKif2 to detect endogenous TbKif2 in wild-type cells and the absence of detectable changes in flagellum length between wild-type and knockout *TbKif2* cells where TbKif2myc expression was suppressed suggests that *TbKif2* is not expressed in procyclic form trypanosomes. The RT-PCR results only show the presence of *TbKif2* mRNA but it is conceivable given the nature of expression regulation in trypanosomes (Vanhamme and Pays, 1995), the mRNA is not translated into protein.

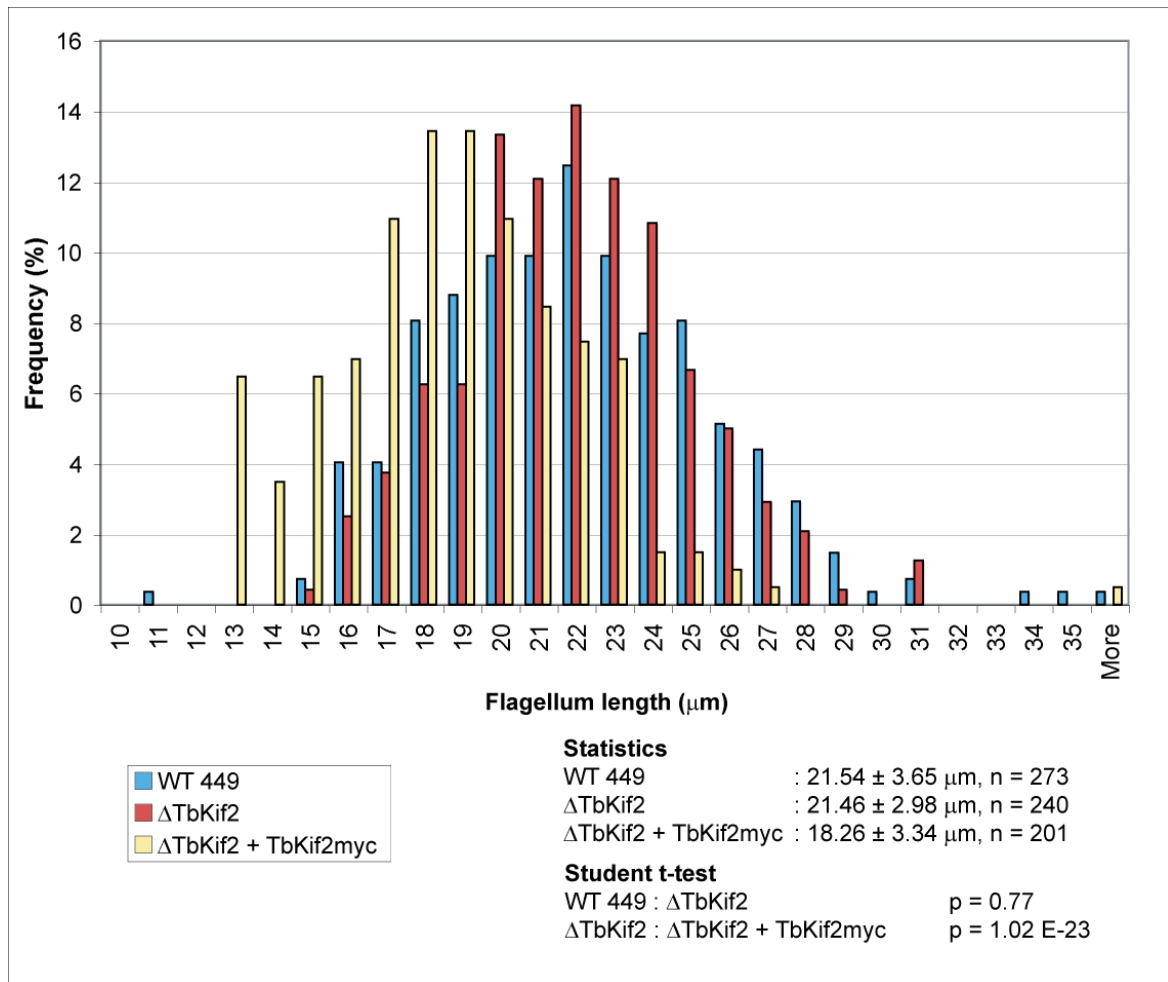


Figure 3.11: Histogram of flagellum length in wild-type (WT) 449 cells, Δ TbKif2/TbKif2myc cells grown with tetracycline (Δ TbKif2 + TbKif2myc) and Δ TbKif2/TbKif2myc cells grown without tetracycline induction (Δ TbKif2). The panel below the histogram contains descriptive statistics on the mean, standard deviation and number of flagellum measurements taken for each of the three different cell types. The student t-test is a statistical method for comparing the means of two normally distributed populations. Generally, a probability (p) of below 0.05 is used to determine if the means compared were significantly different.

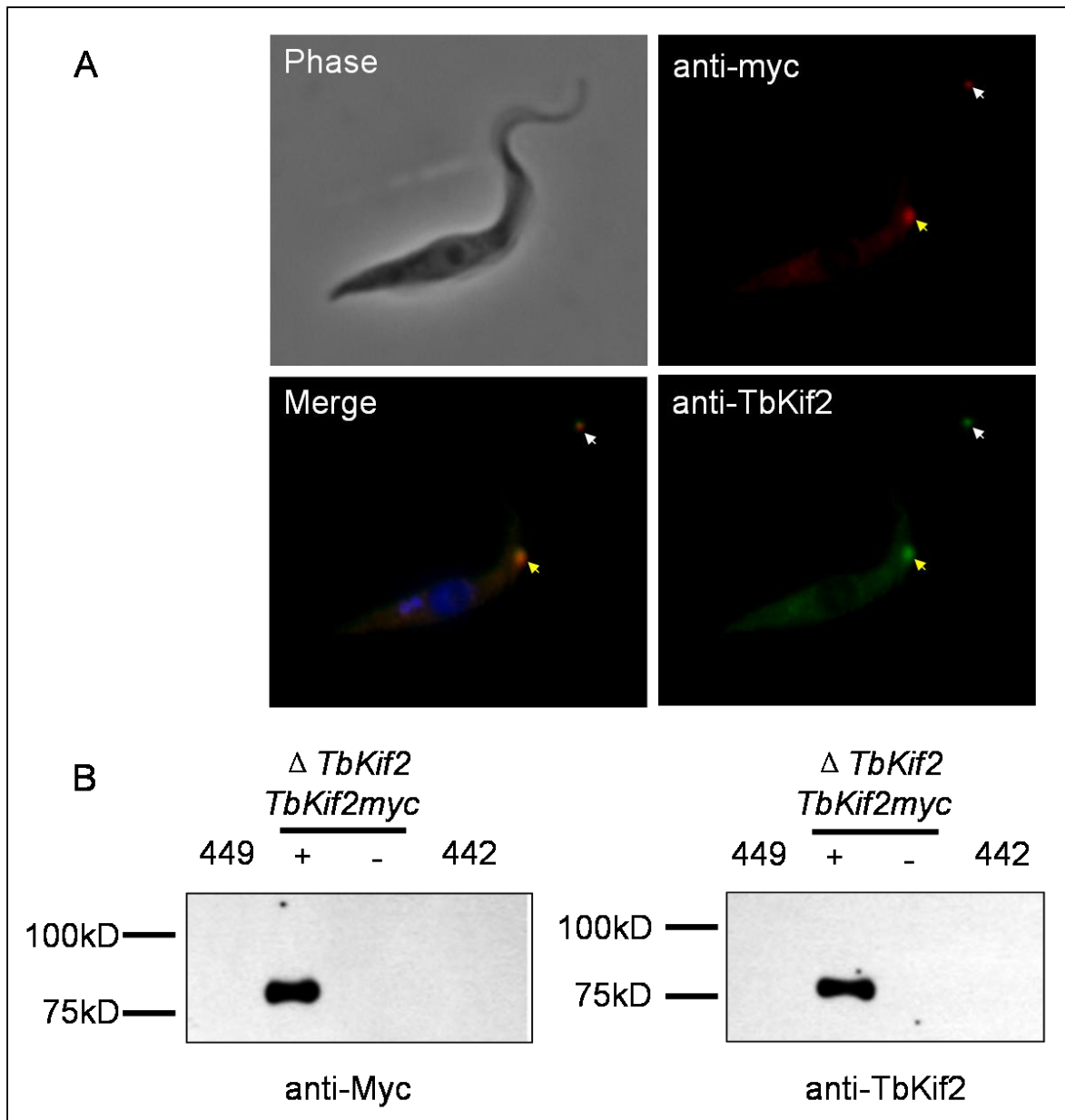


Figure 3.12: Immunofluorescence and Western blot analysis using anti-TbKif2 antibodies. (A) Immunofluorescence microscopy of procyclic $\Delta TbKif2/TbKif2myc$ cells expressing *TbKif2myc* (1,000 times magnification). The green staining is due to the staining from anti-TbKif2 and the red staining is from anti-myc. The merged image shows that both anti-TbKif2 and anti-myc antibodies recognise the same *TbKif2myc* protein. The blue signal in the merged image is due to the staining of the nucleus and the already divided kinetoplast (1N2K) by DAPI. The white arrow indicates the staining of *TbKif2myc* on the tip of the old flagellum while the yellow arrow indicates the staining of *TbKif2myc* on the tip of the new flagellum. **(B)** Western blot analysis using anti-TbKif2 and anti-myc antibodies on procyclic (449), bloodstream (442) and *TbKif2* knockout cells $\Delta TbKif2/TbKif2myc$. The lane marked (+) represents cells which are expressing *TbKif2myc* while the lane marked (-) represents cells not expressing *TbKif2myc*.

3.4.4 *TbKif8myc* is localised to the cell body

To investigate if *TbKif8* was expressed in procyclic and bloodstream forms of trypanosomes, RT-PCR was performed on cDNA of total RNA obtained from both procyclic 427 and bloodstream 442 cell lines. The results from the RT-PCR experiment shows that mRNA transcripts of *TbKif8* were present in both procyclic and bloodstream forms (Figure 3.13).

When the purified *TbKif8* antibodies were used, it was discovered that the presence of *TbKif8* was undetectable in Western blots of whole cell lysate of both procyclic and bloodstream forms of trypanosomes (Figure 3.14C). Likewise, *TbKif8* was undetectable by immunofluorescence microscopy using the same antibody (results were not shown). It was initially assumed that the purified *TbKif8* antibody failed to recognise native *TbKif8*. Therefore, in order to study the cellular distribution of *TbKif8*, a procyclic 449 cell line containing a tetracycline inducible exogenous copy of *TbKif8myc* was created. The expression of *TbKif8myc* in procyclic cells were successful as Western blots using anti-*myc* antibodies performed on tetracycline induced 449/*TbKif8myc* cells resulted in the detection of a single protein band of approximately 80 kD (Figure 3.14A), corresponding to the expected molecular mass of *TbKif8myc*. Immunofluorescence microscopy of procyclic cells expressing *TbKif8myc* revealed that *TbKif8myc* was localised exclusively to the cell body of the trypanosome excluding the nucleus and flagellum. This localisation of the cell body appeared to be diffused in nature and did not appear to be associated with any known organelle in the cell body. Furthermore, the localisation of *TbKif8myc* did not change throughout the cell cycle of the procyclic cells.

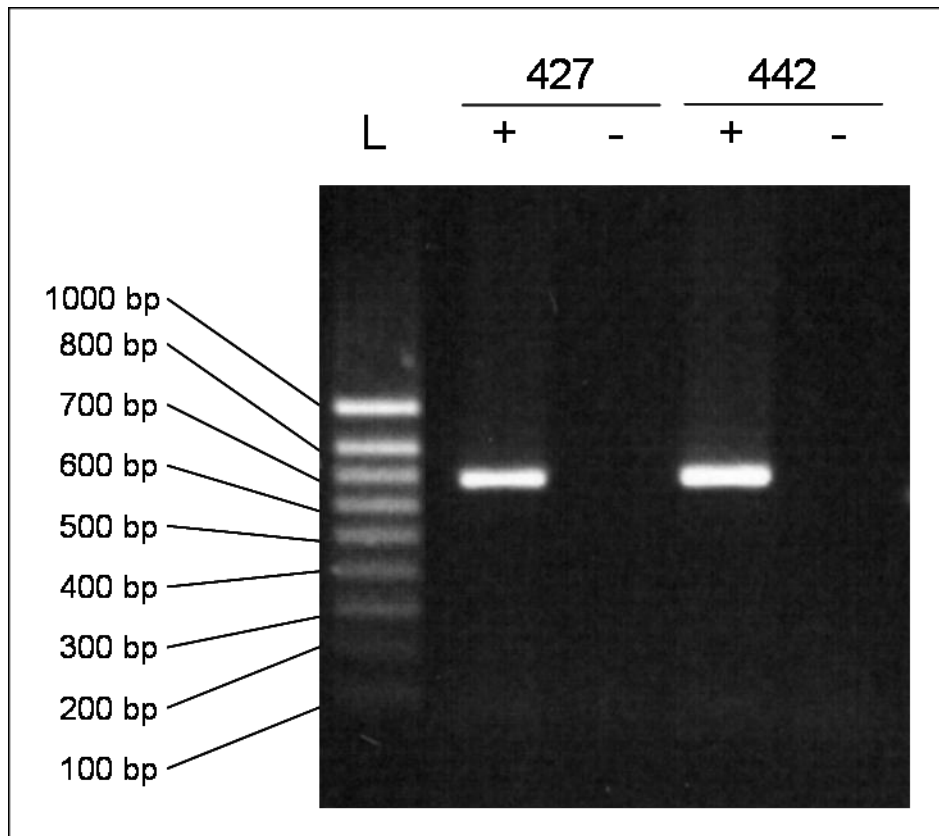


Figure 3.13: The RT-PCR results showing *TbKif8* is expressed in both the procyclic (427) form and bloodstream (442) form of trypanosomes. (L) indicates the DNA ladder with its corresponding length annotated, (+) indicates the results of the RT-PCR experiment using primers specific to *TbKif8*, (-) indicates the negative control (- reverse transcriptase enzyme).

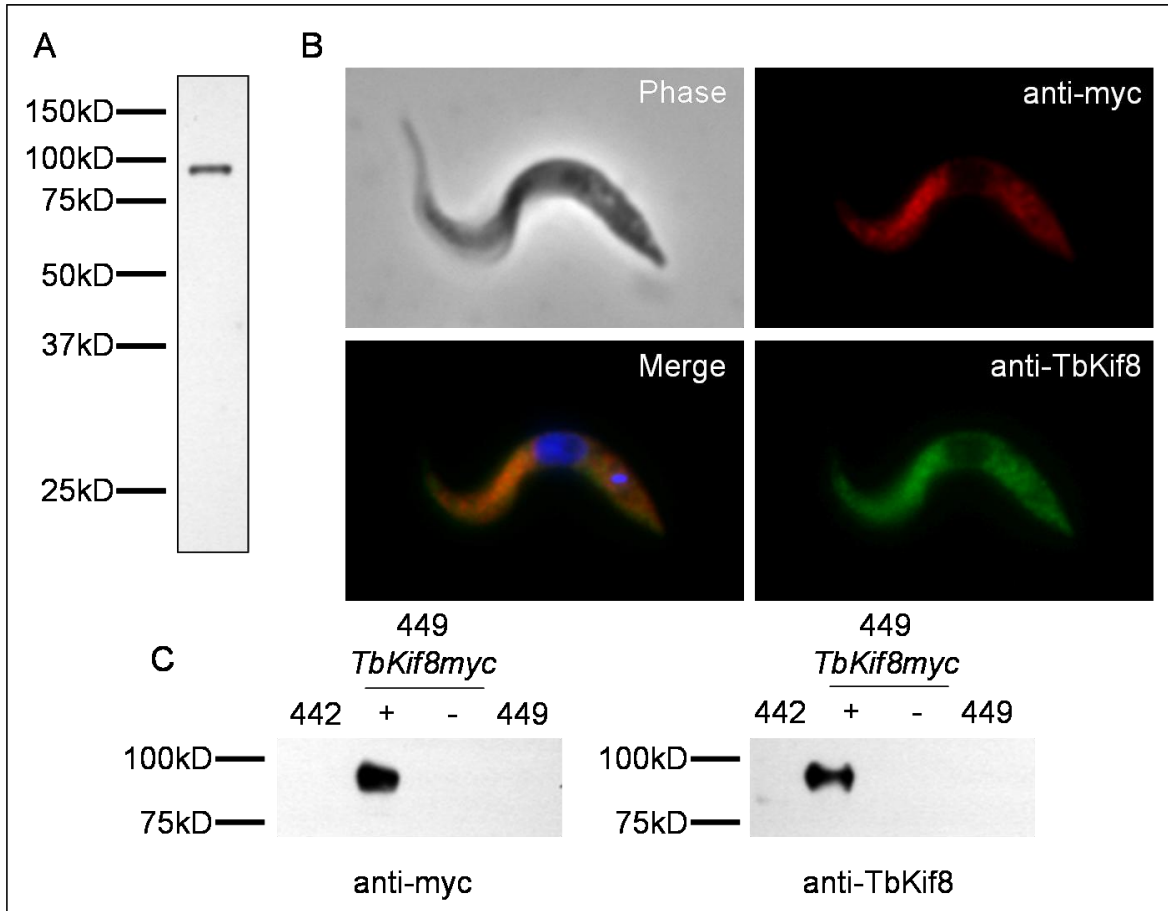


Figure 3.14: Immunofluorescence and Western blot analysis using cell lines expressing TbKif8myc. (A) Western blot of procyclic 449/*TbKif8myc* cells induced with tetracycline for 24 hours. The Western blot was probed by anti-myc. **(B)** Immunofluorescence microscopy of procyclic cells expressing TbKif8myc (1,000 times magnification). Green indicates the staining from anti-TbKif8 and red indicates the staining from anti-myc. The merged image shows that both anti-TbKif8 and anti-myc antibodies have a similar subcellular localisation supporting the idea that anti-TbKif8 was able to detect TbKif8myc. The blue signal in the merged image is due to the staining of the nucleus and kinetoplast by DAPI. **(C)** Western blot analysis using anti-TbKif8 and anti-myc on wild-type procyclic (449), bloodstream (442) and 449/*TbKif8myc* cell line. The lane marked (+) represents 449/*TbKif8myc* cells induced with tetracycline for 24 hours while the lane marked (-) represent control 449/*TbKif8myc* cells (-tetracycline).

3.4.5 TbKif8 expression was not detected in procyclic and bloodstream forms but RNAi targeting *TbKif8* resulted in a mild growth defect

To test if the purified TbKif8 antibody was able to detect TbKif8myc, cells expressing TbKif8myc was probed with anti-TbKif8 in Western blots and in immunofluorescence. In both cases, it was found that anti-TbKif8 was able to detect TbKif8myc (Figure 3.14B and Figure 3.14C). Therefore, the inability of anti-TbKif8 to detect the presence of endogenous TbKif8 was unlikely to be caused by epitope-masking or other technical issues but because the expression of endogenous TbKif8 at the protein level was below the detection threshold of anti-TbKif8 in Western blots and immunofluorescence microscopy.

RNAi directed against *Tbkif8* in 29-13/p2T7-*TbKif8* cells resulted in an impaired growth rate when compared to non-induced cells. However, apart from a mild growth defect in RNAi induced cells, no gross changes in cellular morphology were observed when the cells were examined under phase-contrast light microscopy.

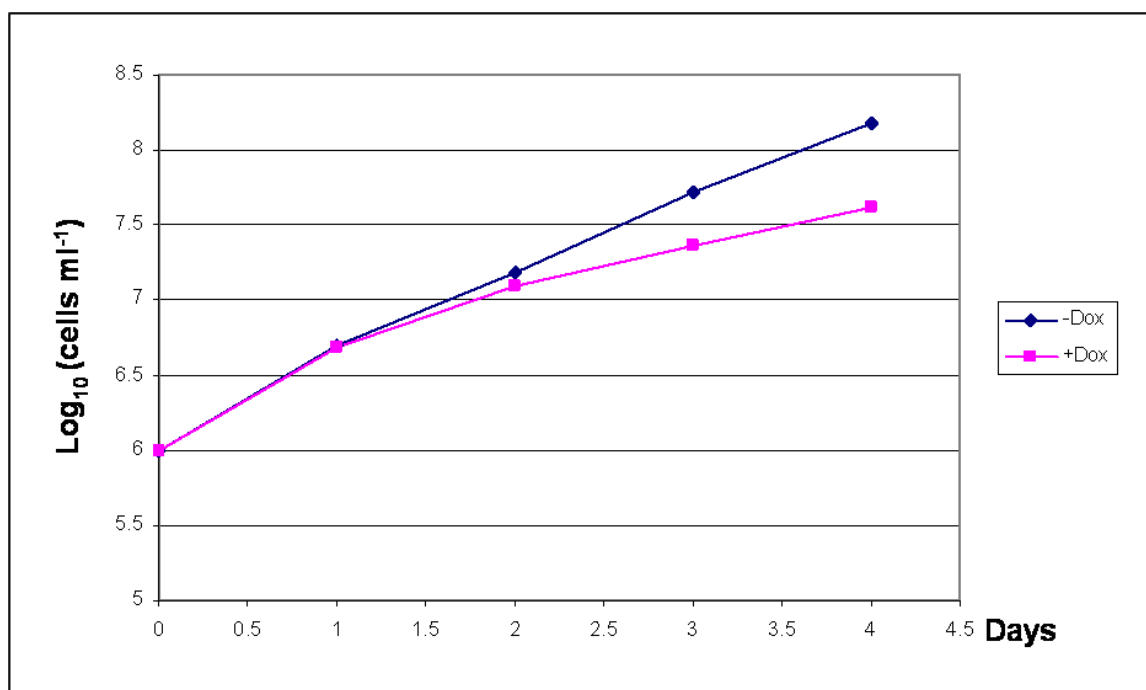


Figure 3.15: The growth curve of 29-13/p2T7-*TbKif8* cells in the presence (+) or absence (-) of 1 µg ml⁻¹ doxycycline (Dox).

3.4.6 TbKif9 is localised to the flagellum of both procyclic and bloodstream cells

To investigate the specificity of the affinity-purified polyclonal antibody anti-TbKif9, a Western blot using the whole cell lysate of procyclic strain 427 cells was performed. The Western blot resulted in the identification of a single protein band of approximately 90 kD in size corresponding to the expected size of TbKif9 of 87 kD (Figure 3.16A). Immunofluorescence microscopy performed using anti-TbKif9 on both procyclic and bloodstream cells revealed a staining along the entire length of the flagellum (Figure 3.16B). The staining in the flagellum is persistent throughout the cell cycle and is present on the new and mature flagellum during cell division. In addition, double labelling experiments using the paraflagellar rod (PFR) antibody L8C4 and anti-TbKif9 confirms that TbKif9 is localised to the entire length of the flagellum. The staining of anti-TbKif9 appear slightly shifted distal to the PFR staining in relation to the cell body, potentially indicating an axonemal localisation.

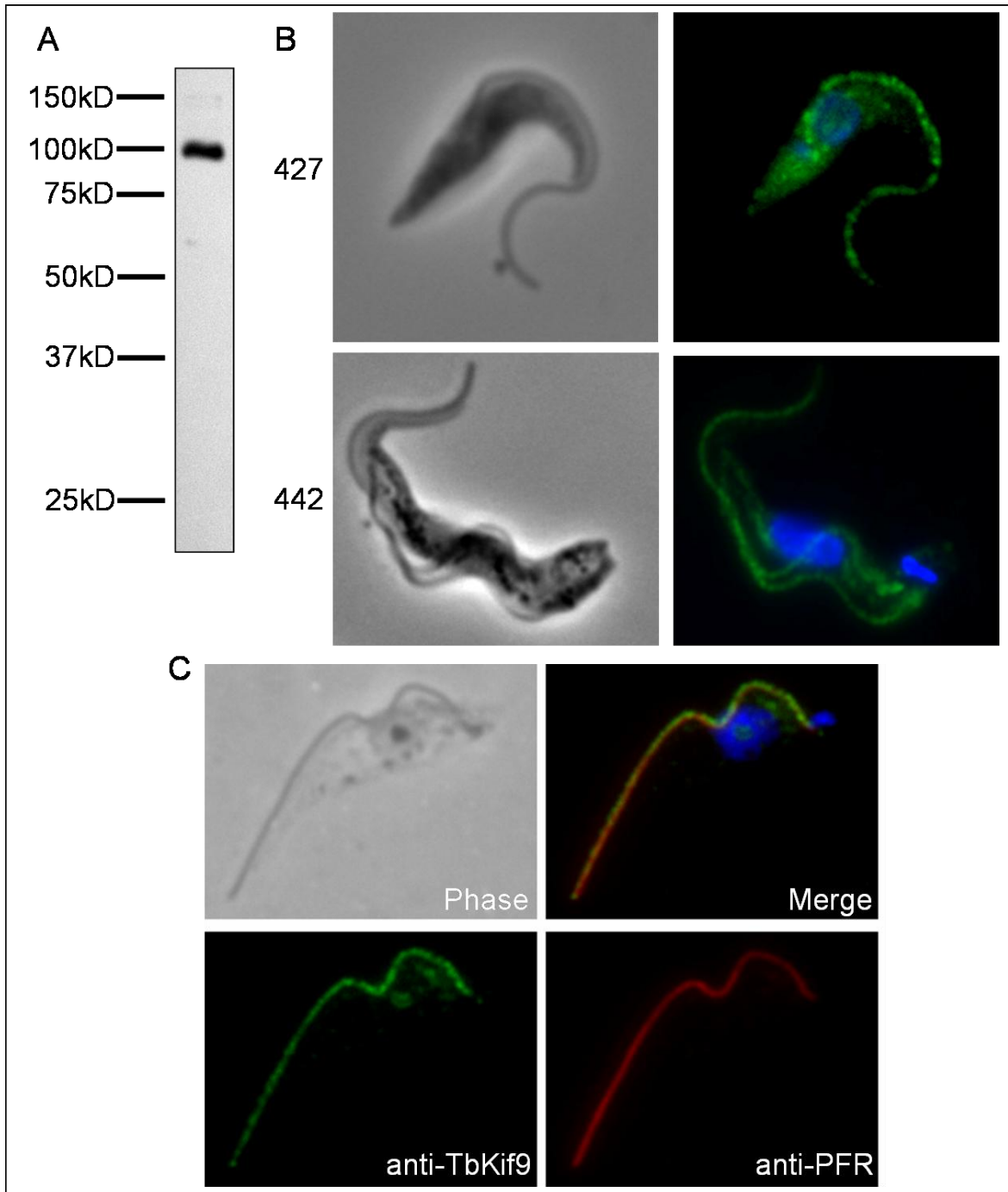


Figure 3.16: Western blot and subcellular localisation of TbKif9. (A) Western blot using anti-TbKif9 on procyclic strain 427 cells. (B) Immunofluorescence microscopy (1,000 times magnification) on procyclic (427) and bloodstream (442) cells. The left panel represents phase contrast images while the right panel represents the merged fluorescence images of anti-TbKif9 (green) and DAPI. DAPI stains the DNA located in the nucleus and kinetoplast of the trypanosome and is shown in blue. (C) A double label experiment on NP40 extracted procyclic strain 427 cells. The paraflagellar rod which outlines the entire length of the flagellum is stained by L8C4 which is indicated in red (Kohl et al., 1999) while the localisation of TbKif9 is shown in green.

3.4.7 TbKif9 detergent solubility is ATP dependent

Kinesins have been shown to interact with microtubules in an ATP-dependent manner (Cole et al., 1992; Hertzler et al., 2006). A recent paper described a *Leishmania donovani* kinesin LdK39, to be partially associated with the detergent-extracted cytoskeleton in an ATP-dependent manner (Gerald et al., 2007). To test if TbKif9 shares similar characteristics, procyclic strain 427 cells were extracted with non-ionic detergent NP40 in the presence and absence of ATP and subsequently analysed by Western blots. Results from Western blot analysis shows that TbKif9 was localised to the detergent-insoluble (cytoskeleton) fraction when extracted in the absence of ATP (Figure 3.17). TbKif9 was partially found in the soluble fraction when cells were extracted in the presence of ATP. This result provides evidence that TbKif9 is associated with the cytoskeleton in an ATP-dependent manner. When immunofluorescence microscopy is performed on detergent extracted cells, the flagellar staining of anti-TbKif9 remained supporting the conclusion that the staining of the flagellum is due to TbKif9 (Figure 3.16C).

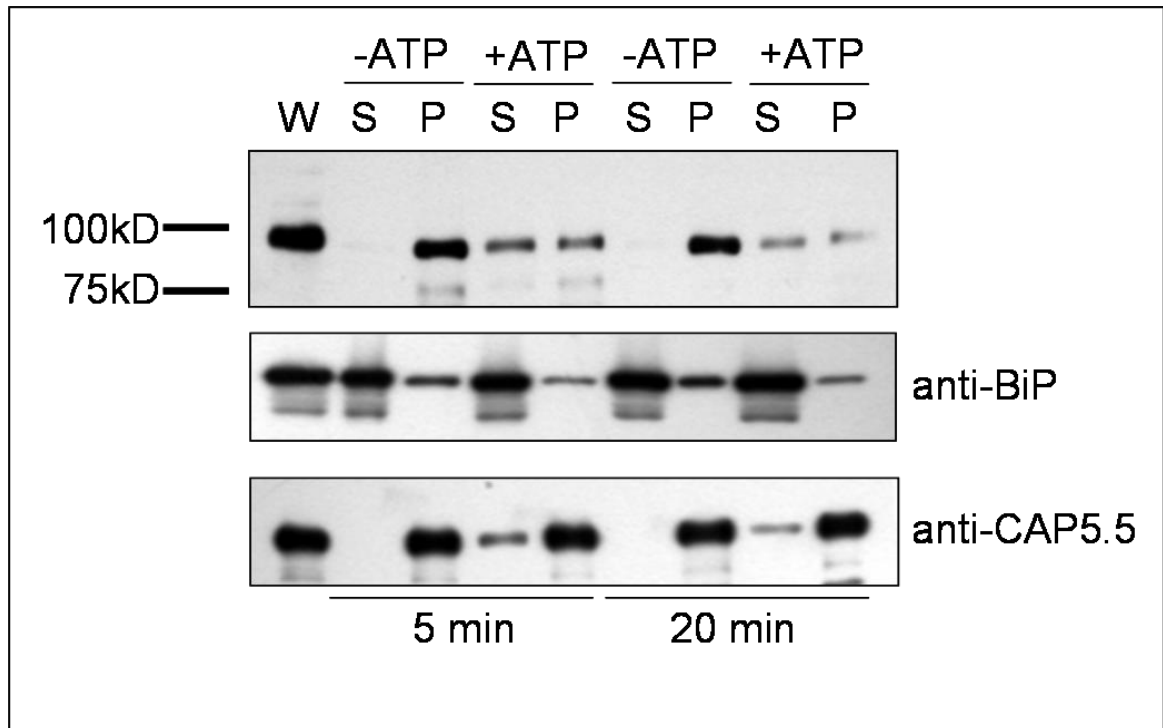


Figure 3.17: Western blot analysis of TbKif9 response to detergent extraction and treatment with ATP. Each lane was loaded with an equivalent of 2×10^6 cells which was either untreated whole cells (W), NP40 soluble (S) or insoluble (P) fractions. The lanes where the cells were extracted in the presence of ATP are indicated with the (+ATP) symbol. Anti-BiP is a marker for the endoplasmic reticulum (Bangs et al., 1993) and anti-CAP5.5 is a marker for the cytoskeleton (Hertz-Fowler et al., 2001). Both BiP and CAP5.5 is used in this experiment as a control to show the level of separation between detergent-soluble and insoluble fractions.

3.4.8 Depletion of TbKif9 through RNAi had no observable effect in procyclic strain 29-13 cells

To study the function of TbKif9 in trypanosomes, procyclic strain 29-13 cells were transfected with the p2T7-*TbKif9* RNAi vector. The production of dsRNA against *TbKif9* was induced by the addition of doxycycline and resulted in the depletion of TbKif9 protein within 24 hours (Figure 3.18A). The presence of TbKif9 on Western blots remained undetectable throughout the experiment which lasted for 10 days (Figure 3.18A). Despite the reduction of TbKif9 protein levels, there was no change in the growth rate between induced and non-induced populations (Figure 3.18B). In addition, comparisons between both populations under light microscopy indicated that there were no observable gross changes in the cellular morphology or motility.

When 29-13/p2T7-*TbKif9* cells induced with doxycycline for 4 days were examined using immunofluorescence microscopy, it was observed that the flagellum staining of anti-TbKif9 remained (Figure 3.18C). The staining of anti-TbKif9 on the flagellum appeared to be of similar intensity when compared with non-induced 29-13/p2T7-*TbKif9* cells. This raised the possibility that anti-TbKif9 is not recognising TbKif9 in fluorescence microscopy and the staining in the flagellum was due to cross-reactivity of anti-TbKif9 with a different protein. In order to test if anti-TbKif9 is able to detect TbKif9 in fluorescence microscopy, procyclic cells expressing a myc tagged version of TbKif9 (TbKif9myc) were created.

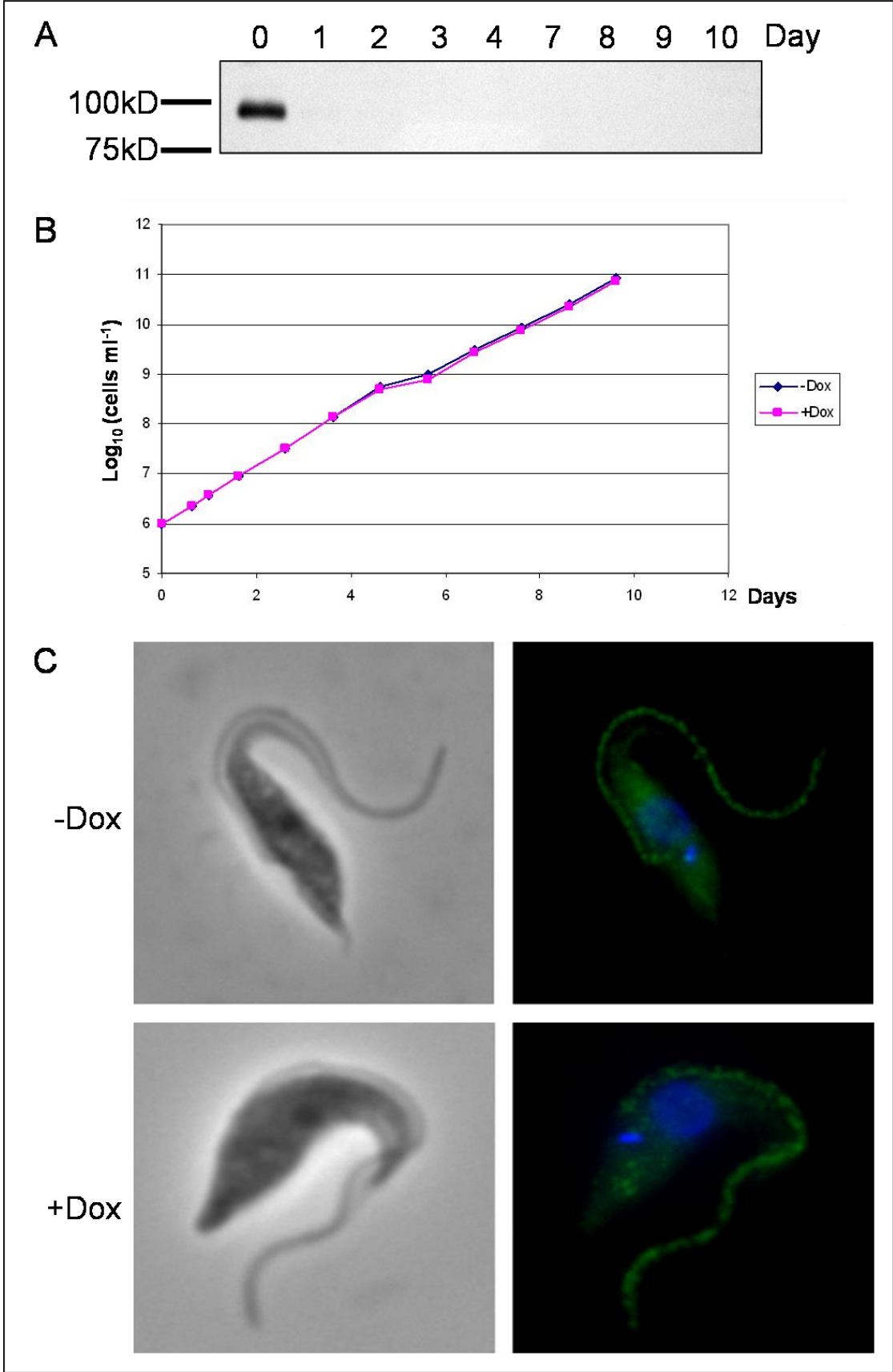


Figure 3.18: RNAi on procyclic 29-13/p2T7-*TbKif9* cells. (A) Western blot analysis of 29-13/p2T7-*TbKif9* cell samples. Samples for Western blotting were taken at 24 hour intervals after the addition of doxycycline (Dox, 1 $\mu\text{g ml}^{-1}$) for 10 days. Only samples from day 0, 1, 2, 3, 4, 7, 8, 9 and day 10 were shown. (B) Growth curve of procyclic 29-13/p2T7-*TbKif9* cells induced with doxycycline (+dox). Non-induced (-dox) 29-13/p2T7-*TbKif9* cells were used as a control. (C) Immunofluorescence microscopy (1,000 times magnification) of 29-13/p2T7-*TbKif9* cells induced with doxycycline for 4 days and probed with anti-*TbKif9*. The images on the left panel are phase contrast images for the corresponding immunofluorescence image on the left panel. The staining of anti-*TbKif9* is shown in green while the staining in blue represents the nucleus and kinetoplast of the trypanosome.

3.4.9 Anti-*TbKif9* is able to detect ectopically tagged *TbKif9myc*

Procyclic strain 449 cells with a tetracycline inducible exogenous copy of *TbKif9myc* were subsequently created. The Western blots on 449/*TbKif9myc* cells induced with tetracycline for 24 hours resulted in the detection of a single protein band of similar size to native *TbKif9* (90 kD) when probed with anti-myc (Figure 3.19A). When 449/*TbKif9myc* induced cells were probed with anti-*TbKif9* in Western blots, it was found that anti-*TbKif9* reacted against a protein band of similar size with *TbKif9* corresponding to the ectopically expressed *TbKif9myc* (Figure 3.19A). However, when induced 449/*TbKif9myc* cells were examined under fluorescence microscopy using anti-myc, a cell body staining excluding the nucleus and flagellum was observed. Double labelling fluorescence microscopy using anti-*TbKif9* and anti-myc was also performed on tetracycline induced 449/*TbKif9myc* cells (Figure 3.19B). The staining of anti-*TbKif9* was shown to have a similar cell body staining to anti-myc in addition to the flagellum stain. An image overlay of anti-*TbKif9* and anti-myc shows a perfect merge of the cell body staining from anti-*TbKif9* and anti-myc supporting the conclusion that anti-*TbKif9* was able to detect *TbKif9myc*. This indicates that the flagellar staining obtained with anti-*TbKif9* is not due to cross-reactivity with a different protein.

It is possible that the addition of the myc tag at the C-terminus of *TbKif9myc* resulted in the mistargeting and exclusion of *TbKif9myc* from the flagellum. However, further work is required to ascertain this possibility.

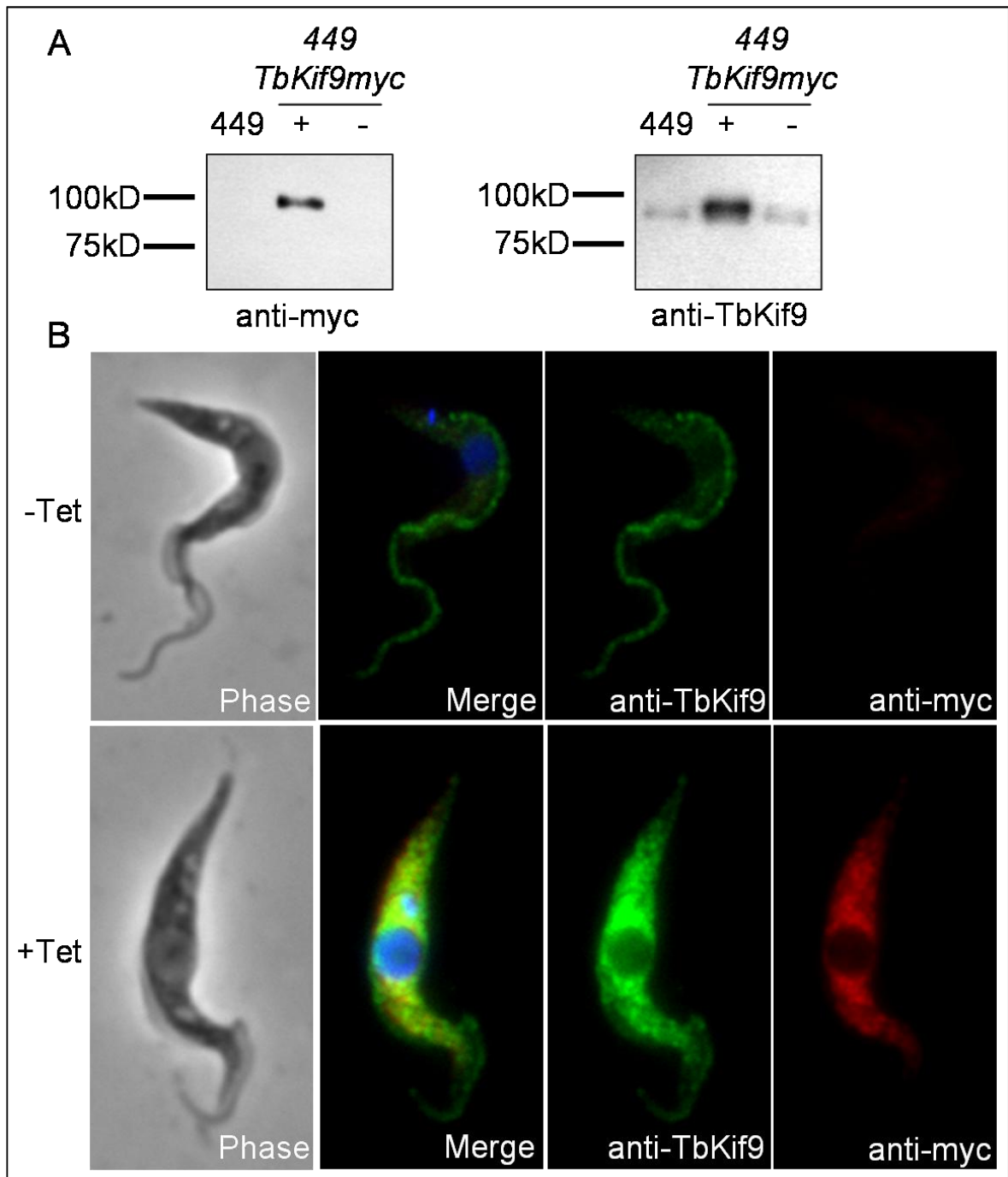


Figure 3.19: Immunofluorescence and Western blot analysis on 449/*TbKif9myc* cells induced with tetracycline ($1\mu\text{g ml}^{-1}$) for 24 hours. (A) Western blot analysis using anti-TbKif9 and anti-myc antibodies on procyclic (449) and 449/*TbKif9myc* cell line. The lane (+) are cells expressing *TbKif9myc* while (-) are cells not expressing *TbKif9myc*. (B) Immunofluorescence microscopy (1,000 times magnification) of procyclic cells expressing *TbKif9myc*. The cells were labelled with anti-TbKif9 (green) and anti-myc (red). The blue stain in the merged image represents the nucleus and kinetoplast.

3.4.10 TbKif15 is associated to the mitochondrion in procyclic and bloodstream cells

To test the specificity of purified TbKif15 polyclonal antibodies, a Western blot was performed on whole cell lysate of procyclic strain 427 cells. It was found that anti-TbKif15 recognises a single protein band of approximately 60 kD (Figure 3.20A). This corresponds well with the expected size of TbKif15 of 54 kD.

When anti-TbKif15 was used in immunofluorescence microscopy on procyclic strain 427 cells, a cell body staining with a pattern congruent with of the distribution of the single mitochondrion was observed. The mitochondrial localisation was confirmed when a mitochondrial specific dye, Mitotracker was used in tandem with anti-TbKif15 (Figure 3.20B). In bloodstream cells, anti-TbKif15 staining was reduced in comparison to procyclic cells (Figure 3.21). This change is expected as the development of the mitochondrion in bloodstream cells is repressed as a response to metabolic adaptation (Priest and Hajduk, 1994; Schneider, 2001). It was also observed that the staining of the cell body by anti-TbKif15 in bloodstream forms increased in cells undergoing cell division suggesting that TbKif15 may play a role during the segregation of the mitochondrion.

Efforts to characterise the function of TbKif15 using RNAi were unsuccessful. Procyclic strain 29-13 cells containing the p2T7-*TbKif15* RNAi vector did not show any reduction in TbKif15 expression when induced with doxycycline and consequently no RNAi-induced phenotype was observed (Figure 3.22).

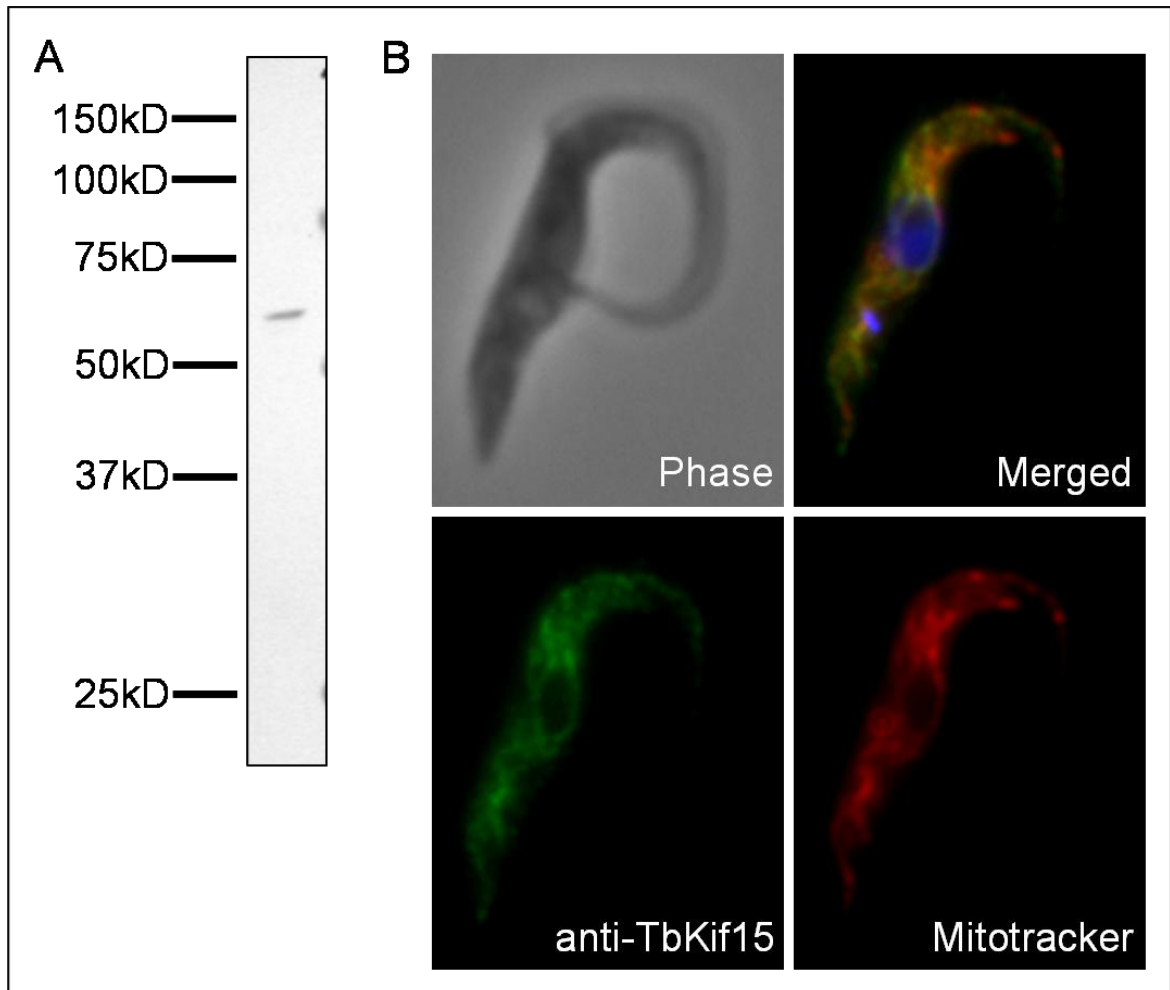


Figure 3.20: Western blot and subcellular localisation of TbKif15. (A) Western blot of whole cell lysate of procyclic strain 427 cells probed with anti-TbKif15. (B) Immunofluorescence microscopy (1,000 times magnification) of procyclic strain 427 cells stained with Mitotracker (red) and anti-TbKif15 (green). The blue stain (DAPI) in the merged image represents the nucleus and kinetoplast.

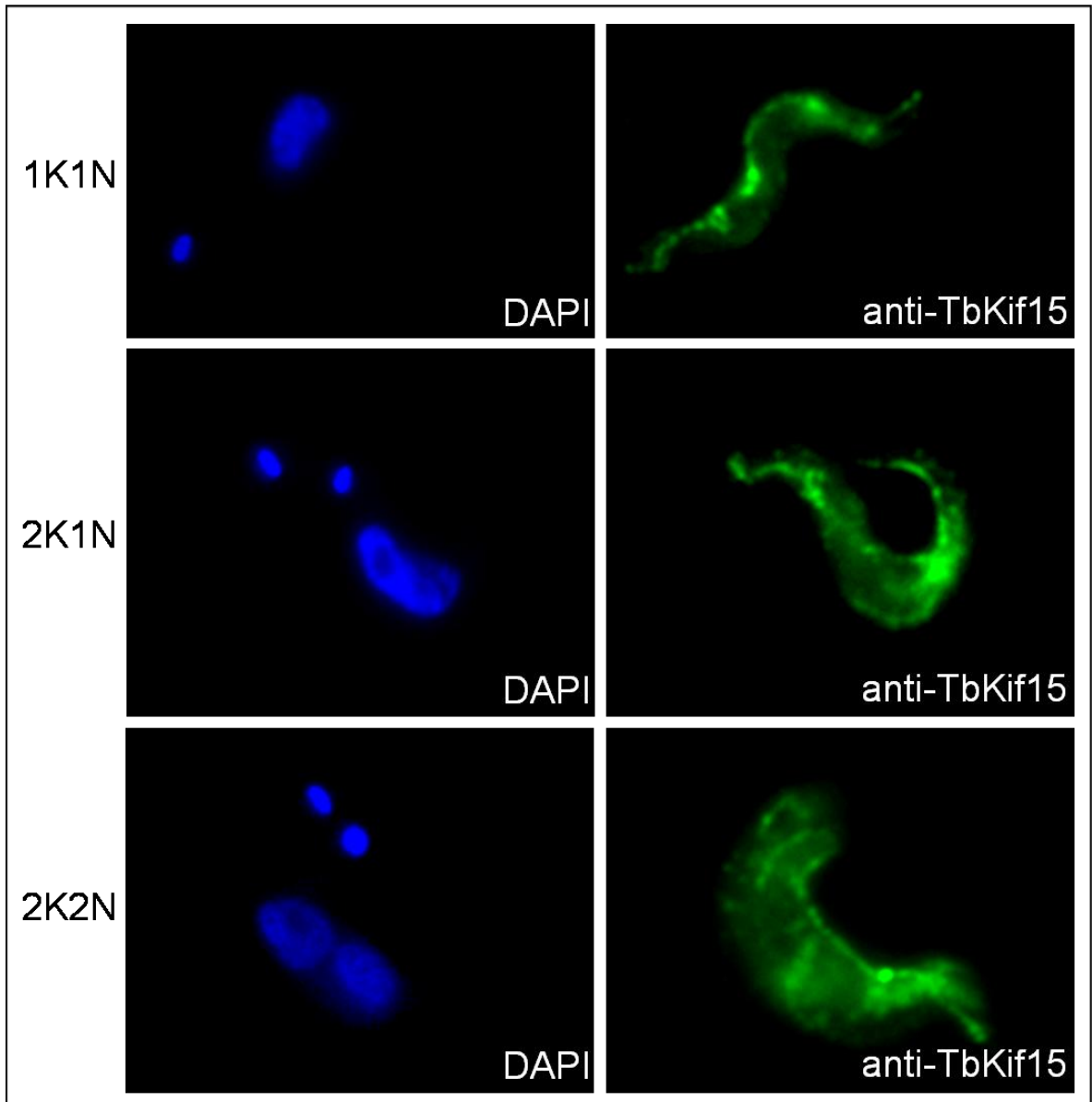


Figure 3.21: Immunofluorescence microscopy (1,000 times magnification) of bloodstream strain 442 cells probed with anti-TbKif15 (green). Nuclear and mitochondrial DNA is stained with DAPI and is shown in blue. Cells in the G_1/S phase have 1 kinetoplast and 1 nucleus (1K1N), cells undergoing G_2/M phase has 2 kinetoplast and 1 nucleus (2K1N) while cells undergoing cytokinesis have 2 kinetoplast and 2 nucleuses (2K2N).

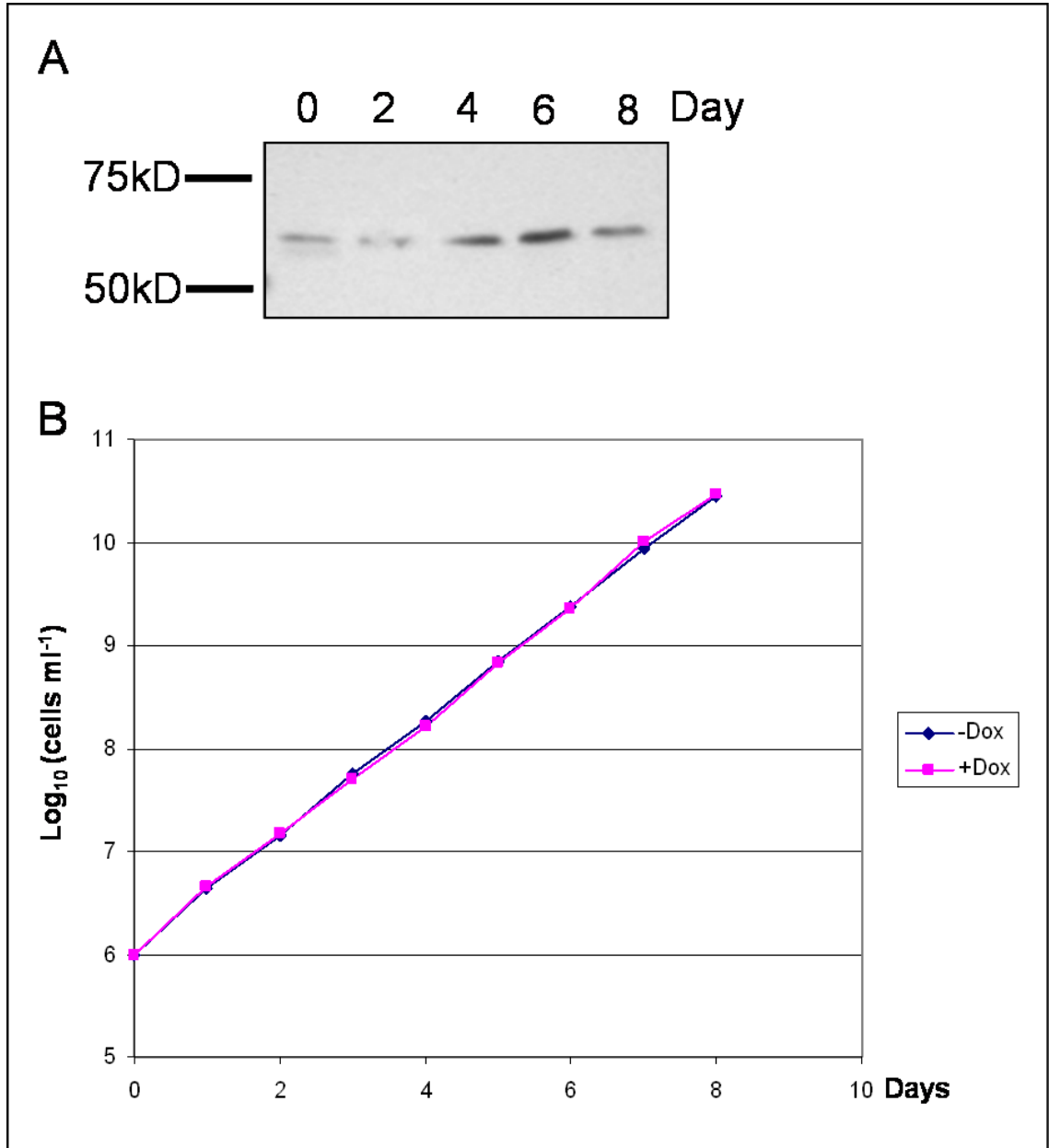


Figure 3.22: Effect of doxycycline induction on 29-13/p2T7-*TbKif15* cells. (A) Western blot of 29-13/p2T7-*TbKif15* cells induced with the addition of 1 $\mu\text{g ml}^{-1}$ doxycycline (Dox). (B) A growth curve of 29-13/p2T7-*TbKif15* cells grown in the presence (+dox) or absence (-dox) of doxycycline.

3.4.11 TbKif27 localises to the cell body in procyclic cells

To test the specificity of affinity-purified antibody anti-TbKif27, a Western blot was performed on the whole cell lysate of procyclic strain 427 cells. It was found that anti-TbKif27 reacts strongly to a single protein band of approximately 60 kD in size (Figure 3.23A). This corresponds well with the expected size of TbKif27 of 63 kD.

Immunofluorescence microscopy on formaldehyde fixed procyclic strain 427 cells using anti-TbKif27 revealed a cell body staining which excludes the nucleus and flagellum of the cell. The staining pattern appeared to be granular and the staining intensity throughout the cell body was homogenous (Figure 3.24A). Based on the staining pattern, cellular structures potentially associated with TbKif27 are the cortical cytoskeleton or the endoplasmic reticulum (ER). When comparisons were made between the staining pattern during immunofluorescence microscopy of anti-TbKif27 and an ER specific antibody BiP was made, it was observed that BiP had a distinctly different staining pattern compared to TbKif27 (Figure 3.24B). A double labelling experiment using anti-CAP5.5 (a cytoskeleton protein marker) and anti-TbKif27 was also performed (Figure 3.24A). It was observed that CAP5.5 had a similar distribution with TbKif27 under fluorescence microscopy. However, CAP5.5 revealed a more pronounced filamentous staining pattern in contrast to the granular staining pattern of TbKif27.

Detergent extraction experiments on procyclic strain 427 cells also reveal that TbKif27 is detergent-soluble (Figure 3.23B). The addition of ATP did not change the response of TbKif27 during extraction with NP40.

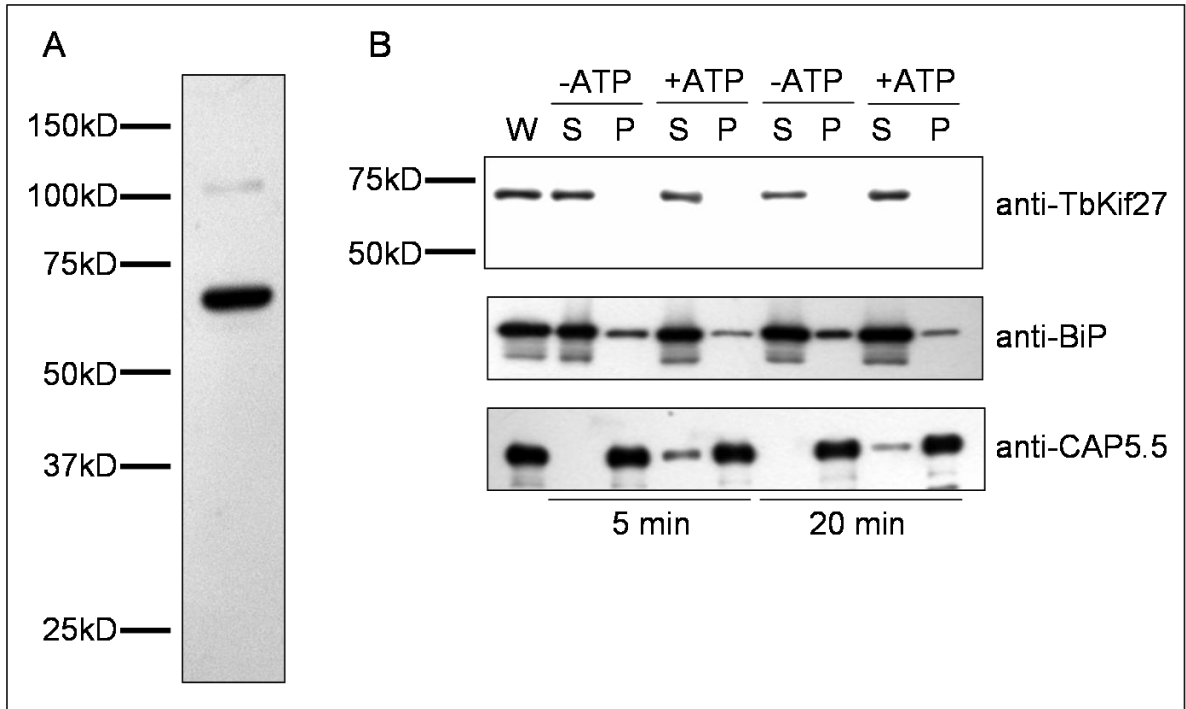


Figure 3.23: Western blot analysis using anti-TbKif27. (A) Western blot of whole cell lysate of procyclic strain 427 cells probed with anti-TbKif27. **(B)** Western blot analysis of TbKif27 response to detergent extraction and treatment with MgATP. Each lane was loaded with an equivalent of 2×10^6 cells which was either untreated whole cells (W), NP40 soluble (S) or insoluble (P) fractions. The lanes where cells were extracted in the presence of MgATP are indicated with the (+ATP) symbol. Anti-BiP is a marker for the endoplasmic reticulum (Bangs et al., 1993) and anti-CAP5.5 is a marker for the cytoskeleton (Hertz-Fowler et al., 2001). Both BiP and CAP5.5 is used in this experiment as a control to show the level of separation between detergent-soluble and insoluble fractions.

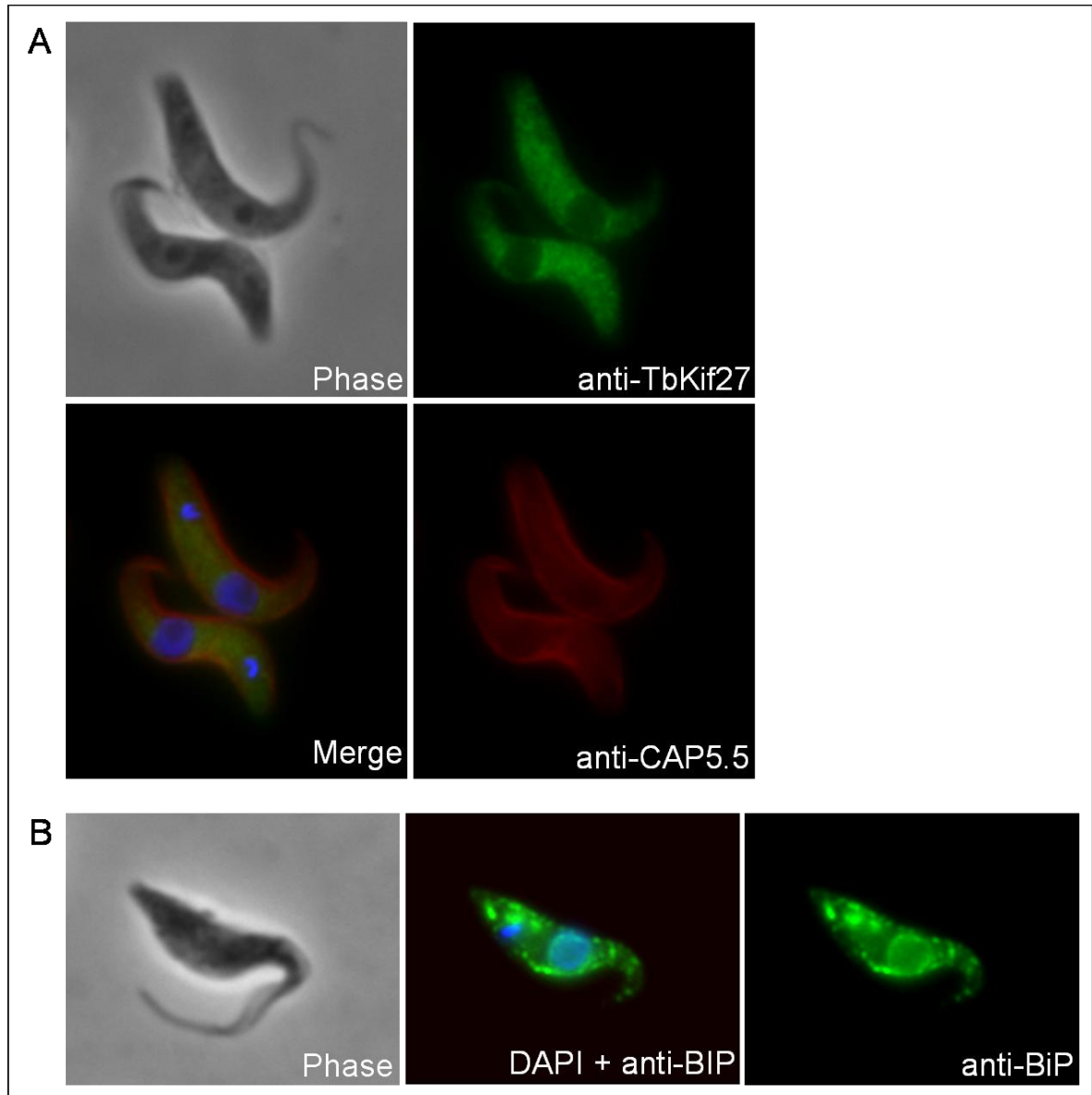


Figure 3.24: Immunofluorescence microscopy (1,000 times magnification) of TbKif27 in procyclic strain 427 cells. (A) A double labelling experiment with anti-TbKif27 (green) and anti-CAP5.5 (red). CAP5.5 is a protein which is associated with the microtubule corset of trypanosomes (Hertz-Fowler et al., 2001). The blue stain in the merged image is due to DAPI staining the kinetoplast and nucleus. (B) An immunofluorescence image of cells stained with anti-BiP (green). BiP is a protein marker for the endoplasmic reticulum (Bangs et al., 1993).

3.4.12 Depletion of TbKif27 via RNA interference resulted in a growth defect in procyclic strain 29-13 cells

To probe for the function of TbKif27, RNAi was performed on procyclic strain 29-13 cells using the vector p2T7-*TbKif27*. The production of *TbKif27* double stranded RNA resulted in the depletion of TbKif27 in Western blots (Figure 3.25A). After three days of induction with doxycycline, TbKif27 was undetectable in Western blots and remained undetectable after day five of induction. The depletion of TbKif27 was also observed during immunofluorescence microscopy where the cell body staining of anti-TbKif27 was almost undetectable at day four of induction (Figure 3.25B).

The depletion of TbKif27 through RNAi resulted in a reduction in the growth rate of procyclic cells (Figure 3.26A). However, no gross morphological phenotypes were observed and TbKif27 depleted cells appeared to be normal when examined under phase contrast and fluorescence microscopy (Figure 3.25B). When TbKif27 depleted cells were analysed via FACS for cellular DNA content, it was observed that there was a slight increase in the amount of zoids (1K0N) between control (1.1%) and TbKif27 depleted (3.1%) cell populations (Figure 3.26B). There was also a decrease in the G1 (1K1N) population from 52.9% in control cells to 46.9% in TbKif27 depleted cells.

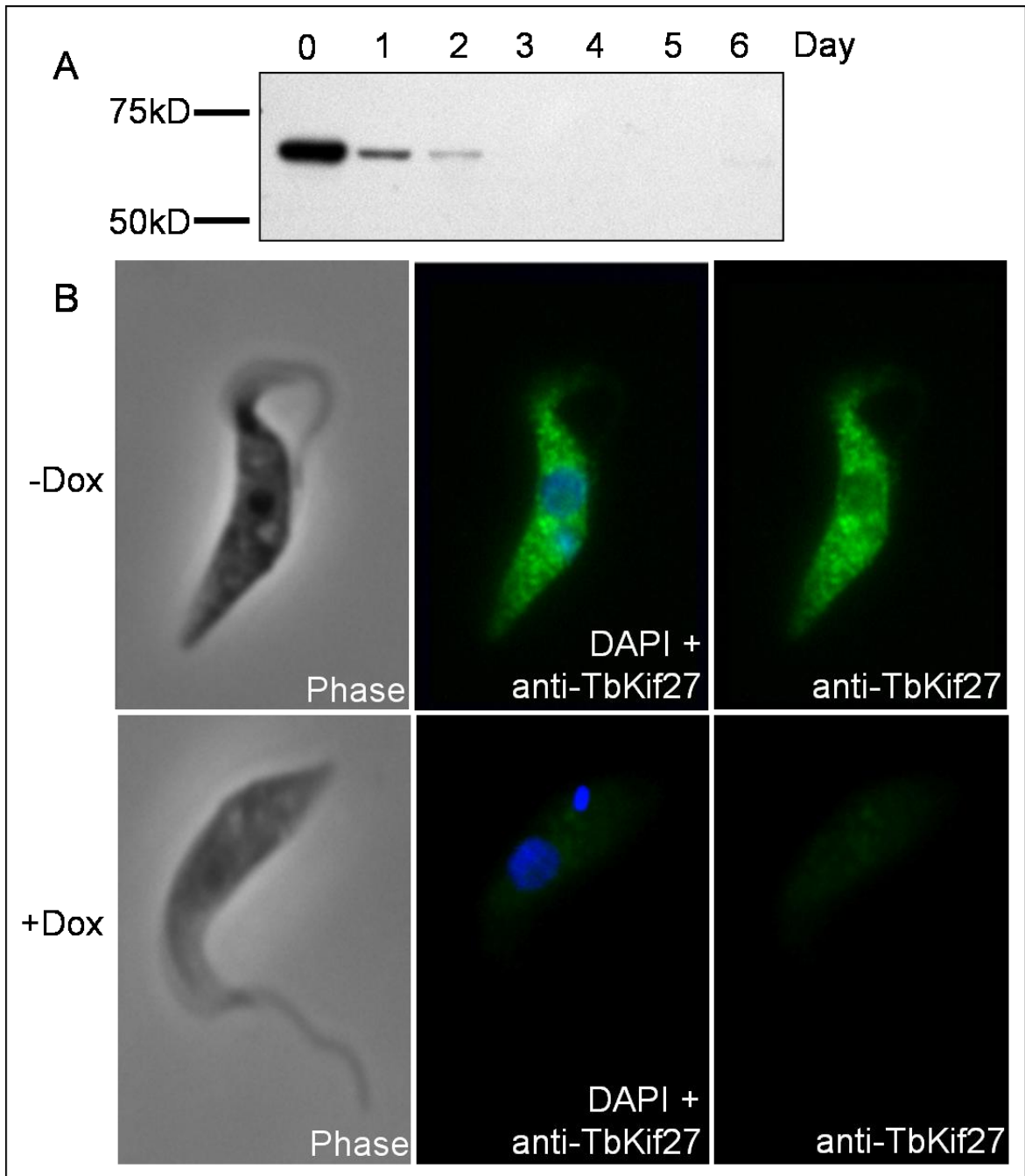


Figure 3.25: RNAi analysis of 29-13/p2T7-*TbKif27* cells. (A) A Western blot showing the effects of RNAi induced depletion of *TbKif27*. Samples for Western blotting were taken at every 24 hour intervals for 6 days. (B) Immunofluorescence microscopy (1,000 times magnification) of 29-13/p2T7-*TbKif27* cells probed with anti-*TbKif27*. (-Dox) control, (+Dox) RNAi cell induced for 4 days. The staining of anti-*TbKif27* is shown in green. The colour blue represents DAPI staining the kinetoplast and nucleus.

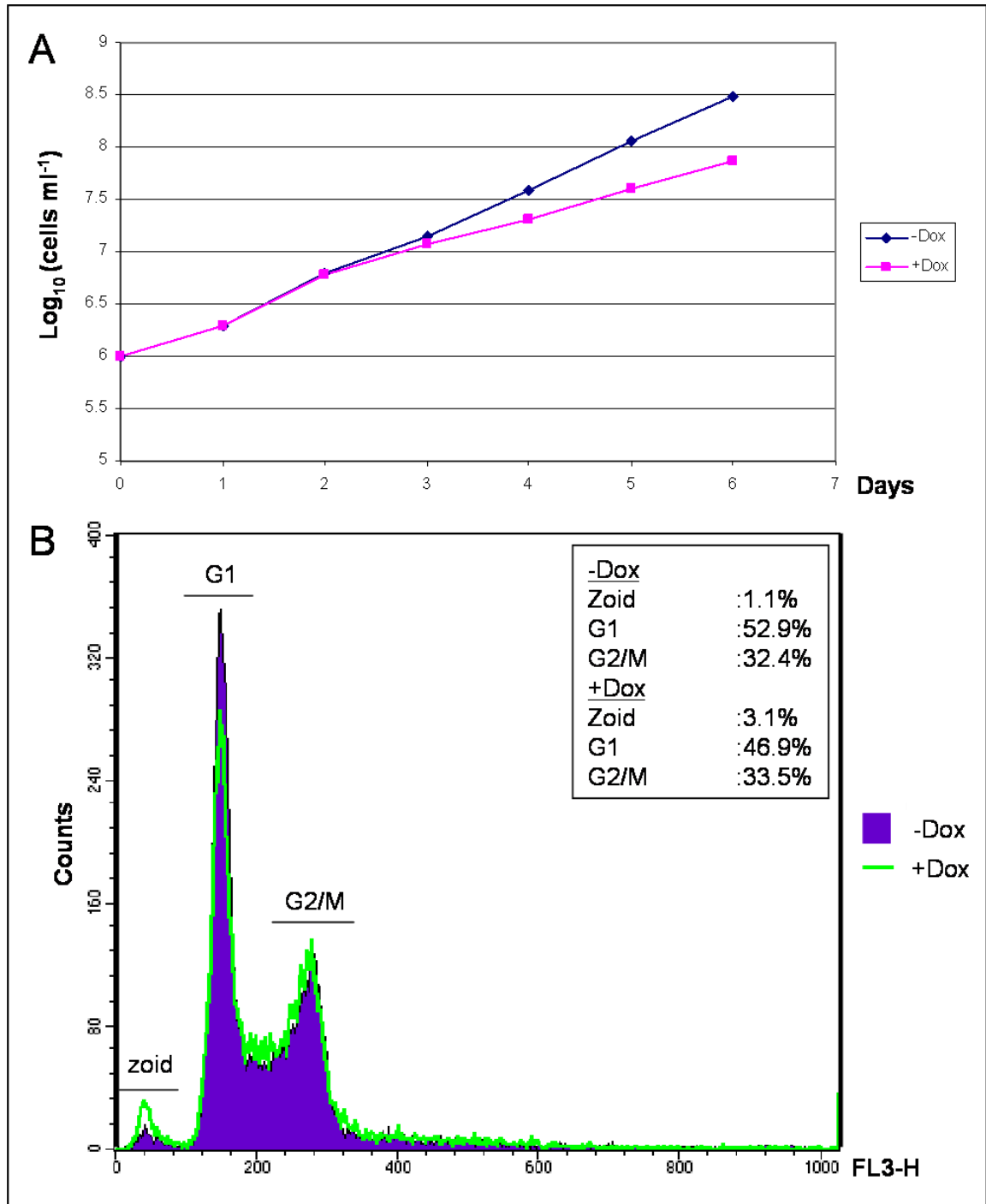


Figure 3.26: Effect of RNAi on p2T7-*TbKif27* cells. (A) Growth curve of p2T7-*TbKif27* cells. The cells were diluted to a density 1×10^6 cells ml⁻¹ and counted every 24 hours in the presence (+Dox) or absence (-Dox) of doxycycline. (B) FACS analysis on the DNA content of control cells (-Dox) and *TbKif27* depleted cells 4 days after RNAi induction (+Dox). The x-axis represents the fluorescence signal of propidium iodide which indicates the DNA content of a cell. The y-axis represents the number of counts for the specific absorbance intensity which is proportional to the number of cells counted.

3.4.13 TbKif45 is detergent-insoluble but anti-TbKif45 failed to detect native TbKif45 during immunofluorescence microscopy

To test the specificity of affinity-purified anti-TbKif45, a Western blot was performed on the whole cell lysate of procyclic strain 427 cells. It was found that anti-TbKif45 reacted strongly to a single protein band of approximately 80 kD in size (Figure 3.27A). This corresponds well with the expected size of TbKif45 of 77 kD. Western blots on NP40 extracted procyclic cells also revealed that TbKif45 is detergent-insoluble but becomes detergent-soluble in the presence of ATP (Figure 3.27B).

Immunofluorescence microscopy on procyclic strain 427 cells using anti-TbKif45 did not reveal any discernable signals (results not shown). Furthermore, anti-TbKif45 also failed produce a staining in NP40 extracted cells or when cells were fixed using methanol (results not shown). Anti-TbKif45 was made from a polyclonal source raised against a large TbKif45 protein fragment (28 kD) and therefore anti-TbKif45 it is likely to recognise more than one epitope of TbKif45. The polyclonal nature of anti-TbKif45 and the detection of TbKif45 through Western blots suggest that the inability for anti-TbKif45 to detect TbKif45 during immunofluorescence microscopy was either due to a low abundance of TbKif45 or the inaccessibility of the TbKif45 epitopes.

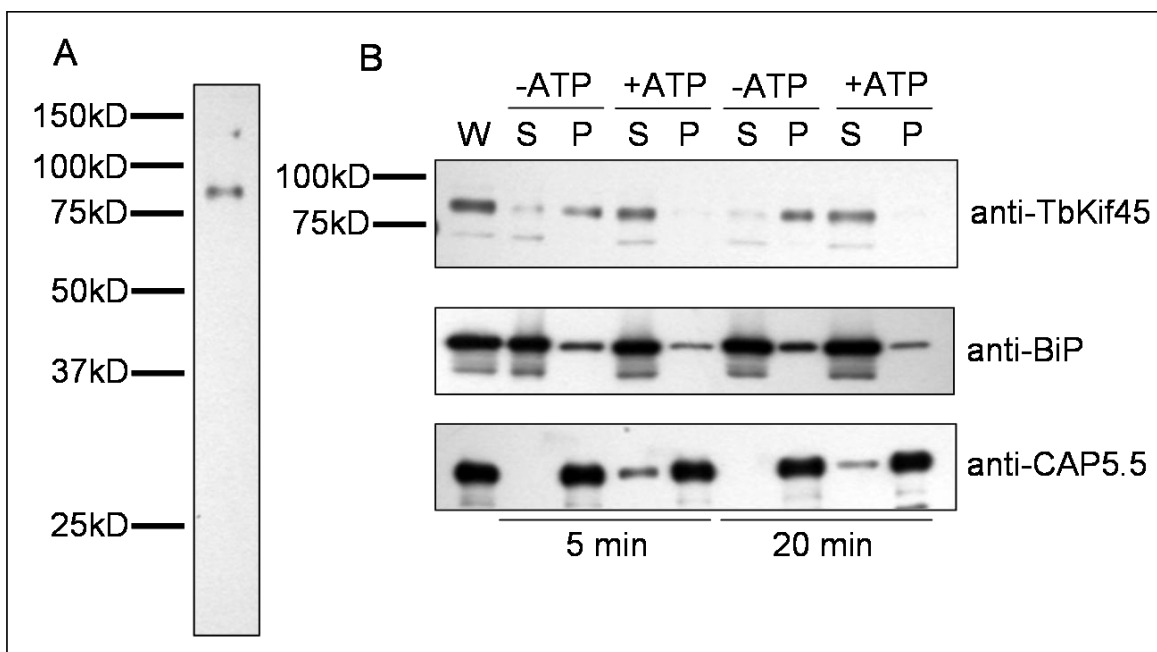


Figure 3.27: Western blot analysis on TbKif45. (A) Western blot on whole cell lysate of procyclic strain 427 probed with anti-TbKif45. (B) Western blot analysis of TbKif45 response to detergent extraction and treatment with MgATP. Each lane was loaded with an equivalent of 2×10^6 cells which was either untreated whole cells (W), NP40 soluble (S) or insoluble (P) fractions. The lanes where the cells were extracted in the presence of MgATP are indicated with the (+ATP) symbol. Anti-BiP is a marker for the endoplasmic reticulum (Bangs et al., 1993) and anti-CAP5.5 is a marker for the cytoskeleton (Hertz-Fowler et al., 2001). Both BiP and CAP5.5 is used in this experiment as a control to show the level of separation between detergent-soluble and insoluble fractions.

3.4.14 TbKif45M was localised to the nucleus

In order to determine the subcellular localisation of TbKif45, cell lines expressing ectopic TbKif45 tagged with a myc epitope was created. However, it was discovered after DNA sequencing, that the *TbKif45myc* vector used in the transfection of procyclic strain 449 cells contained a single base pair deletion at the 3' end of the *TbKif45* coding region (Figure 3.28A). This single base pair deletion is likely to be introduced by the reverse primer used in the amplification of the *TbKif45* coding region during the creation of the *TbKif45myc* vector. The point mutation resulted in a frameshift at the end of the coding region of *TbKif45* changing the last amino acid of TbKif45 from isoleucine (I) to methionine (M) and added 8 other amino acids instead of the myc tag at the C-terminus of *TbKif45* (Figure 3.28B), creating a mutant version of *TbKif45* (*TbKif45M*).

The absence of the myc tag in TbKif45M makes detection using anti-myc impossible. However, the expression of TbKif45M in procyclic strain 449 cells was detectable in Western blots when probed with anti-TbKif45 (Figure 3.30A). The band was as expected, similar in size to the endogenous TbKif45. When cells expressing TbKif45M were examined by immunofluorescence microscopy, it was found that TbKif45M was exclusively localised to the nucleus (Figure 3.30B). TbKif45M was detected only in cells which were preparing or undergoing mitosis. When immunofluorescence microscopy was performed on NP40-extracted cells, part of the nuclear staining of TbKif45M remained and was observed to have a staining pattern that was compatible with the position of the mitotic spindle (Figure 3.30C).

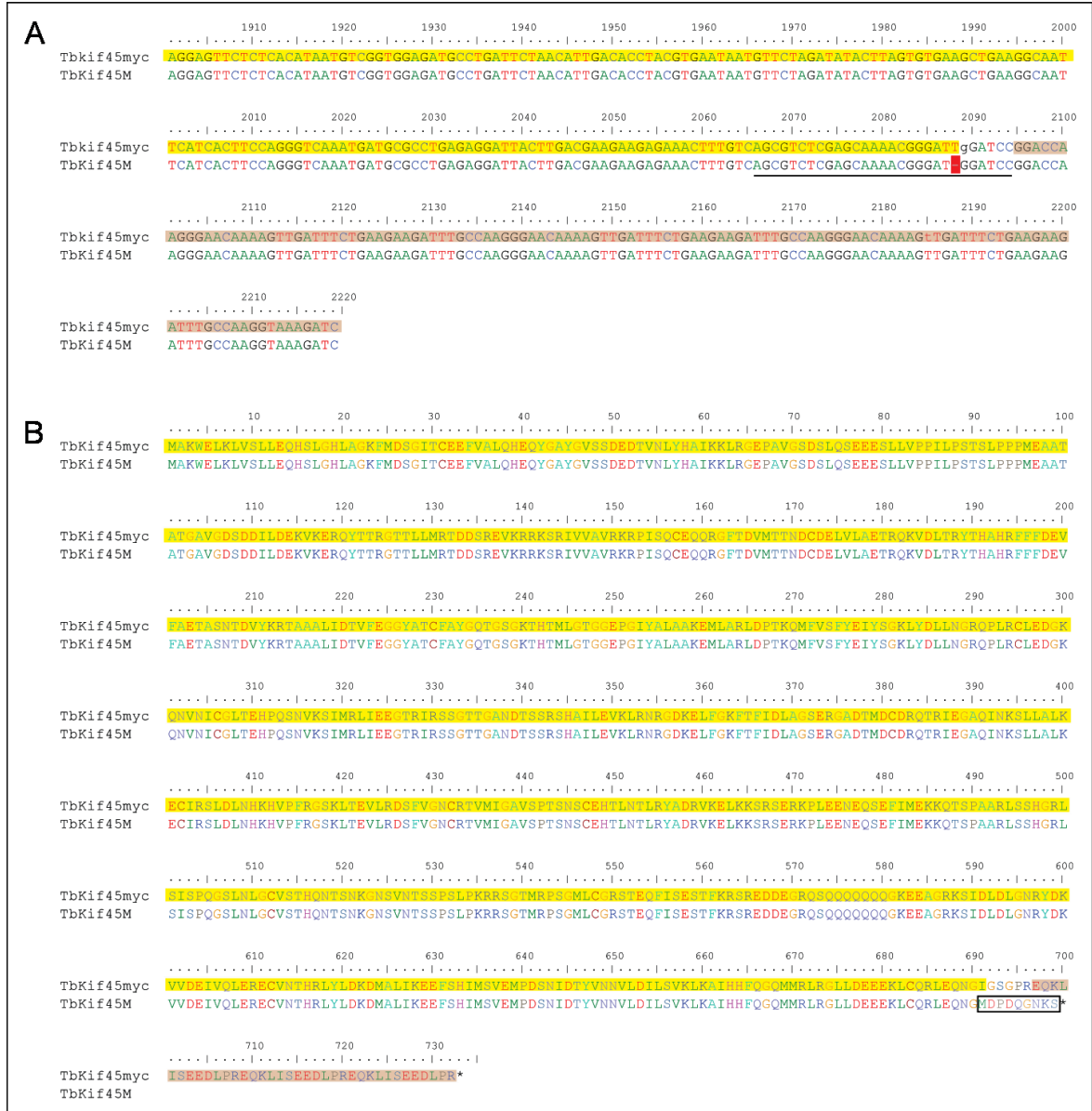


Figure 3.28: DNA and protein sequence analysis of the *TbKif45* mutant, *TbKif45M*. (A) DNA sequence alignment of the 3' region of *TbKif45myc* and *TbKif45M*. (*TbKif45myc*) represents the expected sequence of the 3' region of the *TbKif45myc* expression construct while (*TbKif45M*) represents the actual sequence determined from DNA sequencing. The region shaded in yellow represent the 3' region of the *TbKif45* ORF, the region shaded in brown represents the 3 × myc tag inserted by the p2674 vector. The region underlined represents the reverse primer used to amplify the open reading frame of *TbKif45* gene and the area shaded in red represents the deleted Thymine (T) residue introduced by the *TbKif45myc* reverse primer. (B) Protein alignment of *TbKif45myc* against the predicted *TbKif45M* protein sequence deduced from the sequencing results of *TbKif45M* vector. The region shaded in yellow represents the entire protein sequence of *TbKif45* and the region shaded in brown represents the 3 × myc tag inserted by the p2674 vector resulting in a 3 × myc tagged *TbKif45* gene. The region outlined by the black box represents the additional 9 amino acid residues introduced to the C-terminus of *TbKif45* creating the protein *TbKif45M*.

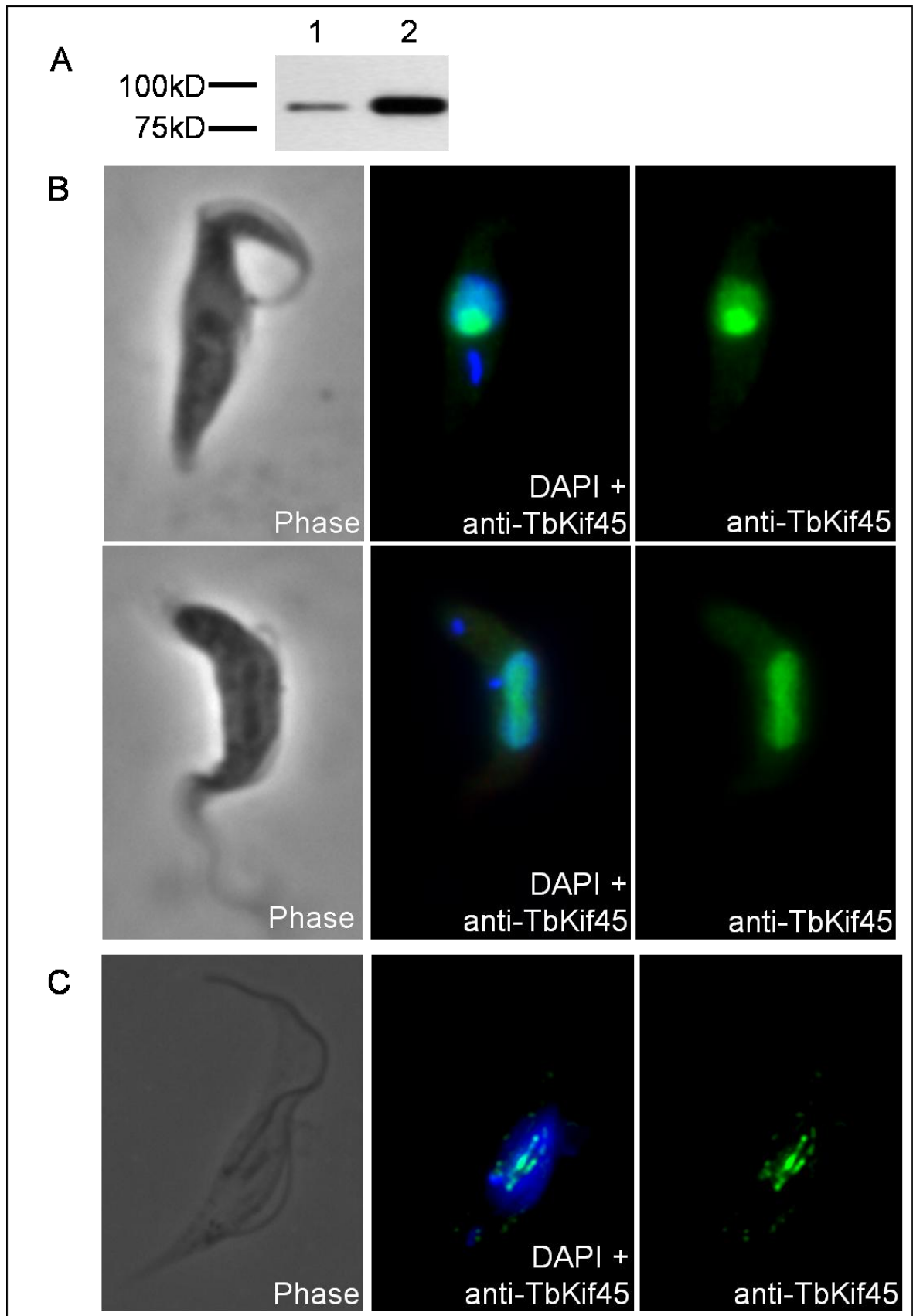


Figure 3.29: Immunofluorescence and Western blot analysis on 449/*TbKif45myc* cells induced with tetracycline (1µg ml⁻¹) for 3 hours. (A) Western blot analysis using anti-TbKif45 on non-induced (1) and induced (2) cells. (B) Immunofluorescence microscopy (1,000 times magnification) of 449/*TbKif45myc* cells induced with tetracycline for 3 hours. (C) Immunofluorescence microscopy (1,000 times magnification) of NP40 extracted 449/*TbKif45myc* cells induced with tetracycline for 3 hours.

3.4.15 Overexpression of TbKif45M resulted in karyokinesis arrest

An induction time course of 449/*TbKif45M* cells revealed that the induction of TbKif45M resulted in severe growth retardation 6 hours after the addition of tetracycline (Figure 3.30B). Western blot analysis of induced 449/*TbKif45M* cells indicated that the decrease in cell growth coincided with the increase in TbKif45M protein levels (Figure 3.30A). FACS analysis revealed an accumulation of G2/M cell population and a corresponding decrease in G1 cell population after 6 hours of TbKif45M induction (Figure 3.30C). After 24 hours, large populations of zoids (1K 0N) are found to be present (Figure 3.31A). Furthermore, after 24 hours of TbKif45M induction, a large proportion of the cells observed appear to have an enlarged nucleus (1K 1N*) likely due the accumulation of TbKif45M and larger nuclear DNA content of unknown ploidy (Figure 3.31A). Zoids are often formed when the trypanosome is unable to complete mitosis but able to progress through cell division leading to the accumulation of anucleate (1K 0N) cells called zoids and 1K 1N* cells which contain a higher nuclear DNA content than normal (Ploubidou et al., 1999). The appearance of aberrant cell types and the accumulation of G2/M phase in FACS analysis strongly support the idea that TbKif45M overexpression inhibits the completion of mitosis/karyokinesis in procyclic cells. This conclusion is also supported by the observation that no aberrant cells with multiple nuclei were observed by microscopy indicating that karyokinesis failed to occur in TbKif45M overexpressing cells.

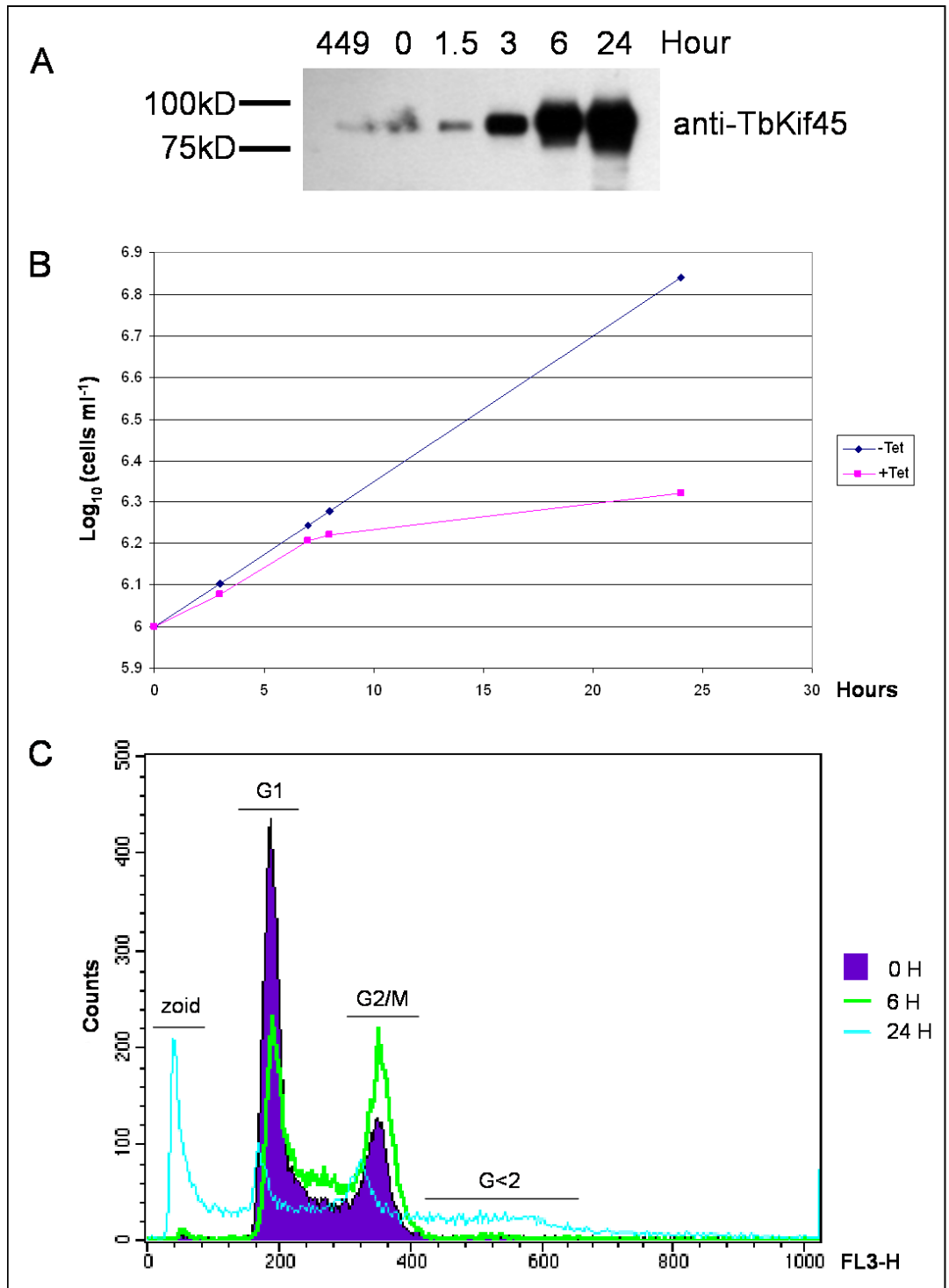


Figure 3.30: The effect of *TbKif45M* overexpression. (A) Western blot of wild-type (449) cells and *TbKif45M* cells induced with tetracycline addition after 0, 1.5, 3, 6 and 24 hours. (B) A growth curve of 449/*TbKif45M* cells. The overproduction of *TbKif45M* was induced with the addition of tetracycline (+Tet). (-Tet) represents the negative control. (C) FACS analysis on the DNA content of 449/*TbKif45M* cells. The x-axis represents the fluorescence signal of propidium iodide which indicates the DNA content of a cell. The y-axis represents the number of counts for the specific absorbance intensity which is proportional to the number of cells counted.

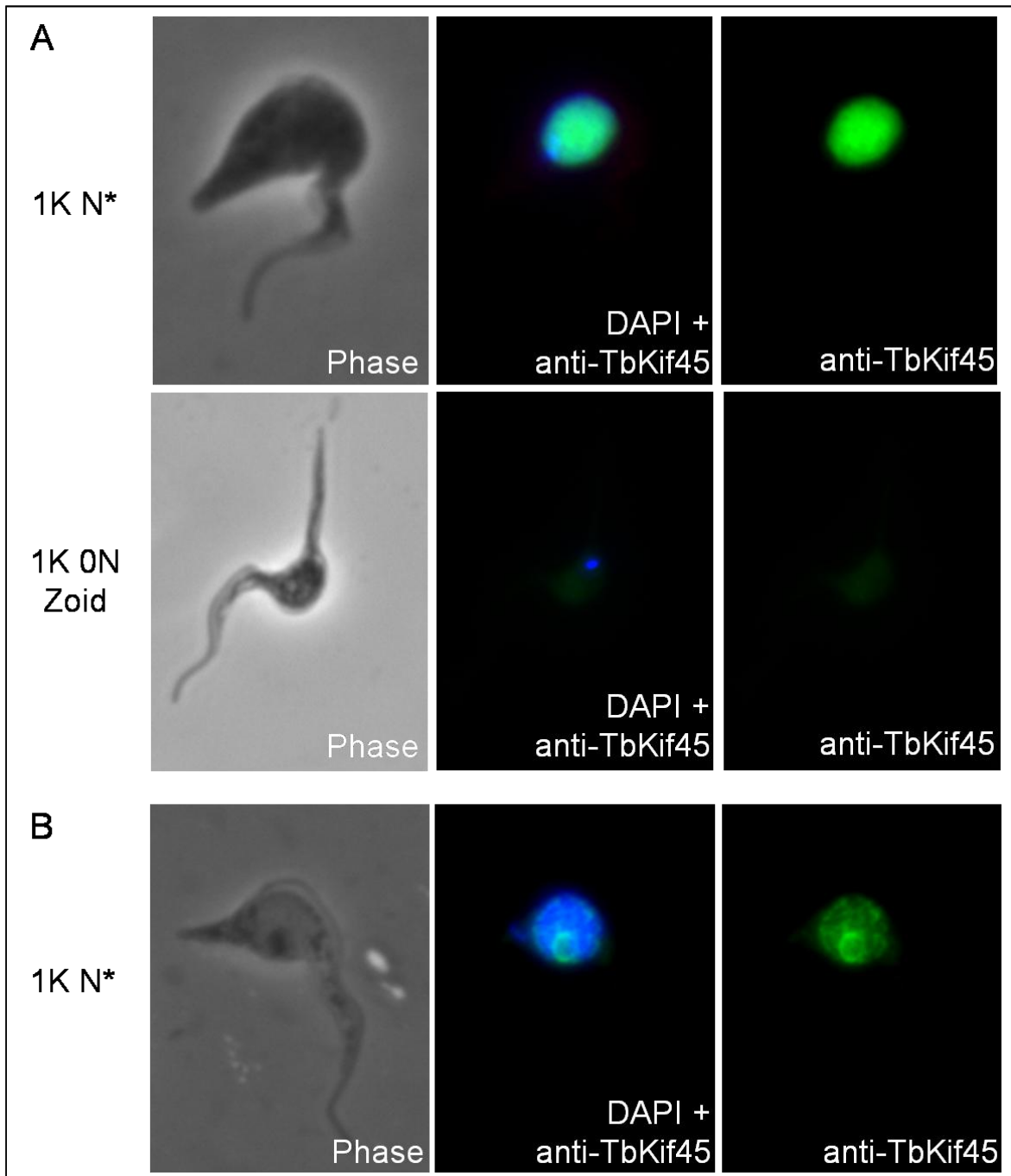


Figure 3.31: Aberrant cell morphologies observed on 449/*TbKif45M* cells overexpressing *TbKif45M*. (A) Immunofluorescence microscopy on formaldehyde fixed 449/*TbKif45M* cells 24 hours after tetracycline induction. (B) Immunofluorescence microscopy (1,000 times magnification) on NP40 extracted 449/*TbKif45M* cells 24 hours after tetracycline induction. The cells were stained with anti-*TbKif45* (green) and DAPI (blue). DAPI stains the DNA of the kinetoplast and nucleus. The abbreviations used were (K) representing kinetoplast, (N) representing nucleus and (N*) representing an enlarged nucleus.

3.4.16 TbKif45 depletion through RNAi in procyclic strain 29-13 cells resulted in a mild growth defect

To test the effect of TbKif45 depletion in procyclic strain 29-13 cells, RNAi was performed using the vector p2T7-*TbKif45*. Doxycycline induction on 29-13/p2T7-*TbKif45* cells was successful in depleting the protein levels of TbKif45 (Figure 3.32A). The protein level of TbKif45 was reduced by >95% on Western blots within 24 hours and remained constant throughout the entire duration of the experiment which lasted for 6 days. The depletion of TbKif45 caused a slight reduction in the growth rate when compared to non-induced cells within 24 hours of induction (Figure 3.32B). Examination of TbKif45 depleted cells under fluorescence microscopy did not reveal any gross changes on cells undergoing mitosis nor were any aberrant cell types observed. Similar observations were obtained when TbKif45 depleted cells were analysed by FACS (Figure 3.32C). However, it was noted that there was a slight increase in zoid cells in TbKif45 depleted cells (3.8%) when compared with control cells (1.2%).

In conclusion, the overexpression of TbKif45M had a more pronounced effect on the cell cycle and growth than the depletion of TbKif45. This observation could be explained by the often observed redundancy built into the function of kinesin proteins in other organisms (Cottingham et al., 1999; Ganem et al., 2005; Nag et al., 2008). In addition, it is also possible that a partial depletion of endogenous TbKif45 was insufficient in inducing an observable change in cellular morphology.

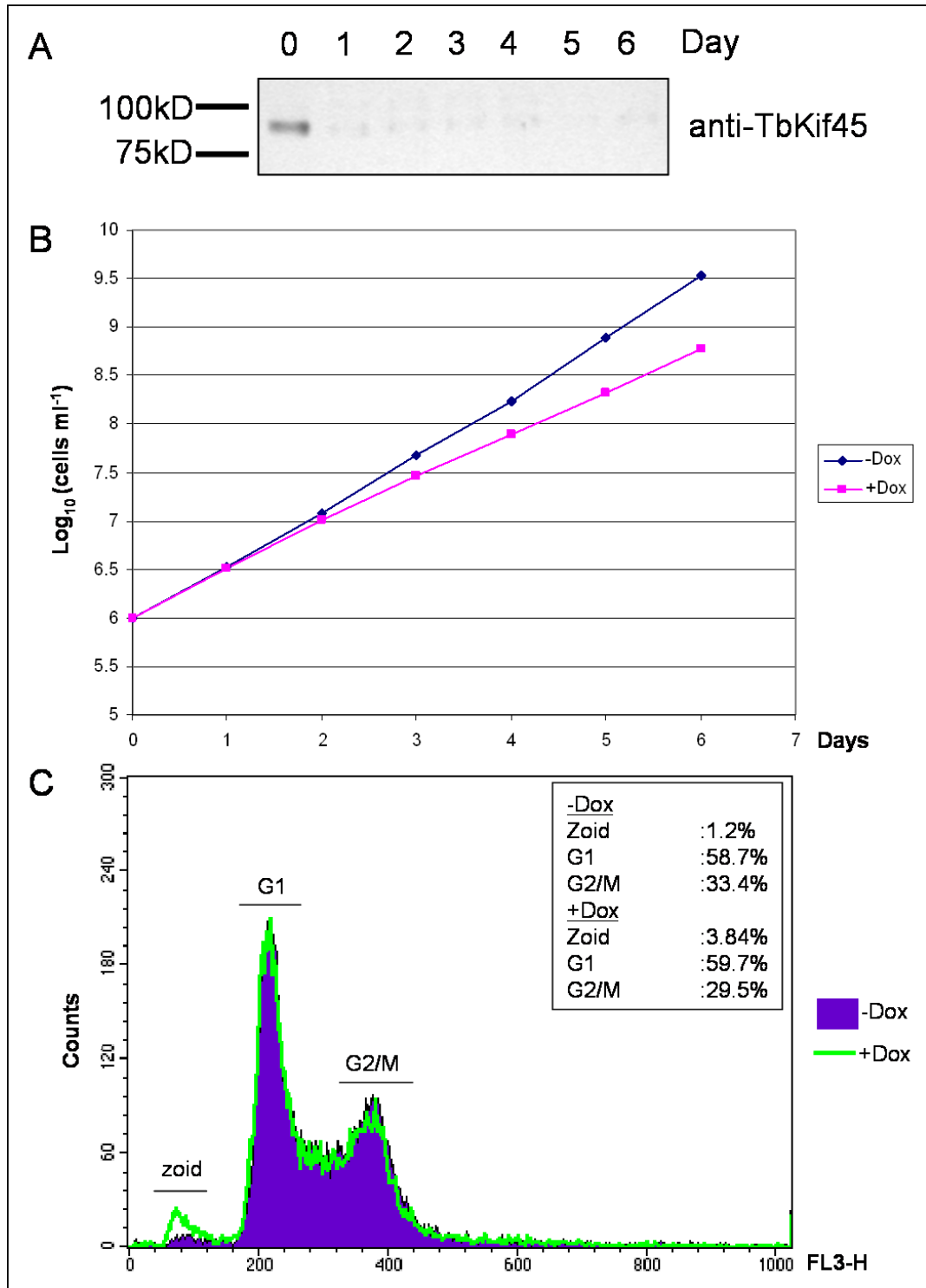


Figure 3.32: The effect of TbKif45 depletion in procyclic 29-13/p2T7-*TbKif45* cells. (A) Western blot of 29-13/p2T7-*TbKif45* cells at 0, 1, 2, 3, 4, 5 and 6 days after the addition of doxycycline. (B) A growth curve of 29-13/p2T7-*TbKif45* cells. The depletion of TbKif45 is induced with the addition of doxycycline (+Dox). (-Dox) represents the negative control. (C) FACS analysis on the DNA content of 29-13/p2T7-*TbKif45* cells. The x-axis represents the fluorescence signal of propidium iodide which indicates the DNA content of a cell. The y-axis represents the number of counts for the specific absorbance intensity which is proportional to the number of cells counted.

3.5 Discussion

This report represents the first comprehensive survey of the Kinesin-13 family in the Kinetoplastid group reporting the subcellular localisation of six of the seven Kinesin-13 family members coded by the trypanosome genome (Table 3.5). Of the six, only one kinesin was found to have a nuclear localisation (TbKif45), two were associated with the flagellum (TbKif2 and TbKif9), two were localised to the cell body (TbKif8 and TbKif27) and one was found to be associated with the mitochondrion (TbKif15).

Initial attempts to functionally characterise the Kinesin-13 members were predominantly restricted to observing growth phenotypes and gross morphological changes from RNAi induced protein depletion. While it was shown that RNAi directed against TbKif9, TbKif27 and TbKif45 did result in the depletion of the targeted gene products, no gross morphological changes were observed in all three kinesins, although TbKif27 and TbKif45 showed a decrease in growth rate. These observations are not uncommon when working with single kinesin gene deletion/depletion studies and are documented from work on various organisms (Cottingham et al., 1999; Goshima and Vale, 2003; Nag et al., 2008; Zhu et al., 2005). This is often due to functional overlaps between several kinesins where the loss of function of a single kinesin is compensated by other kinesins that share similar functions. This is well illustrated in gene deletion studies targeted against kinesins in *Saccharomyces cerevisiae*, where it was shown that cells remain viable even after the loss of four (out of six) kinesin genes coded by its genome (Cottingham et al., 1999). As a consequence of these functional overlaps exhibited by some kinesins, a phenotype can only be observed when the cells are subjected to stress (de Hostos et al., 1998) or when several kinesins of related functions were deleted/depleted simultaneously (Goshima and Vale, 2003; Nag et al., 2008).

Table 3.5: The localisation of the six Kinesin-13 members in *Trypanosoma brucei*.

Kinesin	Endogenous protein	Ectopically expressed protein
TbKif2	No detectable signal in Western blots and immunofluorescence microscopy using anti-TbKif2	<ul style="list-style-type: none"> • Myc tagged at the C-terminus • Localised to the distal tip of the flagellum • Detectable by both anti-myc and anti-TbKif2
TbKif8	No detectable signal in Western blots and immunofluorescence microscopy using anti-TbKif8	<ul style="list-style-type: none"> • Myc tagged at the C-terminus • Localised to the cell body excluding the nucleus and flagellum • Detectable by both anti-myc and anti-TbKif8
TbKif9	Detectable in Western blots and localised to the entire length of the flagellum by anti-TbKif9	<ul style="list-style-type: none"> • Myc tagged at the C-terminus • Localised to the cell body excluding the nucleus and flagellum • Detectable by both anti-myc and anti-TbKif9
TbKif15	Detectable in Western blots and localised to the mitochondrion by anti-TbKif15	N/A
TbKif27	Detectable in Western blots and localised to the cell body excluding the flagellum and nucleus by anti-TbKif27	N/A
TbKif45	Detectable in Western blots but not detectable in immunofluorescence microscopy by anti-TbKif45	<ul style="list-style-type: none"> • Localised to the nucleus • Exhibit a staining pattern similar to the mitotic spindle in detergent extracted cells • Detectable by anti-TbKif45

RNAi directed against *TbKif2* resulted in a severe growth defect contrary to previously published experimental results where RNAi directed against *TbKif2* in procyclic cells did not result in cell growth impairment (Blaineau et al., 2007). As anti-TbKif2 was unable to detect any endogenous TbKif2 protein, it is unknown if the production of *TbKif2* dsRNA resulted in the depletion of *TbKif2* mRNA as a northern blot was not performed. A possible explanation for such a contrasting result would be that the dsRNA produced by the RNAi vector p2T7-*TbKif2* was cross-reacting with the mRNA of another gene product. Blast searches using the DNA sequence used in the construction of the RNAi vector p2T7-*TbKif2* did not reveal any other genes that share any significant sequence similarities except for *TbKif2*. However, it is possible that the dsRNA produced by the RNAi vector p2T7-*TbKif2* may target the UTR regions of mRNA coded by other genes resulting in non-specific gene silencing. It is therefore prudent to confirm the results of the initial gene silencing experiment by performing a second RNAi knockdown directed against a different region of the gene of interest or to generate a gene knockout cell line.

Attempts to deplete *TbKif15* using RNAi were unsuccessful. One possible cause for *TbKif15* to be non-responsive to RNAi induction would be due to the leaky nature of the p2T7 RNAi vector when used in conjunction with the 29-13 cell line which expresses high levels of T7 RNA polymerase. If *TbKif15* is an essential gene, even a small amount of dsRNA may be hazardous to trypanosomes resulting in the selection for mutants which are non-responsive to RNAi induction. To overcome this problem, one could use a tightly-regulated RNAi system which involves cell lines containing higher levels of tetracycline repressor proteins (Alibu et al., 2005) and/or use a stem-loop RNAi construct which uses a single T7 promoter (Chanez et al., 2006). Alternatively, other non-RNAi methods can be employed to aid functional characterisation such as overexpression studies (Blaineau et al., 2007; Kline-Smith and Walczak, 2002; Saunders et al., 1997), creating cell lines with conditional gene knockouts (Homma et al., 2003; Lu et al., 2005; Nag et al., 2008) or inducible dominant negative mutants (Dawson et al., 2007; Kline-Smith et al., 2004).

Apart from issues involving the use of RNAi in trypanosomes, it was observed that the presence of *TbKif2* at the RNA level does not necessarily mean that TbKif2 was expressed. Using antibodies, TbKif2 was not detectable in procyclic and bloodstream cells and the removal of TbKif2 in procyclic cells did not result in any observable phenotype

indicating that TbKif2 was not expressed or at least dispensable for cultured life cycle forms. This illustrates the importance of the use of antibodies to detect endogenous protein levels as the presence of mRNA does not necessarily mean that the gene is expressed at the protein level. In addition, it also outlines the drawbacks of end-point RT-PCR as it provides only a qualitative result in detecting the presence of RNA but does not provide a quantitative measure in terms of RNA levels present. Northern blots and real-time PCR, using genes with known expression levels as a point of reference, would be able to give a more accurate account of mRNA levels.

3.5.1 *TbKif2 and TbKif9 - kinesins localised to the flagellum*

The characterisation of the Kinesin-13 family in trypanosomes resulted in the discovery of two kinesins associated to the flagellum, TbKif2 and TbKif9. We were unable to detect endogenous TbKif2 using anti-TbKif2 but ectopically expressed TbKif2myc was found to localise to the distal tip of the flagellum. Members of the Kinesin-13 family have been reported to be associated to the flagellar tip in *Leishmania major* (Blaineau et al., 2007) and *Giardia intestinalis* (Dawson et al., 2007). In both organisms, the localisation was determined using ectopically tagged versions of the protein of interest. In *L. major*, the overexpression of a Kinesin-13 family member LmjKIN13-2 (a homologue to TbKif2) resulted in a short flagellum phenotype. This prompted the suggestion that LmjKIN13-2 promotes flagellum shortening by depolymerising axonemal microtubules at the distal tip of the flagellum (Blaineau et al., 2007). Their conclusion is supported by two lines of evidence. (1) Mutation studies of the KLD or KEC motif in the motor domain of LmjKIN13-2 which resulted in the loss of flagellum localisation and the restoration of wild type morphology. The KLD and KEC motifs are Kinesin-13 specific motifs which play an important role in microtubule depolymerisation and tubulin binding (Hertzler et al., 2003; Shipley et al., 2004). As the substitution of the KLD or KEC motifs did result in the restoration of wild type morphology, they argued it was due to the inhibition of the microtubule depolymerisation of LmjKIN13-2. However, it could be due to the also observed mislocalisation of LmjKIN13-2 to the base of the flagellum, which resulted in the restoration of wild type morphology. (2) The depletion of *TbKif2* mRNA levels using

RNAi (LmjKIN13-2 homologue) in procyclic trypanosomes resulted in flagellum lengthening. This result was compatible with the idea that TbKif2 promotes flagellum shortening and the depletion of TbKif2 would result in the lengthening of the flagellum.

Some of the results from my experiments on TbKif2 agree with previously published data (Blaineau et al., 2007) as the expression of TbKif2myc in $\Delta TbKif2/TbKif2myc$ cells was found to have a negative effect (15% reduction, Figure 3.11) on the length of the flagellum when compared to wild-type 449 cells. In addition, immunofluorescence microscopy on procyclic cells expressing TbKif2myc revealed that during cell division, TbKif2myc was found to be more abundant (in terms of fluorescence intensity and area of flagellar tip staining, Figure 3.7) on the actively growing new flagellum when compared to the mature flagellum. The preferential staining of Kinesin-13 family members to actively polymerising microtubule ends has been documented before in interphase Chinese Hamster Ovary (CHO) cells (Moore et al., 2005) and at growing flagellar tips in *Giardia* (Dawson et al., 2007).

However, in contrast to published results (Blaineau et al., 2007), the absence of TbKif2myc expression in the procyclic $\Delta TbKif2/TbKif2myc$ cell lines did not result in flagellum lengthening when compared with wild-type 449 cells. The reason for such a discrepancy in results is unknown but may be attributed to the different approach used in depletion of TbKif2 expression (conditional knock-out in contrast to RNAi) in procyclic cells. In addition, it is uncertain that TbKif2 regulates flagellar length by directly promoting microtubule depolymerisation at the distal tip of the flagellum. Previous phylogenetic and sequence analysis of TbKif2 and other Kinesin-13 family members revealed that TbKif2 does not possess a neck domain (Figure 2.4). The neck domain plays an essential role in the depolymerisation of microtubules *in vivo* (Maney et al., 2001; Ovechkina et al., 2002). The absence of the neck domain in TbKif2 would severely inhibit its microtubule depolymerising ability. TbKif2 also appears not to be expressed in procyclic forms of trypanosomes. This is supported by the observation that endogenous TbKif2 was not detected in Western blots or in immunofluorescence microscopy when probed with anti-TbKif2 and the absence of TbKif2 did not result in any change in flagellum length of $\Delta TbKif2/TbKif2myc$ cells when compared with wild-type 449 cells. While it is theoretically possible that small amounts of TbKif2myc, undetectable by Western blotting, can be

expressed in non-induced $\Delta TbKif2/TbKif2myc$ cells preventing flagellum lengthening, this is unlikely to have happened as RT-PCR on RNA extracts from non-induced cells did not detect the presence of *TbKif2myc* mRNA (Figure 3.10B). The absence of *TbKif2* in procyclic cells would suggest that *TbKif2* is developmentally regulated and its primary function, at least in procyclic cells, is not flagellum length regulation. As *TbKif2* does not appear to be expressed in the procyclic form life stage, it would of interest to determine if *TbKif2* expression is detectable in other stages of the trypanosome life cycle. One potential stage where *TbKif2* may play a role would be the epimastigote stage, where the trypanosome undergoes extensive flagella remodelling and attaches itself to the epithelial lining of the salivary gland.

TbKif9 was observed to be associated with the entire length of the flagellum. It represents the first kinesin in the Kinesin-13 family to exhibit such a staining pattern at the flagellum. The function of *TbKif9* is still unknown as RNAi failed to deplete *TbKif9* protein to sufficient levels to produce any observable phenotype. Kinesin motor proteins involved in the flagellum are most comprehensively studied in the biflagellate alga, *Chlamydomonas reinhardtii* and to a certain extent the nematode, *Caenorhabditis elegans* (Blacque et al., 2008; Scholey, 2008). The studies of motor proteins in the flagellum to date are predominantly confined to those related to the movement of proteinaceous particles from the base of the flagellum to the distal tip of the flagellum (Kozminski et al., 1993; Rosenbaum and Witman, 2002). These proteinaceous particles, called intraflagellar transport (IFT) particles move along the microtubules of the axoneme. They play a role in transporting flagellum precursor proteins to the distal tip of the flagellum which is the site of flagellum assembly (Johnson and Rosenbaum, 1992). Two different classes of motor proteins are involved in movement of IFT particles. The Kinesin-2 family which is responsible for anterograde IFT towards the flagellum tip and dyneins which is responsible for retrograde IFT back to the cell body (Blacque et al., 2008; Rosenbaum and Witman, 2002; Scholey, 2008). The trypanosome genome codes for many of the conserved IFT transport proteins, and homologues to the conserved motor proteins involved in IFT have been identified (Berriman et al., 2005). Some of these IFT proteins have been characterised and results suggest that they are functionally conserved (Absalon et al., 2008; Adhiambo et al., 2005).

Assuming that TbKif9 is a microtubule depolymeriser, it is not obvious the function of a lateral association along the length of the flagellum might have. This is because the sites where previously characterised Kinesin-13 members exert their microtubule depolymerisation activity are at microtubule ends.

A group of kinesin family members known to have a flagellar localisation is the Kinesin-9 family which was found to play a role in flagellar movement (Yokoyama et al., 2004). CrKlp1, which is a member of the Kinesin-9 family, exhibits a staining pattern similar to TbKif9 which is along the flagellum in *Chlamydomonas* (Bernstein et al., 1994; Yokoyama et al., 2004). However, it is unlikely that TbKif9 would share similar functions to CrKlp1 as the trypanosome does possess a single Kinesin-9 family member, TbKif40 which is likely a functional homologue to CrKlp1 [refer Table 2.3 and (Wickstead and Gull, 2006)]. In addition, TbKif9 also exhibits a different response when compared to CrKlp1 during detergent extraction experiments, where TbKif9 is partially detergent-soluble in the presence of ATP while CrKlp1 was found to be soluble only when extracted in the presence 0.5 M NaCl (Yokoyama et al., 2004), indicating a difference in biochemical properties possessed by TbKif9 and CrKlp1.

It is also possible that TbKif9 is involved in flagellar structures/functions not found in other model eukaryotic systems. The homologues of TbKif9 are present in the kinetoplastid counterparts *L. major* and *T. cruzi*, which suggests that TbKif9 is involved in a function found only in the kinetoplastid group. The kinetoplastid flagellum contains the classical axonemal structure made of nine doublets of microtubules around a central pair of single microtubules (Branche et al., 2006). However, unlike other flagellated eukaryotes, the kinetoplastid flagellum also possesses a paraflagellar rod (PFR) which runs in parallel with the axoneme within the flagellar membrane (Hill, 2003; Maga and LeBowitz, 1999). As TbKif9 does have a similar distribution to the PFR, it is possible that TbKif9 interacts with the PFR. The localisation of TbKif9 by the electron microscope would provide more information about its function by revealing its exact localisation in the flagellum.

3.5.2 TbKif8 and TbKif27 - kinesins localised to the cell body

The expression of the ectopic copy of TbKif8 tagged with a myc epitope resulted in a cell body staining which excludes the nucleus and flagellum. The distribution of TbKif8myc does not appear to correlate with known trypanosome cell body organelles and exhibits a diffused cell body staining. The polyclonal anti-TbKif8 is able to detect ectopically expressed TbKif8myc by immunofluorescence microscopy and Western blot. Therefore, as the expression of the endogenous TbKif8 was undetectable by anti-TbKif8, it is possible that TbKif8 is not expressed in both procyclic and bloodstream forms. If TbKif8 is not expressed in procyclic cells, the diffused cell body distribution of TbKif8myc could simply represent the mistargeting of TbKif8myc due to the absence of TbKif8 targeting site. It is uncertain if the growth defect observed during doxycycline induction in 29-13/p2T7-*TbKif8* cells is an actual phenotype, as endogenous expression of TbKif8 was undetected and RNAi can cause cross-interference. Therefore, in order to confirm that the growth defect of RNAi directed against TbKif8 is reproducible, a second RNAi experiment targeting a different region of the gene should be performed. In addition, it is important to investigate if endogenous TbKif8 can be detected in other life cycle stages of *Trypanosoma brucei*.

TbKif27 was also localised to the cell body and was found to exhibit a uniform intensity throughout the cell body excluding the nucleus and flagellum. RNAi induced reduction of TbKif27 resulted in the loss of cell body staining by more than 95% confirming that the cell body staining is due to TbKif27. The distribution of TbKif27 does not appear to associate with any known membrane-bound organelles in the cell body. The motor domain of TbKif27 is well conserved when compared with other characterised kinesin family members (refer Figure 2.3). It is therefore likely that the motor domain of TbKif27 is capable of microtubule interaction. It was previously reported that a Kinesin-13 family member, MCAK being localised to microtubule tips in interphase CHO cells resulting in a homogenous granular/filamentous staining in the cell body (Moore et al., 2005). The TbKif27 cell body staining is compatible with the possibility that TbKif27 is associated to the trypanosome sub-pellicular microtubule corset (Kohl and Gull, 1998; Woods et al., 1989).

Western blot analysis on the detergent extraction experiment revealed that TbKif27 was detergent-soluble. Kinesins which are unable to maintain association with microtubules in the absence of ATP are not uncommon, as some kinesins have been shown to stably associate to microtubules only in the presence of a non-hydrolysable analogue of ATP, AMPPNP (Brady, 1985; Cole et al., 1992; Vale et al., 1985). Therefore, in order to properly verify if TbKif27 is detergent-soluble, a second detergent extraction experiment is planned where procyclic cells will be extracted in the presence of AMPPNP. If TbKif27 is detergent soluble, it is possible that TbKif27 is cytosolic. Therefore, a double labelling experiment with a cytosolic marker should be performed. Conversely, if TbKif27 is shown to associate to the cytoskeleton, it will be essential to examine the localisation of TbKif27 under an electron microscope to determine how TbKif27 interacts with the microtubule corset. Depletion of TbKif27 through RNAi resulted in a reduction of growth rate in procyclic strain 29-13 cells. While there were no gross changes in the cellular morphology in TbKif27 depleted cells, a slight increase in zoid populations in TbKif27 depleted cells suggests that TbKif27 may play a role in cytokinesis. Currently, a conditional knockout of *TbKif27* is being created in our lab in order to further characterise the function of TbKif27. It is speculated that TbKif27 could be involved in the organisation and dynamics of the microtubule corset. It has been previously shown that the microtubule corset duplicates in a semi-conservative fashion during cytokinesis by intercalating new microtubule filaments between the existing microtubule array (Sherwin and Gull, 1989b). Kinesins might play a role in regulating the assembly process.

3.5.3 TbKif15, a kinesin associated with the mitochondrion

TbKif15 represents the first Kinesin-13 family member of any organism to be found associated to the mitochondrion. There are two classes of microtubule associated motor proteins known to be involved in the movement of mitochondria along the cell body of eukaryotes, the kinesin and dynein motor proteins. Members of the Kinesin-1 and Kinesin-3 family play a role in mitochondrial transport towards the microtubule plus-end (Glater et al., 2006; Khodjakov et al., 1998; Klopfenstein et al., 2002; Nangaku et al., 1994; Tanaka et al., 1998) while dyneins are involved in the transport of mitochondria towards the minus-

end of microtubules (Pilling et al., 2006; Tanaka et al., 1998). Members of the Kinesin-13 family represent the only kinesin family known not to exhibit microtubule processivity (Desai et al., 1999). Unlike most eukaryotes, trypanosomes possess only a single large mitochondrion which spans the entire length of the cell body in procyclic cells (Gull, 2001). This negates the need for the trypanosome mitochondrion to be transported within the trypanosome cell body. It is possible that TbKif15 is involved in anchoring the mitochondrion to the cell body and plays a role in the segregation of the mitochondrion during cell division. Very little is known about proteins involved in mitochondrial segregation in trypanosomes, with the exception for a motor protein called dynamin, which plays a role in mitochondrial fission (Chanez et al., 2006; Morgan et al., 2004). Currently, our lab is collaborating with André Schneider, University of Fribourg, in characterising TbKif15. Preliminary results on procyclic cells depleted of TbKif15 by stem-loop RNAi, resulted in a growth defect when cultivated in a low glucose medium. This could indicate that the depletion of TbKif15 resulted in the disruption of the integrity of the single mitochondrion, which is essential for the survival of procyclic trypanosomes.

3.5.4 TbKif45, a kinesin localised to the nucleus

Of the six Kinesin-13 family members characterised, only TbKif45 exhibited a nuclear localisation. This is surprising as most of the Kinesin-13 family members in other organisms characterised have mitotic functions. The functions of the Kinesin-13 family in mitosis are well studied in many metazoan organisms (Ganem and Compton, 2004; Manning et al., 2007; Rogers et al., 2004; Walczak et al., 2002; Walczak et al., 1996; Wordeman et al., 2007) but little work has been performed on protozoans regarding the exact roles of the Kinesin-13 family during mitosis. To date, only two publications involving the characterisation of the Kinesin-13 family members that have a nuclear localisation in protozoans have been reported. In *Giardia*, a Kinesin-13 member was reported to be localised to flagellar tips, the median body and to the entire mitotic spindle (Dawson et al., 2007). The function of the *Giardia* Kinesin-13 was deduced by expressing a dominant-negative GFP-tagged Kinesin-13 rigor mutant. The expression of the Kinesin-13 rigour mutant resulted in severe cytokinesis defects and the appearance of lagging

chromosomes during anaphase, a common spindle defect observed when the function of Kinesin-13 motor proteins are disturbed during mitosis (Kline-Smith et al., 2004; Maney et al., 1998; Rogers et al., 2004).

In *L. major*, LmjKIN13-1 (a homologue of TbKif45) was reported to have a nuclear localisation and was observed to be associated to the poles of the mitotic spindle (Dubessay et al., 2006). However, in contrast to my work on TbKif45, overexpression of GFP-tagged LmjKIN13-1 in *L. major* did not result in any observable defects in mitosis. The exact cause of such discrepancy in results is unknown but it is possible that the degree of overexpression of LmjKIN13-1 was not high enough to promote a spindle defect or that the GFP tag interfered with the normal function of LmjKIN13-1. The effect of a Kinesin-13 protein overexpression has been previously demonstrated (Kline-Smith and Walczak, 2002; Maney et al., 1998; Newton et al., 2004). In vertebrate cells, an overexpression of a Kinesin-13 family member, XKCM1 resulted in the formation of monoastral and monopolar spindles with small pro-metaphase spindles causing mitotic arrest or delay in affected cells (Kline-Smith and Walczak, 2002). The formation of aberrant mitotic spindles has been attributed by the microtubule depolymerising ability of XKCM1 as the depletion of XKCM1 resulted in spindle elongation. The result of TbKif45M overexpression in procyclic cells correlates well with previous findings as TbKif45M overexpression resulted in karyokinesis inhibition. Examination of detergent extracted cells with aberrant nuclear morphology produced an unusual filamentous staining within the nucleus when probed with anti-TbKif45 (Figure 3.31B). It is possible that this filamentous stain is a result from the failure of the mitotic spindle to form a normal bipolar spindle as a result of TbKif45M overexpression. To test this hypothesis, these cells would need to be stained with an antibody that is specific to the mitotic spindle such as the anti-tubulin antibody, KMX (Birkett et al., 1985).

The depletion of TbKif45 using the p2T7-*TbKif45* RNAi construct resulted in mild growth retardation and a slight elevation in zoid cell populations. The mild defects could have been caused by an overlap in function of other motor proteins or a partial depletion of TbKif45 may have been insufficient in producing a more pronounced phenotype. The latter reasoning would appear to be the case, as an RNAi induction experiment performed by a member of our lab using a stem-loop construct targeting TbKif45 was recently performed,

resulting in a severe growth defect within two days of RNAi induction (results not shown). FACS analysis on induced cells revealed a large population of zoid cells and an accumulation of G1 phase cells which indicate a cell cycle defect (results not shown). A more detailed examination on the mitotic defects is currently being carried out. It is speculated that TbKif45 will possess similar functions to the mitotic Kinesin-13 family members in metazoan organisms where the depletion of TbKif45 results in the appearance of elongated spindles and lagging chromosomes (Maney et al., 1998; Rogers et al., 2004; Walczak et al., 1996).

The inability of anti-TbKif45 to detect endogenous TbKif45 during immunofluorescence microscopy is possibly due to its epitope being masked. Anti-TbKif45 is able to detect endogenous TbKif45 in western blots and the overexpression of TbKif45M is detectable by immunofluorescence microscopy. Cells can be treated with a different fixation method or subjected to various unmasking procedures (e.g. mild protease treatment) to unmask the epitope of TbKif45. Alternatively, the inability of anti-TbKif45 to detect endogenous TbKif45 during immunofluorescence microscopy may be due to the low abundance of TbKif45 in individual cells.

3.5.5 Functional diversity of the Kinesin-13 family

The characterisation of Kinesin-13 members has predominantly been confined to metazoans and those functions related to mitosis. While the mitotic functions of Kinesin-13 family members are well understood, the non-mitotic functions of the Kinesin-13 family are only beginning to be uncovered (Moores and Milligan, 2006). An example would be Kif2A, which is associated to the mitotic spindle during mitosis and is associated to tips of polymerising microtubules in interphase cells (Moore et al., 2005). During mitosis, Kif2A is associated to centrosome and play important role in promoting spindle bipolarity and powering chromosome segregation during anaphase (Ganem and Compton, 2004). In interphase cells, Kif2A has been implicated in collateral branch suppression in neuronal cells (Homma et al., 2003). Non-mitotic functions of Kinesin-13 members have also been observed in plants (Lu et al., 2005) and in protozoa (Blaineau et al., 2007; Dawson et al., 2007). My work on the Kinesin-13 family members in *T. brucei* where majority of the

Kinesin-13 members were found to have distinct non-nuclear localisations during the entire cell cycle provides an excellent opportunity to study the functional diversity of the Kinesin-13 family. Furthermore, as many of these kinesins appear to perform functions unique to the trypanosome cell biology, making them attractive targets for future drug development.

4 References

- Absalon, S., T. Blisnick, L. Kohl, G. Toutirais, G. Dore, D. Julkowska, A. Tavenet, and P. Bastin. 2008. Intraflagellar Transport and Functional Analysis of Genes Required for Flagellum Formation in Trypanosomes. *Mol Biol Cell*. 19:929-944.
- Adams, R.R., A.A. Tavares, A. Salzberg, H.J. Bellen, and D.M. Glover. 1998. pavarotti encodes a kinesin-like protein required to organize the central spindle and contractile ring for cytokinesis. *Genes Dev*. 12:1483-94.
- Adhiambo, C., J.D. Forney, D.J. Asai, and J.H. LeBowitz. 2005. The two cytoplasmic dynein-2 isoforms in *Leishmania mexicana* perform separate functions. *Mol Biochem Parasitol*. 143:216-25.
- Afshar, K., N.R. Barton, R.S. Hawley, and L.S. Goldstein. 1995. DNA binding and meiotic chromosomal localization of the *Drosophila nod* kinesin-like protein. *Cell*. 81:129-38.
- Alibu, V.P., L. Storm, S. Haile, C. Clayton, and D. Horn. 2005. A doubly inducible system for RNA interference and rapid RNAi plasmid construction in *Trypanosoma brucei*. *Mol Biochem Parasitol*. 139:75-82.
- Antonio, C., I. Ferby, H. Wilhelm, M. Jones, E. Karsenti, A.R. Nebreda, and I. Vernos. 2000. Xkid, a chromokinesin required for chromosome alignment on the metaphase plate. *Cell*. 102:425-35.
- Asada, T., R. Kuriyama, and H. Shibaoka. 1997. TKRP125, a kinesin-related protein involved in the centrosome-independent organization of the cytokinetic apparatus in tobacco BY-2 cells. *J Cell Sci*. 110 (Pt 2):179-89.
- Bangs, J.D., L. Uyetake, M.J. Brickman, A.E. Balber, and J.C. Boothroyd. 1993. Molecular cloning and cellular localization of a BiP homologue in *Trypanosoma brucei*. Divergent ER retention signals in a lower eukaryote. *J Cell Sci*. 105 (Pt 4):1101-13.
- Banks, J.D., and R. Heald. 2001. Chromosome movement: dynein-out at the kinetochore. *Curr Biol*. 11:R128-31.
- Barry, J.D. 1997. The relative significance of mechanisms of antigenic variation in African trypanosomes. *Parasitol Today*. 13:212-8.
- Barry, J.D., and R. McCulloch. 2001. Antigenic variation in trypanosomes: enhanced phenotypic variation in a eukaryotic parasite. *Adv Parasitol*. 49:1-70.
- Bathe, F., K. Hahlen, R. Dombi, L. Driller, M. Schliwa, and G. Woehlke. 2005. The complex interplay between the neck and hinge domains in kinesin-1 dimerization and motor activity. *Mol Biol Cell*. 16:3529-37.
- Bernstein, M. 1995. Flagellar kinesins: new moves with an old beat. *Cell Motil Cytoskeleton*. 32:125-8.
- Bernstein, M., P.L. Beech, S.G. Katz, and J.L. Rosenbaum. 1994. A new kinesin-like protein (Klp1) localized to a single microtubule of the *Chlamydomonas* flagellum. *J Cell Biol*. 125:1313-26.
- Berriman, M., E. Ghedin, C. Hertz-Fowler, G. Blandin, H. Renauld, D.C. Bartholomeu, N.J. Lennard, E. Caler, N.E. Hamlin, B. Haas, U. Bohme, L. Hannick, M.A. Aslett, J. Shallom, L. Marcello, L. Hou, B. Wickstead, U.C. Alsmark, C. Arrowsmith, R.J. Atkin, A.J. Barron, F. Bringaud, K. Brooks, M. Carrington, I. Cherevach, T.J. Chillingworth, C. Churcher, L.N. Clark, C.H. Corton, A. Cronin, R.M. Davies, J.

- Doggett, A. Djikeng, T. Feldblyum, M.C. Field, A. Fraser, I. Goodhead, Z. Hance, D. Harper, B.R. Harris, H. Hauser, J. Hostetler, A. Ivens, K. Jagels, D. Johnson, J. Johnson, K. Jones, A.X. Kerhornou, H. Koo, N. Larke, S. Landfear, C. Larkin, V. Leech, A. Line, A. Lord, A. Macleod, P.J. Mooney, S. Moule, D.M. Martin, G.W. Morgan, K. Mungall, H. Norbertczak, D. Ormond, G. Pai, C.S. Peacock, J. Peterson, M.A. Quail, E. Rabbinowitsch, M.A. Rajandream, C. Reitter, S.L. Salzberg, M. Sanders, S. Schobel, S. Sharp, M. Simmonds, A.J. Simpson, L. Tallon, C.M. Turner, A. Tait, A.R. Tivey, S. Van Aken, D. Walker, D. Wanless, S. Wang, B. White, O. White, S. Whitehead, J. Woodward, J. Wortman, M.D. Adams, T.M. Embley, K. Gull, E. Ullu, J.D. Barry, A.H. Fairlamb, F. Opperdoes, B.G. Barrell, J.E. Donelson, N. Hall, C.M. Fraser, et al. 2005. The genome of the African trypanosome *Trypanosoma brucei*. *Science*. 309:416-22.
- Berriman, M., N. Hall, K. Shearer, F. Bringaud, B. Tiwari, T. Isobe, S. Bowman, C. Corton, L. Clark, G.A. Cross, M. Hoek, T. Zanders, M. Berberof, P. Borst, and G. Rudenko. 2002. The architecture of variant surface glycoprotein gene expression sites in *Trypanosoma brucei*. *Mol Biochem Parasitol*. 122:131-40.
- Beverly, S.M., and C.E. Clayton. 1993. Transfection of *Leishmania* and *Trypanosoma brucei* by electroporation. *Methods Mol Biol*. 21:333-48.
- Biebinger, S., L.E. Wirtz, P. Lorenz, and C. Clayton. 1997. Vectors for inducible expression of toxic gene products in bloodstream and procyclic *Trypanosoma brucei*. *Mol Biochem Parasitol*. 85:99-112.
- Birkett, C.R., K.E. Foster, L. Johnson, and K. Gull. 1985. Use of monoclonal antibodies to analyse the expression of a multi-tubulin family. *FEBS Lett*. 187:211-8.
- Blacque, O.E., S. Cevik, and O.I. Kaplan. 2008. Intraflagellar transport: from molecular characterisation to mechanism. *Front Biosci*. 13:2633-52.
- Blaineau, C., M. Tessier, P. Dubessay, L. Tasse, L. Crobu, M. Pages, and P. Bastien. 2007. A novel microtubule-depolymerizing kinesin involved in length control of a eukaryotic flagellum. *Curr Biol*. 17:778-82.
- Blangy, A., H.A. Lane, P. d'Herin, M. Harper, M. Kress, and E.A. Nigg. 1995. Phosphorylation by p34cdc2 regulates spindle association of human Eg5, a kinesin-related motor essential for bipolar spindle formation in vivo. *Cell*. 83:1159-69.
- Boleti, H., E. Karsenti, and I. Vernos. 1996. Xklp2, a novel *Xenopus* centrosomal kinesin-like protein required for centrosome separation during mitosis. *Cell*. 84:49-59.
- Bowser, J., and A.S. Reddy. 1997. Localization of a kinesin-like calmodulin-binding protein in dividing cells of *Arabidopsis* and tobacco. *Plant J*. 12:1429-37.
- Brady, S.T. 1985. A novel brain ATPase with properties expected for the fast axonal transport motor. *Nature*. 317:73-5.
- Brady, S.T., K.K. Pfister, and G.S. Bloom. 1990. A monoclonal antibody against kinesin inhibits both anterograde and retrograde fast axonal transport in squid axoplasm. *Proc Natl Acad Sci U S A*. 87:1061-5.
- Branche, C., L. Kohl, G. Toutirais, J. Buisson, J. Cosson, and P. Bastin. 2006. Conserved and specific functions of axoneme components in trypanosome motility. *J Cell Sci*. 119:3443-55.
- Brun, R., and Schonberger. 1979. Cultivation and in vitro cloning or procyclic culture forms of *Trypanosoma brucei* in a semi-defined medium. Short communication. *Acta Trop*. 36:289-92.

- Carter, N.J., and R.A. Cross. 2006. Kinesin's moonwalk. *Curr Opin Cell Biol.* 18:61-7.
- Case, R.B., D.W. Pierce, N. Hom-Booher, C.L. Hart, and R.D. Vale. 1997. The directional preference of kinesin motors is specified by an element outside of the motor catalytic domain. *Cell.* 90:959-66.
- Cassimeris, L. 2004. Cell division: eg'ing on microtubule flux. *Curr Biol.* 14:R1000-2.
- Cassimeris, L., and J. Morabito. 2004. TOGp, the human homolog of XMAP215/Dis1, is required for centrosome integrity, spindle pole organization, and bipolar spindle assembly. *Mol Biol Cell.* 15:1580-90.
- Caviston, J.P., and E.L. Holzbaur. 2006. Microtubule motors at the intersection of trafficking and transport. *Trends Cell Biol.* 16:530-7.
- Chanez, A.L., A.B. Hehl, M. Engstler, and A. Schneider. 2006. Ablation of the single dynamin of *T. brucei* blocks mitochondrial fission and endocytosis and leads to a precise cytokinesis arrest. *J Cell Sci.* 119:2968-74.
- Chen, C., A. Marcus, W. Li, Y. Hu, J.P. Calzada, U. Grossniklaus, R.J. Cyr, and H. Ma. 2002. The Arabidopsis ATK1 gene is required for spindle morphogenesis in male meiosis. *Development.* 129:2401-9.
- Cimini, D., and F. Degraffi. 2005. Aneuploidy: a matter of bad connections. *Trends Cell Biol.* 15:442-51.
- Colasante, C., V.P. Alibu, S. Kirchberger, J. Tjaden, C. Clayton, and F. Voncken. 2006. Characterization and developmentally regulated localization of the mitochondrial carrier protein homologue MCP6 from *Trypanosoma brucei*. *Eukaryot Cell.* 5:1194-205.
- Cole, D.G. 1999. Kinesin-II, the heteromeric kinesin. *Cell Mol Life Sci.* 56:217-26.
- Cole, D.G., W.Z. Cande, R.J. Baskin, D.A. Skoufias, C.J. Hogan, and J.M. Scholey. 1992. Isolation of a sea urchin egg kinesin-related protein using peptide antibodies. *J Cell Sci.* 101 (Pt 2):291-301.
- Compton, D.A. 2000. Spindle assembly in animal cells. *Annu Rev Biochem.* 69:95-114.
- Cottingham, F.R., L. Gheber, D.L. Miller, and M.A. Hoyt. 1999. Novel roles for *Saccharomyces cerevisiae* mitotic spindle motors. *J Cell Biol.* 147:335-50.
- Cottingham, F.R., and M.A. Hoyt. 1997. Mitotic spindle positioning in *Saccharomyces cerevisiae* is accomplished by antagonistically acting microtubule motor proteins. *J Cell Biol.* 138:1041-53.
- Dawson, S.C., M.S. Sagolla, J.J. Mancuso, D.J. Woessner, S.A. House, L. Fritz-Laylin, and W.Z. Cande. 2007. Kinesin-13 Regulates Flagellar, Interphase, and Mitotic Microtubule Dynamics in *Giardia intestinalis*. *Eukaryot Cell.* 6:2354-64.
- de Hostos, E.L., G. McCaffrey, R. Sucgang, D.W. Pierce, and R.D. Vale. 1998. A developmentally regulated kinesin-related motor protein from *Dictyostelium discoideum*. *Mol Biol Cell.* 9:2093-106.
- Desai, A., S. Verma, T.J. Mitchison, and C.E. Walczak. 1999. Kin I kinesins are microtubule-destabilizing enzymes. *Cell.* 96:69-78.
- Donelson, J.E. 2003. Antigenic variation and the African trypanosome genome. *Acta Trop.* 85:391-404.
- Dubessay, P., C. Blaineau, P. Bastien, L. Tasse, J. Van Dijk, L. Crobu, and M. Pages. 2006. Cell cycle-dependent expression regulation by the proteasome pathway and characterization of the nuclear targeting signal of a *Leishmania major* Kin-13 kinesin. *Mol Microbiol.* 59:1162-74.

- Dutoya, S., S. Gibert, G. Lemercier, X. Santarelli, D. Baltz, T. Baltz, and N. Bakalara. 2001. A novel C-terminal kinesin is essential for maintaining functional acidocalcisomes in *Trypanosoma brucei*. *J Biol Chem.* 276:49117-24.
- Dymek, E.E., D. Goduti, T. Kramer, and E.F. Smith. 2006. A kinesin-like calmodulin-binding protein in *Chlamydomonas*: evidence for a role in cell division and flagellar functions. *J Cell Sci.* 119:3107-16.
- Ems-McClung, S.C., K.M. Hertzler, X. Zhang, M.W. Miller, and C.E. Walczak. 2007. The interplay of the N- and C-terminal domains of MCAK control microtubule depolymerization activity and spindle assembly. *Mol Biol Cell.* 18:282-94.
- Endow, S.A., and K.W. Waligora. 1998. Determinants of kinesin motor polarity. *Science.* 281:1200-2.
- Enos, A.P., and N.R. Morris. 1990. Mutation of a gene that encodes a kinesin-like protein blocks nuclear division in *A. nidulans*. *Cell.* 60:1019-27.
- Ersfeld, K., and K. Gull. 1997. Partitioning of large and minichromosomes in *Trypanosoma brucei*. *Science.* 276:611-4.
- Ersfeld, K., S.E. Melville, and K. Gull. 1999. Nuclear and genome organization of *Trypanosoma brucei*. *Parasitol Today.* 15:58-63.
- Funabiki, H., and A.W. Murray. 2000. The *Xenopus* chromokinesin Xkid is essential for metaphase chromosome alignment and must be degraded to allow anaphase chromosome movement. *Cell.* 102:411-24.
- Gaglio, T., M.A. Dionne, and D.A. Compton. 1997. Mitotic spindle poles are organized by structural and motor proteins in addition to centrosomes. *J Cell Biol.* 138:1055-66.
- Gaglio, T., A. Saredi, J.B. Bingham, M.J. Hasbani, S.R. Gill, T.A. Schroer, and D.A. Compton. 1996. Opposing motor activities are required for the organization of the mammalian mitotic spindle pole. *J Cell Biol.* 135:399-414.
- Ganem, N.J., and D.A. Compton. 2004. The KinI kinesin Kif2a is required for bipolar spindle assembly through a functional relationship with MCAK. *J Cell Biol.* 166:473-8.
- Ganem, N.J., K. Upton, and D.A. Compton. 2005. Efficient mitosis in human cells lacking poleward microtubule flux. *Curr Biol.* 15:1827-32.
- Gardner, M.J., N. Hall, E. Fung, O. White, M. Berriman, R.W. Hyman, J.M. Carlton, A. Pain, K.E. Nelson, S. Bowman, I.T. Paulsen, K. James, J.A. Eisen, K. Rutherford, S.L. Salzberg, A. Craig, S. Kyes, M.S. Chan, V. Nene, S.J. Shallom, B. Suh, J. Peterson, S. Angiuoli, M. Pertea, J. Allen, J. Selengut, D. Haft, M.W. Mather, A.B. Vaidya, D.M. Martin, A.H. Fairlamb, M.J. Fraunholz, D.S. Roos, S.A. Ralph, G.I. McFadden, L.M. Cummings, G.M. Subramanian, C. Mungall, J.C. Venter, D.J. Carucci, S.L. Hoffman, C. Newbold, R.W. Davis, C.M. Fraser, and B. Barrell. 2002. Genome sequence of the human malaria parasite *Plasmodium falciparum*. *Nature.* 419:498-511.
- Gerald, N.J., I. Coppens, and D.M. Dwyer. 2007. Molecular dissection and expression of the LdK39 kinesin in the human pathogen, *Leishmania donovani*. *Mol Microbiol.* 63:962-79.
- Ghosh, S.K., S. Hajra, A. Paek, and M. Jayaram. 2006. Mechanisms for chromosome and plasmid segregation. *Annu Rev Biochem.* 75:211-41.

- Gindhart, J.G. 2006. Towards an understanding of kinesin-1 dependent transport pathways through the study of protein-protein interactions. *Brief Funct Genomic Proteomic.* 5:74-86.
- Glater, E.E., L.J. Megeath, R.S. Stowers, and T.L. Schwarz. 2006. Axonal transport of mitochondria requires Milton to recruit kinesin heavy chain and is light chain independent. *J Cell Biol.* 173:545-57.
- Goodson, H.V., S.J. Kang, and S.A. Endow. 1994. Molecular phylogeny of the kinesin family of microtubule motor proteins. *J Cell Sci.* 107 (Pt 7):1875-84.
- Goshima, G., and R.D. Vale. 2003. The roles of microtubule-based motor proteins in mitosis: comprehensive RNAi analysis in the Drosophila S2 cell line. *J Cell Biol.* 162:1003-16.
- Grishchuk, E.L., and J.R. McIntosh. 2006. Microtubule depolymerization can drive poleward chromosome motion in fission yeast. *Embo J.* 25:4888-96.
- Gull, K. 2001. The biology of kinetoplastid parasites: insights and challenges from genomics and post-genomics. *International Journal for Parasitology.* 31:443.
- Gull, K., S. Alsford, and K. Ersfeld. 1998. Segregation of minichromosomes in trypanosomes: implications for mitotic mechanisms. *Trends Microbiol.* 6:319-23.
- Gull, K., C. Birkett, R. Gerke-Bonet, A. Parma, D. Robinson, T. Sherwin, and R. Woodward. 1990. The cell cycle and cytoskeletal morphogenesis in *Trypanosoma brucei*. *Biochem Soc Trans.* 18:720-2.
- Gupta, M.L., Jr., P. Carvalho, D.M. Roof, and D. Pellman. 2006. Plus end-specific depolymerase activity of Kip3, a kinesin-8 protein, explains its role in positioning the yeast mitotic spindle. *Nat Cell Biol.* 8:913-23.
- Hanlon, D.W., Z. Yang, and L.S. Goldstein. 1997. Characterization of KIFC2, a neuronal kinesin superfamily member in mouse. *Neuron.* 18:439-51.
- Hertz-Fowler, C., K. Ersfeld, and K. Gull. 2001. CAP5.5, a life-cycle-regulated, cytoskeleton-associated protein is a member of a novel family of calpain-related proteins in *Trypanosoma brucei*. *Mol Biochem Parasitol.* 116:25-34.
- Hertzer, K.M., S.C. Ems-McClung, S.L. Kline-Smith, T.G. Lipkin, S.P. Gilbert, and C.E. Walczak. 2006. Full-length dimeric MCAK is a more efficient microtubule depolymerase than minimal domain monomeric MCAK. *Mol Biol Cell.* 17:700-10.
- Hertzer, K.M., S.C. Ems-McClung, and C.E. Walczak. 2003. Kin I kinesins: insights into the mechanism of depolymerization. *Crit Rev Biochem Mol Biol.* 38:453-69.
- Heywood, P., and D. Weinman. 1978. Mitosis in the hemoflagellate *Trypanosoma cyclops*. *J Protozool.* 25:287-92.
- Hildebrandt, E.R., and M.A. Hoyt. 2000. Mitotic motors in *Saccharomyces cerevisiae*. *Biochim Biophys Acta.* 1496:99-116.
- Hill, E., M. Clarke, and F.A. Barr. 2000. The Rab6-binding kinesin, Rab6-KIFL, is required for cytokinesis. *Embo J.* 19:5711-9.
- Hill, K.L. 2003. Biology and mechanism of trypanosome cell motility. *Eukaryot Cell.* 2:200-8.
- Hirokawa, N. 1998. Kinesin and dynein superfamily proteins and the mechanism of organelle transport. *Science.* 279:519-26.
- Hirokawa, N., Y. Noda, and Y. Okada. 1998. Kinesin and dynein superfamily proteins in organelle transport and cell division. *Curr Opin Cell Biol.* 10:60-73.

- Hirokawa, N., and R. Takemura. 2004. Kinesin superfamily proteins and their various functions and dynamics. *Exp Cell Res.* 301:50-9.
- Hirumi, H., and K. Hirumi. 1989. Continuous cultivation of *Trypanosoma brucei* blood stream forms in a medium containing a low concentration of serum protein without feeder cell layers. *J Parasitol.* 75:985-9.
- Holzinger, A., and U. Lutz-Meindl. 2002. Kinesin-like proteins are involved in postmitotic nuclear migration of the unicellular green alga *Micrasterias denticulata*. *Cell Biol Int.* 26:689-97.
- Homma, N., Y. Takei, Y. Tanaka, T. Nakata, S. Terada, M. Kikkawa, Y. Noda, and N. Hirokawa. 2003. Kinesin superfamily protein 2A (KIF2A) functions in suppression of collateral branch extension. *Cell.* 114:229-39.
- Hoyt, M.A., L. He, K.K. Loo, and W.S. Saunders. 1992. Two *Saccharomyces cerevisiae* kinesin-related gene products required for mitotic spindle assembly. *J Cell Biol.* 118:109-20.
- Inoue, H., H. Nojima, and H. Okayama. 1990. High efficiency transformation of *Escherichia coli* with plasmids. *Gene.* 96:23-8.
- Johnson, K.A., and J.L. Rosenbaum. 1992. Polarity of flagellar assembly in *Chlamydomonas*. *J Cell Biol.* 119:1605-11.
- Kapoor, T.M., M.A. Lampson, P. Hergert, L. Cameron, D. Cimini, E.D. Salmon, B.F. McEwen, and A. Khodjakov. 2006. Chromosomes can congress to the metaphase plate before biorientation. *Science.* 311:388-91.
- Karki, S., and E.L. Holzbaur. 1999. Cytoplasmic dynein and dynactin in cell division and intracellular transport. *Curr Opin Cell Biol.* 11:45-53.
- Kelly, S., J. Reed, S. Kramer, L. Ellis, H. Webb, J. Sunter, J. Salje, N. Marinsek, K. Gull, B. Wickstead, and M. Carrington. 2007. Functional genomics in *Trypanosoma brucei*: a collection of vectors for the expression of tagged proteins from endogenous and ectopic gene loci. *Mol Biochem Parasitol.* 154:103-9.
- Khodjakov, A., E.M. Lizunova, A.A. Minin, M.P. Koonce, and F.K. Gyoeva. 1998. A specific light chain of kinesin associates with mitochondria in cultured cells. *Mol Biol Cell.* 9:333-43.
- Kikkawa, M., Y. Okada, and N. Hirokawa. 2000. A resolution model of the monomeric kinesin motor, KIF1A. *Cell.* 100:241-52.
- Kim, A.J., and S.A. Endow. 2000. A kinesin family tree. *J Cell Sci.* 113 Pt 21:3681-2.
- Kline-Smith, S.L., A. Khodjakov, P. Hergert, and C.E. Walczak. 2004. Depletion of centromeric MCAK leads to chromosome congression and segregation defects due to improper kinetochore attachments. *Mol Biol Cell.* 15:1146-59.
- Kline-Smith, S.L., and C.E. Walczak. 2002. The microtubule-destabilizing kinesin XKCM1 regulates microtubule dynamic instability in cells. *Mol Biol Cell.* 13:2718-31.
- Kline-Smith, S.L., and C.E. Walczak. 2004. Mitotic spindle assembly and chromosome segregation: refocusing on microtubule dynamics. *Mol Cell.* 15:317-27.
- Klopfenstein, D.R., E.A. Holleran, and R.D. Vale. 2002. Kinesin motors and microtubule-based organelle transport in *Dictyostelium discoideum*. *J Muscle Res Cell Motil.* 23:631-8.
- Kohl, L., and K. Gull. 1998. Molecular architecture of the trypanosome cytoskeleton. *Mol Biochem Parasitol.* 93:1-9.

- Kohl, L., T. Sherwin, and K. Gull. 1999. Assembly of the paraflagellar rod and the flagellum attachment zone complex during the *Trypanosoma brucei* cell cycle. *J Eukaryot Microbiol.* 46:105-9.
- Kollmar, M., and G. Glockner. 2003. Identification and phylogenetic analysis of *Dictyostelium discoideum* kinesin proteins. *BMC Genomics.* 4:47.
- Kozminski, K.G., K.A. Johnson, P. Forscher, and J.L. Rosenbaum. 1993. A motility in the eukaryotic flagellum unrelated to flagellar beating. *Proc Natl Acad Sci U S A.* 90:5519-23.
- LaCount, D.J., S. Bruse, K.L. Hill, and J.E. Donelson. 2000. Double-stranded RNA interference in *Trypanosoma brucei* using head-to-head promoters. *Mol Biochem Parasitol.* 111:67-76.
- Lawrence, C.J., R.K. Dawe, K.R. Christie, D.W. Cleveland, S.C. Dawson, S.A. Endow, L.S. Goldstein, H.V. Goodson, N. Hirokawa, J. Howard, R.L. Malmberg, J.R. McIntosh, H. Miki, T.J. Mitchison, Y. Okada, A.S. Reddy, W.M. Saxton, M. Schliwa, J.M. Scholey, R.D. Vale, C.E. Walczak, and L. Wordeman. 2004. A standardized kinesin nomenclature. *J Cell Biol.* 167:19-22.
- Lawrence, C.J., R.L. Malmberg, M.G. Muszynski, and R.K. Dawe. 2002. Maximum likelihood methods reveal conservation of function among closely related kinesin families. *J Mol Evol.* 54:42-53.
- Lawrence, C.J., N.R. Morris, R.B. Meagher, and R.K. Dawe. 2001. Dyneins have run their course in plant lineage. *Traffic.* 2:362-3.
- Lee, S., J.C. Wisniewski, W.L. Dentler, and D.J. Asai. 1999. Gene knockouts reveal separate functions for two cytoplasmic dyneins in *Tetrahymena thermophila*. *Mol Biol Cell.* 10:771-84.
- Letunic, I., R.R. Copley, B. Pils, S. Pinkert, J. Schultz, and P. Bork. 2006. SMART 5: domains in the context of genomes and networks. *Nucleic Acids Res.* 34:D257-60.
- Lips, S., P. Revelard, and E. Pays. 1993. Identification of a new expression site-associated gene in the complete 30.5 kb sequence from the AnTat 1.3A variant surface protein gene expression site of *Trypanosoma brucei*. *Mol Biochem Parasitol.* 62:135-7.
- Loftus, B., I. Anderson, R. Davies, U.C. Alsmark, J. Samuelson, P. Amedeo, P. Roncaglia, M. Berriman, R.P. Hirt, B.J. Mann, T. Nozaki, B. Suh, M. Pop, M. Duchene, J. Ackers, E. Tannich, M. Leippe, M. Hofer, I. Bruchhaus, U. Willhoeft, A. Bhattacharya, T. Chillingworth, C. Churcher, Z. Hance, B. Harris, D. Harris, K. Jagels, S. Moule, K. Mungall, D. Ormond, R. Squares, S. Whitehead, M.A. Quail, E. Rabbinowitsch, H. Norbertczak, C. Price, Z. Wang, N. Guillen, C. Gilchrist, S.E. Stroup, S. Bhattacharya, A. Lohia, P.G. Foster, T. Sicheritz-Ponten, C. Weber, U. Singh, C. Mukherjee, N.M. El-Sayed, W.A. Petri, Jr., C.G. Clark, T.M. Embley, B. Barrell, C.M. Fraser, and N. Hall. 2005. The genome of the protist parasite *Entamoeba histolytica*. *Nature.* 433:865-8.
- Lu, L., Y.R. Lee, R. Pan, J.N. Maloof, and B. Liu. 2005. An internal motor kinesin is associated with the Golgi apparatus and plays a role in trichome morphogenesis in *Arabidopsis*. *Mol Biol Cell.* 16:811-23.
- Maga, J.A., and J.H. LeBowitz. 1999. Unravelling the kinetoplastid paraflagellar rod. *Trends Cell Biol.* 9:409-13.

- Maney, T., A.W. Hunter, M. Wagenbach, and L. Wordeman. 1998. Mitotic centromere-associated kinesin is important for anaphase chromosome segregation. *J Cell Biol.* 142:787-801.
- Maney, T., M. Wagenbach, and L. Wordeman. 2001. Molecular dissection of the microtubule depolymerizing activity of mitotic centromere-associated kinesin. *J Biol Chem.* 276:34753-8.
- Manning, A.L., N.J. Ganem, S.F. Bakhoun, M. Wagenbach, L. Wordeman, and D.A. Compton. 2007. The kinesin-13 proteins Kif2a, Kif2b, and Kif2c/MCAK have distinct roles during mitosis in human cells. *Mol Biol Cell.* 18:2970-9.
- Marcus, A.I., W. Li, H. Ma, and R.J. Cyr. 2003. A kinesin mutant with an atypical bipolar spindle undergoes normal mitosis. *Mol Biol Cell.* 14:1717-26.
- Matthews, K.R. 2005. The developmental cell biology of *Trypanosoma brucei*. *J Cell Sci.* 118:283-90.
- Matthews, K.R., J.R. Ellis, and A. Paterou. 2004. Molecular regulation of the life cycle of African trypanosomes. *Trends Parasitol.* 20:40-7.
- McCulloch, R. 2004. Antigenic variation in African trypanosomes: monitoring progress. *Trends Parasitol.* 20:117-21.
- McDonald, H.B., R.J. Stewart, and L.S. Goldstein. 1990. The kinesin-like *ncd* protein of *Drosophila* is a minus end-directed microtubule motor. *Cell.* 63:1159-65.
- McKean, P.G. 2003. Coordination of cell cycle and cytokinesis in *Trypanosoma brucei*. *Curr Opin Microbiol.* 6:600-7.
- Medina-Acosta, E., and G.A. Cross. 1993. Rapid isolation of DNA from trypanosomatid protozoa using a simple 'mini-prep' procedure. *Mol Biochem Parasitol.* 59:327-9.
- Meluh, P.B., and M.D. Rose. 1990. KAR3, a kinesin-related gene required for yeast nuclear fusion. *Cell.* 60:1029-41.
- Miki, H., Y. Okada, and N. Hirokawa. 2005. Analysis of the kinesin superfamily: insights into structure and function. *Trends Cell Biol.* 15:467-76.
- Miki, H., M. Setou, K. Kaneshiro, and N. Hirokawa. 2001. All kinesin superfamily protein, KIF, genes in mouse and human. *Proc Natl Acad Sci U S A.* 98:7004-11.
- Miller, R.K., K.K. Heller, L. Frisen, D.L. Wallack, D. Loayza, A.E. Gammie, and M.D. Rose. 1998. The kinesin-related proteins, Kip2p and Kip3p, function differently in nuclear migration in yeast. *Mol Biol Cell.* 9:2051-68.
- Moore, A.T., K.E. Rankin, G. von Dassow, L. Peris, M. Wagenbach, Y. Ovechkina, A. Andrieux, D. Job, and L. Wordeman. 2005. MCAK associates with the tips of polymerizing microtubules. *J. Cell Biol.* 169:391-397.
- Moores, C.A., J. Cooper, M. Wagenbach, Y. Ovechkina, L. Wordeman, and R.A. Milligan. 2006. The role of the kinesin-13 neck in microtubule depolymerization. *Cell Cycle.* 5:1812-5.
- Moores, C.A., M. Hekmat-Nejad, R. Sakowicz, and R.A. Milligan. 2003. Regulation of KinI kinesin ATPase activity by binding to the microtubule lattice. *J Cell Biol.* 163:963-71.
- Moores, C.A., and R.A. Milligan. 2006. Lucky 13-microtubule depolymerisation by kinesin-13 motors. *J Cell Sci.* 119:3905-13.
- Morgan, G.W., D. Goulding, and M.C. Field. 2004. The single dynamin-like protein of *Trypanosoma brucei* regulates mitochondrial division and is not required for endocytosis. *J Biol Chem.* 279:10692-701.

- Morrison, H.G., A.G. McArthur, F.D. Gillin, S.B. Aley, R.D. Adam, G.J. Olsen, A.A. Best, W.Z. Cande, F. Chen, M.J. Cipriano, B.J. Davids, S.C. Dawson, H.G. Elmendorf, A.B. Hehl, M.E. Holder, S.M. Huse, U.U. Kim, E. Lasek-Nesselquist, G. Manning, A. Nigam, J.E. Nixon, D. Palm, N.E. Passamaneck, A. Prabhu, C.I. Reich, D.S. Reiner, J. Samuelson, S.G. Svard, and M.L. Sogin. 2007. Genomic minimalism in the early diverging intestinal parasite *Giardia lamblia*. *Science*. 317:1921-6.
- Morrison, L.J., P. Majiwa, A.F. Read, and J.D. Barry. 2005. Probabilistic order in antigenic variation of *Trypanosoma brucei*. *Int J Parasitol*. 35:961-72.
- Nag, D.K., I. Tikhonenko, I. Soga, and M.P. Koonce. 2008. Disruption of Four Kinesin Genes in *Dictyostelium*. *BMC Cell Biol*. 9:21.
- Nangaku, M., R. Sato-Yoshitake, Y. Okada, Y. Noda, R. Takemura, H. Yamazaki, and N. Hirokawa. 1994. KIF1B, a novel microtubule plus end-directed monomeric motor protein for transport of mitochondria. *Cell*. 79:1209-20.
- Newton, C.N., M. Wagenbach, Y. Ovechkina, L. Wordeman, and L. Wilson. 2004. MCAK, a Kin I kinesin, increases the catastrophe frequency of steady-state HeLa cell microtubules in an ATP-dependent manner in vitro. *FEBS Lett*. 572:80-4.
- Nislow, C., V.A. Lombillo, R. Kuriyama, and J.R. McIntosh. 1992. A plus-end-directed motor enzyme that moves antiparallel microtubules in vitro localizes to the interzone of mitotic spindles. *Nature*. 359:543-7.
- Obado, S.O., C. Bot, D. Nilsson, B. Andersson, and J.M. Kelly. 2007. Repetitive DNA is associated with centromeric domains in *Trypanosoma brucei* but not *Trypanosoma cruzi*. *Genome Biol*. 8:R37.
- Ogawa, T., R. Nitta, Y. Okada, and N. Hirokawa. 2004. A common mechanism for microtubule destabilizers-M type kinesins stabilize curling of the protofilament using the class-specific neck and loops. *Cell*. 116:591-602.
- Ogbadoyi, E., K. Ersfeld, D. Robinson, T. Sherwin, and K. Gull. 2000. Architecture of the *Trypanosoma brucei* nucleus during interphase and mitosis. *Chromosoma*. 108:501-13.
- Ohi, R., K. Burbank, Q. Liu, and T.J. Mitchison. 2007. Nonredundant functions of Kinesin-13s during meiotic spindle assembly. *Curr Biol*. 17:953-9.
- Okada, Y., H. Yamazaki, Y. Sekine-Aizawa, and N. Hirokawa. 1995. The neuron-specific kinesin superfamily protein KIF1A is a unique monomeric motor for anterograde axonal transport of synaptic vesicle precursors. *Cell*. 81:769-80.
- Ovechkina, Y., M. Wagenbach, and L. Wordeman. 2002. K-loop insertion restores microtubule depolymerizing activity of a "neckless" MCAK mutant. *J Cell Biol*. 159:557-62.
- Ovechkina, Y., and L. Wordeman. 2003. Unconventional motoring: an overview of the Kin C and Kin I kinesins. *Traffic*. 4:367-75.
- Overath, P., and M. Engstler. 2004. Endocytosis, membrane recycling and sorting of GPI-anchored proteins: *Trypanosoma brucei* as a model system. *Mol Microbiol*. 53:735-44.
- Pays, E., L. Vanhamme, and D. Perez-Morga. 2004. Antigenic variation in *Trypanosoma brucei*: facts, challenges and mysteries. *Curr Opin Microbiol*. 7:369-74.
- Pereira, A.J., B. Dalby, R.J. Stewart, S.J. Doxsey, and L.S. Goldstein. 1997. Mitochondrial association of a plus end-directed microtubule motor expressed during mitosis in *Drosophila*. *J Cell Biol*. 136:1081-90.

- Pilling, A.D., D. Horiuchi, C.M. Lively, and W.M. Saxton. 2006. Kinesin-1 and Dynein are the primary motors for fast transport of mitochondria in *Drosophila* motor axons. *Mol Biol Cell*. 17:2057-68.
- Ploubidou, A., D.R. Robinson, R.C. Docherty, E.O. Ogbadoyi, and K. Gull. 1999. Evidence for novel cell cycle checkpoints in trypanosomes: kinetoplast segregation and cytokinesis in the absence of mitosis. *J Cell Sci*. 112 (Pt 24):4641-50.
- Priest, J.W., and S.L. Hajduk. 1994. Developmental regulation of mitochondrial biogenesis in *Trypanosoma brucei*. *J Bioenerg Biomembr*. 26:179-91.
- Reddy, A.S., and I.S. Day. 2001. Kinesins in the Arabidopsis genome: a comparative analysis among eukaryotes. *BMC Genomics*. 2:2.
- Robinson, N.P., N. Burman, S.E. Melville, and J.D. Barry. 1999. Predominance of duplicative VSG gene conversion in antigenic variation in African trypanosomes. *Mol Cell Biol*. 19:5839-46.
- Rogers, G.C., S.L. Rogers, T.A. Schwimmer, S.C. Ems-McClung, C.E. Walczak, R.D. Vale, J.M. Scholey, and D.J. Sharp. 2004. Two mitotic kinesins cooperate to drive sister chromatid separation during anaphase. *Nature*. 427:364-70.
- Rosenbaum, J.L., D.G. Cole, and D.R. Diener. 1999. Intraflagellar transport: the eyes have it. *J Cell Biol*. 144:385-8.
- Rosenbaum, J.L., and G.B. Witman. 2002. Intraflagellar transport. *Nat Rev Mol Cell Biol*. 3:813-25.
- Rosenblatt, J. 2005. Spindle assembly: asters part their separate ways. *Nat Cell Biol*. 7:219-22.
- Rudenko, G., I. Chaves, A. Dirks-Mulder, and P. Borst. 1998. Selection for activation of a new variant surface glycoprotein gene expression site in *Trypanosoma brucei* can result in deletion of the old one. *Mol Biochem Parasitol*. 95:97-109.
- Saito, N., Y. Okada, Y. Noda, Y. Kinoshita, S. Kondo, and N. Hirokawa. 1997. KIFC2 is a novel neuron-specific C-terminal type kinesin superfamily motor for dendritic transport of multivesicular body-like organelles. *Neuron*. 18:425-38.
- Saitou, N., and M. Nei. 1987. The neighbor-joining method: a new method for reconstructing phylogenetic trees. *Mol Biol Evol*. 4:406-25.
- Sambrook, J., Fritsch, E. F., Maniatis, T. 1989. *Molecular Cloning: A Laboratory Manual* (Second Edition).
- Saunders, W., V. Lengyel, and M.A. Hoyt. 1997. Mitotic spindle function in *Saccharomyces cerevisiae* requires a balance between different types of kinesin-related motors. *Mol Biol Cell*. 8:1025-33.
- Saunders, W.S., D. Koshland, D. Eshel, I.R. Gibbons, and M.A. Hoyt. 1995. *Saccharomyces cerevisiae* kinesin- and dynein-related proteins required for anaphase chromosome segregation. *J Cell Biol*. 128:617-24.
- Savoian, M.S., M.K. Gatt, M.G. Riparbelli, G. Callaini, and D.M. Glover. 2004. *Drosophila* Klp67A is required for proper chromosome congression and segregation during meiosis I. *J Cell Sci*. 117:3669-77.
- Sawin, K.E., K. LeGuellec, M. Philippe, and T.J. Mitchison. 1992. Mitotic spindle organization by a plus-end-directed microtubule motor. *Nature*. 359:540-3.
- Schmidt, M., and H. Bastians. 2007. Mitotic drug targets and the development of novel anti-mitotic anticancer drugs. *Drug Resist Updat*. 10:162-81.

- Schneider, A. 2001. Unique aspects of mitochondrial biogenesis in trypanosomatids. *Int J Parasitol.* 31:1403-15.
- Scholey, J.M. 2008. Intraflagellar transport motors in cilia: moving along the cell's antenna. *J Cell Biol.* 180:23-9.
- Schultz, J., F. Milpetz, P. Bork, and C.P. Ponting. 1998. SMART, a simple modular architecture research tool: identification of signaling domains. *Proc Natl Acad Sci U S A.* 95:5857-64.
- Sekine, Y., Y. Okada, Y. Noda, S. Kondo, H. Aizawa, R. Takemura, and N. Hirokawa. 1994. A novel microtubule-based motor protein (KIF4) for organelle transports, whose expression is regulated developmentally. *J Cell Biol.* 127:187-201.
- Setou, M., T. Nakagawa, D.H. Seog, and N. Hirokawa. 2000. Kinesin superfamily motor protein KIF17 and mLin-10 in NMDA receptor-containing vesicle transport. *Science.* 288:1796-802.
- Sharp, D.J., G.C. Rogers, and J.M. Scholey. 2000a. Cytoplasmic dynein is required for poleward chromosome movement during mitosis in *Drosophila* embryos. *Nat Cell Biol.* 2:922-30.
- Sharp, D.J., G.C. Rogers, and J.M. Scholey. 2000b. Microtubule motors in mitosis. *Nature.* 407:41-7.
- Sharp, D.J., G.C. Rogers, and J.M. Scholey. 2000c. Roles of motor proteins in building microtubule-based structures: a basic principle of cellular design. *Biochim Biophys Acta.* 1496:128-41.
- Sherwin, T., and K. Gull. 1989a. The cell division cycle of *Trypanosoma brucei brucei*: timing of event markers and cytoskeletal modulations. *Philos Trans R Soc Lond B Biol Sci.* 323:573-88.
- Sherwin, T., and K. Gull. 1989b. Visualization of dephosphorylation along single microtubules reveals novel mechanisms of assembly during cytoskeletal duplication in trypanosomes. *Cell.* 57:211-21.
- Shipley, K., M. Hekmat-Nejad, J. Turner, C. Moores, R. Anderson, R. Milligan, R. Sakowicz, and R. Fletterick. 2004. Structure of a kinesin microtubule depolymerization machine. *Embo J.* 23:1422-32.
- Siddiqui, S.S. 2002. Metazoan motor models: kinesin superfamily in *C. elegans*. *Traffic.* 3:20-8.
- Tamura, K., J. Dudley, M. Nei, and S. Kumar. 2007. MEGA4: Molecular Evolutionary Genetics Analysis (MEGA) software version 4.0. *Mol Biol Evol.* 24:1596-9.
- Tanaka, Y., Y. Kanai, Y. Okada, S. Nonaka, S. Takeda, A. Harada, and N. Hirokawa. 1998. Targeted disruption of mouse conventional kinesin heavy chain, kif5B, results in abnormal perinuclear clustering of mitochondria. *Cell.* 93:1147-58.
- Taylor, J.E., and G. Rudenko. 2006. Switching trypanosome coats: what's in the wardrobe? *Trends Genet.* 22:614-20.
- Thompson, J.D., T.J. Gibson, F. Plewniak, F. Jeanmougin, and D.G. Higgins. 1997. The CLUSTAL_X windows interface: flexible strategies for multiple sequence alignment aided by quality analysis tools. *Nucleic Acids Res.* 25:4876-82.
- Tokai, N., A. Fujimoto-Nishiyama, Y. Toyoshima, S. Yonemura, S. Tsukita, J. Inoue, and T. Yamamoto. 1996. Kid, a novel kinesin-like DNA binding protein, is localized to chromosomes and the mitotic spindle. *Embo J.* 15:457-67.

- Turner, C.M. 1997. The rate of antigenic variation in fly-transmitted and syringe-passaged infections of *Trypanosoma brucei*. *FEMS Microbiol Lett.* 153:227-31.
- Turner, C.M., and J.D. Barry. 1989. High frequency of antigenic variation in *Trypanosoma brucei* rhodesiense infections. *Parasitology.* 99 Pt 1:67-75.
- Vale, R.D. 2003. The Molecular Motor Toolbox for Intracellular Transport. *Cell.* 112:467.
- Vale, R.D., and R.J. Fletterick. 1997. The design plan of kinesin motors. *Annu Rev Cell Dev Biol.* 13:745-77.
- Vale, R.D., T.S. Reese, and M.P. Sheetz. 1985. Identification of a novel force-generating protein, kinesin, involved in microtubule-based motility. *Cell.* 42:39-50.
- Van der Ploeg, L.H., D.C. Schwartz, C.R. Cantor, and P. Borst. 1984. Antigenic variation in *Trypanosoma brucei* analyzed by electrophoretic separation of chromosome-sized DNA molecules. *Cell.* 37:77-84.
- Van der Ploeg, L.H., C.L. Smith, R.I. Polvere, and K.M. Gottesdiener. 1989. Improved separation of chromosome-sized DNA from *Trypanosoma brucei*, stock 427-60. *Nucleic Acids Res.* 17:3217-27.
- Van der Ploeg, L.H., D. Valerio, T. De Lange, A. Bernards, P. Borst, and F.G. Grosveld. 1982. An analysis of cosmid clones of nuclear DNA from *Trypanosoma brucei* shows that the genes for variant surface glycoproteins are clustered in the genome. *Nucleic Acids Res.* 10:5905-23.
- Vanhamme, L., and E. Pays. 1995. Control of gene expression in trypanosomes. *Microbiol. Rev.* 59:223-240.
- Vanstraelen, M., D. Inze, and D. Geelen. 2006. Mitosis-specific kinesins in *Arabidopsis*. *Trends Plant Sci.* 11:167-75.
- Vickerman, K., and T.M. Preston. 1970. Spindle microtubules in the dividing nuclei of trypanosomes. *J Cell Sci.* 6:365-83.
- Vos, J.W., F. Safadi, A.S. Reddy, and P.K. Hepler. 2000. The kinesin-like calmodulin binding protein is differentially involved in cell division. *Plant Cell.* 12:979-90.
- Walczak, C.E., E.C. Gan, A. Desai, T.J. Mitchison, and S.L. Kline-Smith. 2002. The microtubule-destabilizing kinesin XKCM1 is required for chromosome positioning during spindle assembly. *Curr Biol.* 12:1885-9.
- Walczak, C.E., T.J. Mitchison, and A. Desai. 1996. XKCM1: a *Xenopus* kinesin-related protein that regulates microtubule dynamics during mitotic spindle assembly. *Cell.* 84:37-47.
- Wang, S.Z., and R. Adler. 1995. Chromokinesin: a DNA-binding, kinesin-like nuclear protein. *J Cell Biol.* 128:761-8.
- Weaver, B.A., Z.Q. Bonday, F.R. Putkey, G.J. Kops, A.D. Silk, and D.W. Cleveland. 2003. Centromere-associated protein-E is essential for the mammalian mitotic checkpoint to prevent aneuploidy due to single chromosome loss. *J Cell Biol.* 162:551-63.
- West, R.R., T. Malmstrom, and J.R. McIntosh. 2002. Kinesins klp5(+) and klp6(+) are required for normal chromosome movement in mitosis. *J Cell Sci.* 115:931-40.
- Westerholm-Parvinen, A., I. Vernos, and L. Serrano. 2000. Kinesin subfamily UNC104 contains a FHA domain: boundaries and physicochemical characterization. *FEBS Lett.* 486:285-90.
- Wickstead, B., K. Ersfeld, and K. Gull. 2002. Targeting of a tetracycline-inducible expression system to the transcriptionally silent minichromosomes of *Trypanosoma brucei*. *Mol Biochem Parasitol.* 125:211-6.

- Wickstead, B., K. Ersfeld, and K. Gull. 2003. The mitotic stability of the minichromosomes of *Trypanosoma brucei*. *Mol Biochem Parasitol.* 132:97-100.
- Wickstead, B., K. Ersfeld, and K. Gull. 2004. The small chromosomes of *Trypanosoma brucei* involved in antigenic variation are constructed around repetitive palindromes. *Genome Res.* 14:1014-24.
- Wickstead, B., and K. Gull. 2006. A "holistic" kinesin phylogeny reveals new kinesin families and predicts protein functions. *Mol Biol Cell.* 17:1734-43.
- Wirtz, E., S. Leal, C. Ochatt, and G.A. Cross. 1999. A tightly regulated inducible expression system for conditional gene knock-outs and dominant-negative genetics in *Trypanosoma brucei*. *Mol Biochem Parasitol.* 99:89-101.
- Wittmann, T., A. Hyman, and A. Desai. 2001. The spindle: a dynamic assembly of microtubules and motors. *Nat Cell Biol.* 3:E28-34.
- Woehlke, G., and M. Schliwa. 2000. Walking on two heads: the many talents of kinesin. *Nat Rev Mol Cell Biol.* 1:50-8.
- Wolf, F.W., M.S. Hung, B. Wightman, J. Way, and G. Garriga. 1998. vab-8 is a key regulator of posteriorly directed migrations in *C. elegans* and encodes a novel protein with kinesin motor similarity. *Neuron.* 20:655-66.
- Wood, K.W., R. Sakowicz, L.S. Goldstein, and D.W. Cleveland. 1997. CENP-E is a plus end-directed kinetochore motor required for metaphase chromosome alignment. *Cell.* 91:357-66.
- Woods, A., T. Sherwin, R. Sasse, T.H. MacRae, A.J. Baines, and K. Gull. 1989. Definition of individual components within the cytoskeleton of *Trypanosoma brucei* by a library of monoclonal antibodies. *J Cell Sci.* 93 (Pt 3):491-500.
- Wordeman, L., and T.J. Mitchison. 1995. Identification and partial characterization of mitotic centromere-associated kinesin, a kinesin-related protein that associates with centromeres during mitosis. *J Cell Biol.* 128:95-104.
- Wordeman, L., M. Wagenbach, and G. von Dassow. 2007. MCAK facilitates chromosome movement by promoting kinetochore microtubule turnover. *J Cell Biol.* 179:869-79.
- Xu, Y., S. Takeda, T. Nakata, Y. Noda, Y. Tanaka, and N. Hirokawa. 2002. Role of KIFC3 motor protein in Golgi positioning and integration. *J Cell Biol.* 158:293-303.
- Yamazaki, H., T. Nakata, Y. Okada, and N. Hirokawa. 1995. KIF3A/B: a heterodimeric kinesin superfamily protein that works as a microtubule plus end-directed motor for membrane organelle transport. *J Cell Biol.* 130:1387-99.
- Yang, J.T., R.A. Laymon, and L.S. Goldstein. 1989. A three-domain structure of kinesin heavy chain revealed by DNA sequence and microtubule binding analyses. *Cell.* 56:879-89.
- Yen, T.J., G. Li, B.T. Schaar, I. Szilak, and D.W. Cleveland. 1992. CENP-E is a putative kinetochore motor that accumulates just before mitosis. *Nature.* 359:536-9.
- Yildiz, A., and P.R. Selvin. 2005. Kinesin: walking, crawling or sliding along? *Trends Cell Biol.* 15:112-20.
- Yokoyama, R., E. O'Toole, S. Ghosh, and D.R. Mitchell. 2004. Regulation of flagellar dynein activity by a central pair kinesin. *Proc Natl Acad Sci U S A.* 101:17398-403.
- Zhu, C., J. Zhao, M. Bibikova, J.D. Levenson, E. Bossy-Wetzel, J.B. Fan, R.T. Abraham, and W. Jiang. 2005. Functional Analysis of Human Microtubule-based Motor Proteins, the Kinesins and Dyneins, in Mitosis/Cytokinesis Using RNA Interference (RNAi). *Mol Biol Cell.*

Zomerdijk, J.C., R. Kieft, and P. Borst. 1992. A ribosomal RNA gene promoter at the telomere of a mini-chromosome in *Trypanosoma brucei*. *Nucleic Acids Res.* 20:2725-34.

5 Supplementary data

Table S 5.1: A list of kinesin sequences of known families used in the phylogenetic analysis of Trypanosome kinesins.

Sequence Name	GenBank	ProtID	Family	Species
LpKHC	J05258	AAA29990	Kinesin-1	<i>Loligo pealii</i>
MmKif5A	AF067179	AAC79803	Kinesin-1	<i>Mus musculus</i>
NcKHC	L47106	AAB52961	Kinesin-1	<i>Neurospora crassa</i>
DdK7	U41289	AAB07748	Kinesin-1	<i>Dictyostelium discoideum</i>
SpKRP85	L16993	AAA16098	Kinesin-2	<i>Strongylocentrotus purpuratus</i>
SpKRP95	U00996	AAA87393	Kinesin-2	<i>Strongylocentrotus purpuratus</i>
MmKif3A	D12645	BAA02166	Kinesin-2	<i>Mus musculus</i>
MmKif3B	D26077	BAA05070	Kinesin-2	<i>Mus musculus</i>
CrFLA10	L33697	AAA21738	Kinesin-2	<i>Chlamydomonas reinhardtii</i>
MmKif1A	D29951	BAA06221	Kinesin-3	<i>Mus musculus</i>
CeUnc104	M58582	AAA03517	Kinesin-3	<i>Caenorhabditis elegans</i>
LdKIN	L07879	AAA29254	Kinesin-3	<i>Leishmania donovani</i>
DdUnc104	AF245277	AAF63384	Kinesin-3	<i>Dictyostelium discoideum</i>
MmKif4	D12646	BAA02167	Kinesin-4	<i>Mus musculus</i>
GgCHRKIN	U18309	AAC59666	Kinesin-4	<i>Gallus gallus</i>
XIKLP1	X82012	CAA57539	Kinesin-4	<i>Xenopus laevis</i>
F11C1.80	AB061676	BAB55445	Kinesin-4	<i>Arabidopsis thaliana</i>
AY224568	AY224568	AAO72688	Kinesin-4	<i>Oryza sativa</i>
DdK8	U69985	AAB09083	Kinesin-4	<i>Dictyostelium discoideum</i>
MmKif11	AB001427	BAA22387	Kinesin-5	<i>Mus musculus</i>
XIEG5	X54002	CAA37950	Kinesin-5	<i>Xenopus laevis</i>
AnBimC	M32075	AAA33298	Kinesin-5	<i>Aspergillus nidulans</i>
HsMKLP1	X67155	CAA47628	Kinesin-6	<i>Homo sapiens</i>
MmKif20A	NM_009004	NP_033030	Kinesin-6	<i>Mus musculus</i>
DdK12	AY484465	AAR39441	Kinesin-6	<i>Dictyostelium discoideum</i>
HsCENP-E	Z15005	CAA78727	Kinesin-7	<i>Homo sapiens</i>
MmKif10	AB001426	BAA22386	Kinesin-7	<i>Mus musculus</i>
ScKIP2p	Z11963	CAA78021	Kinesin-7	<i>Saccharomyces cerevisiae</i>
AtKlp	AB028470	BAA88114	Kinesin-7	<i>Arabidopsis thaliana</i>
MmKif19A	AB054026	BAB32490	Kinesin-8	<i>Mus musculus</i>
ScKip3p	Z72739	CAA96933	Kinesin-8	<i>Saccharomyces cerevisiae</i>
AtKlp1	NM_114825	NP_190534	Kinesin-8	<i>Arabidopsis thaliana</i>
MmKif9	AJ132889	CAB46016	Kinesin-9	<i>Mus musculus</i>
CrKlp1	X78589	CAA55326	Kinesin-9	<i>Chlamydomonas reinhardtii</i>
HsKID	AB017430	BAA33019	Kinesin-10	<i>Homo sapiens</i>
MmKif22	NM_145588	NP_663563	Kinesin-10	<i>Mus musculus</i>
AtKlp2	NM_120315	NP_195857	Kinesin-10	<i>Arabidopsis thaliana</i>
CeVab-8	NM_073662	NP_506063	Kinesin-11	<i>Caenorhabditis elegans</i>
MmKif26A	XM_138275	XP_138275	Kinesin-11	<i>Mus musculus</i>
ScSMY1p	M69021	AAA35056	Kinesin-11	<i>Saccharomyces cerevisiae</i>
MmKif15	AJ560623	CAD90258	Kinesin-12	<i>Mus musculus</i>
XIKlp2	X94082	CAA63826	Kinesin-12	<i>Xenopus laevis</i>
AtPaKrp1	NM_117492	NP_567423	Kinesin-12	<i>Arabidopsis thaliana</i>

Table S 5.1: A list of kinesin sequences of known families used in the phylogenetic analysis of Trypanosome kinesins.

Sequence Name	GenBank	ProtID	Family	Species
AtPaKrp11	NM_113271	NP_189009	Kinesin-12	<i>Arabidopsis thaliana</i>
CgMCAK	U11790	AAB17358	Kinesin-13	<i>Cricetulus griseus</i>
MmKif2	D12644	BAA02165	Kinesin-13	<i>Mus musculus</i>
AtKlp3	NM_112476	NP_566534	Kinesin-13	<i>Arabidopsis thaliana</i>
CfDSK1	U51680	AAB05681	Kinesin-13	<i>Cylindrotheca fusiformis</i>
DmNCD	X52814	CAA36998	Kinesin-14	<i>Drosophila melanogaster</i>
MmKifC1	D49544	BAA19676	Kinesin-14	<i>Mus musculus</i>
ScKar3	M31719	AAA34715	Kinesin-14	<i>Saccharomyces cerevisiae</i>
AtKATA	D11371	BAA01972	Kinesin-14	<i>Arabidopsis thaliana</i>
AtKCBP	L40358	AAC37475	Kinesin-14	<i>Arabidopsis thaliana</i>

Table S 5.2: A list of kinesin sequences used in Figure 2.3.

Kinesin name	Species	ProtID	Kinesin family
AtKlp3	<i>Arabidopsis thaliana</i>	NP_566534	Kinesin-13
CfDSK1	<i>Cylindrotheca fusiformis (Marine diatom)</i>	Q39493	Kinesin-13
CgMCAK	<i>Cricetulus griseus (Chinese Hamster)</i>	AAB17358	Kinesin-13
GIKin13	<i>Giardia lamblia</i>	EAA40236	Kinesin-13
LmMCAK	<i>Leishmania major</i>	NP_047029	Kinesin-13
MmKif2	<i>Mus musculus</i>	BAA02165	Kinesin-13
PfKin13	<i>Plasmodium falciparum</i>	NP_701793	Kinesin-13

Table S 5.3: A list of kinesin-13 family sequences used in the phylogenetic tree in Figure 2.4 and Figure 2.5.

Kinesin Name	Species	Protein ID	Kinesin Family
MmKif19A	<i>Mus musculus</i>	BAB32490	Kinesin-8
ScKip3p	<i>Saccharomyces cerevisiae</i>	CAA96933	Kinesin-8
AtKlp1	<i>Arabidopsis thaliana</i>	NP_190534	Kinesin-8
HsKIF2A	<i>Homo sapiens</i>	NP_004511	Kinesin-13
MmKIF2A	<i>Mus musculus</i>	P28740	Kinesin-13
RnKIF2A	<i>Rattus norvegicus</i>	XP_345151	Kinesin-13
XlXKIF2	<i>Xenopus laevis</i>	Q91637	Kinesin-13
HsKIF2B	<i>Homo sapiens</i>	AAH33802	Kinesin-13
MfKIF2B	<i>Macaca fascicularis</i>	BAB64505	Kinesin-13
MmKIF2B	<i>Mus musculus</i>	BAC26831	Kinesin-13
RnKIF2B	<i>Rattus norvegicus</i>	XP_220865	Kinesin-13
HsKIF2C	<i>Homo sapiens</i>	Q99661	Kinesin-13
MfKIF2C	<i>Macaca fascicularis</i>	BAB69716	Kinesin-13
MmKIF2C	<i>Mus musculus</i>	BAC40116	Kinesin-13
RnKIF2C	<i>Rattus norvegicus</i>	XP_346747	Kinesin-13
CgMCAK	<i>Cricetulus griseus</i>	P70096	Kinesin-13
XlXKCM1	<i>Xenopus laevis</i>	Q91636	Kinesin-13
FrKIF2C	<i>Fugu rubripes</i>	SINFRUP00000162741	Kinesin-13
MsFKIF4	<i>Morone saxatilis</i>	AAB03190	Kinesin-13
CeKlp7	<i>Caenorhabditis elegans</i>	NP_499384	Kinesin-13
CbKlp7	<i>Caenorhabditis briggsae</i>	CAE71399	Kinesin-13
DmKlp59C	<i>Drosophila melanogaster</i>	NP_611759	Kinesin-13
DmKlp59D	<i>Drosophila melanogaster</i>	NP_611762	Kinesin-13
DmKlp10A	<i>Drosophila melanogaster</i>	NP_727494	Kinesin-13
AgKlp10A	<i>Anopheles gambiae</i>	XP_310979	Kinesin-13
HsKIF24	<i>Homo sapiens</i>	XP_294563	Kinesin-13
MmKIF24	<i>Mus musculus</i>	BAC39323	Kinesin-13
NtTBK10	<i>Nicotiana tabacum</i>	BAB40710	Kinesin-13
AtKlp3	<i>Arabidopsis thaliana</i>	BAB02671	Kinesin-13
OsP0006C01.8	<i>Oryza sativa</i>	NP_917771	Kinesin-13
AtMGL6.9	<i>Arabidopsis thaliana</i>	BAB00068	Kinesin-13
OsNM_185267	<i>Oryza sativa</i>	NP_910156	Kinesin-13
DdK6	<i>Dictyostelium discoideum</i>	AAB09082	Kinesin-13
GIKin13	<i>Giardia lamblia</i>	EAA40236	Kinesin-13
Py03174	<i>Plasmodium yoelii yoelii</i>	EAA22720	Kinesin-13
PfKin13	<i>Plasmodium falciparum</i>	NP_701793	Kinesin-13
EcECU11_0470	<i>Encephalitozoon cuniculi</i>	CAD25957	Kinesin-13
CfDSK1	<i>Cylindrotheca fusiformis</i>	Q39493	Kinesin-13

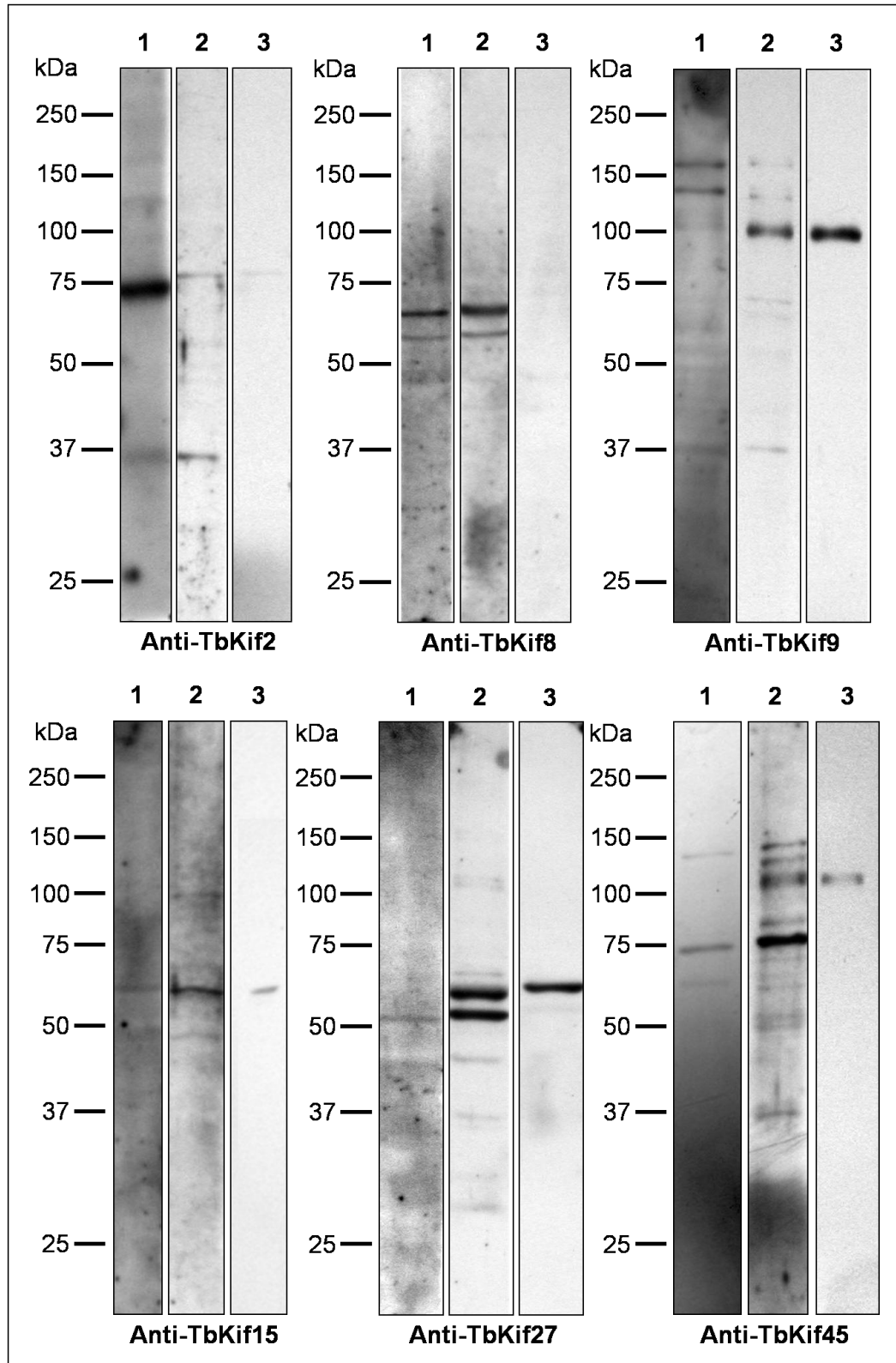
Table S 5.4: The following are the protein sequences of the 6 Kinesin-13 family members studied in this report. The sequences highlighted in blue represent the region used in the production of polyclonal rabbit antibodies.

Name	Protein sequence
TbKif2	MTSLCPITSSITVAIRKRPIANNNGSGDKDIVTCEDCRTISVHEPKTRVDLKAUVETSAF AFDYVFDESANDVYKVCQPLSDVQNGGSSVVIAFGQGTGSGKTHTMLGHGSKTIGLY GYAIRELIGEETTRKLAVSFYEVYGSKLFDLLNGRTQLKMMQDEADNLRIVGLSEKVVTC DKEVYKLI SKGESLRSSGSTLANDTSSRSHAVLEIKVLNYQGEPHGGRVTLIDLASERA ADTTSSDTRGRHEGAEINKSLLALKECIRAMSRNRRHIPFRASKLTQVLRSEFIGNCKTC FIATVSPQRHCEDTLNLTLYANRIRDLKAPSDDGFSRKISMTCPNCNGPVRPDASHTCV RLS TRCPHCRQVVEKHNLEGHIEECSEFPVRCPRCNELLVRGDI PRHNRRCSRSIVRCPL CTCHVMRCGLEKHTLMDCGAKLEKCRYCGQGFPRHSLKRHEDVCTMMKIACPYCLQYFRK VCVDAHASVCVRNPNCRRVSPSRI RDSGEEVWKITNGKEWRQRPRLRNQSLKQLEAISR TKSSVQLREGRKPLGPLLEDNFSLPALHAPSSAPDRKHPPVTSAFTESLQSHPNSEDDAD KEVCRTAPTISGENSSRVGGEGCVC PYAAYGCLHTVCDSSLEKHKD SVMHLQLVRDYA ERVSEENNILRERVNEGTTKASKL LHELESV
TbKif8	MERQLRELLEQGGLSHTIQGFVDGGVLTQLQKQLTMQDYQSVGVIVMTDRRKL FELIQY MKREQANPPSVLNTSDAPRVPEHTPQAVTGARNTTPNCRNATPSSAQRKAENENARMNES RQLSGAGGRDPLHVIDDMELSAMKMTPNRPLSRVARASPTAATRKPGESGTTKRKASR ITVVVRKRPLSTSEINDGLYDILATDPDNLQAIALLEPKQKVDLTKYIEKHFRTYDLVLD DKYSNRDVYEKACKPLIETVFEGGCATCFAYGQGTGSGKTYTMLGKGQDEGIYLM AARDLY ARLESGMSIMVSFFEIYGGKLFDLLNEREKLACREDSRGVINVCGLTEHRVEDTGHLMRV IDYGN SIRAGSTGMNADSSRSHAILHITVLNSKNRFFGRFTFIDLASERGADTLDSDR TTRLEGAEINKSLLALKECIRALDQNRHIPFRGSKLTAVLRDCFTGNSRTVMIGNVSPA SGSCEHTLNTLYADRVKELKDKSSRIAAEEIMIGQMPSEEIETLGLSSNFAQRREAREK KAGT RSSSHLSQREPGTPNAKSHSSYGSYGLKQHSRVMSCKEEDYPNFSDSIRSGKV PSSGGTKSFNRVTPKHSRVGSEISIRDASPYEMTSFASGDSLDEEDNTILGHRHRIDAM MELLQEMTELNGVEMP GASIEVYCKNVESILNRQAKSISSVRNIRQLLN LESQR
TbKif9	MQDEQHEELPPSPFETLDSLRLQDNDNEAIQPPNAPSPILERRVASSDAFPQLSSRHR GEGSNAPSLNLNRQLEDLSRDIQQLNARCRSDSMPNINKTPLRPQHLLPEKQLQLLKQR LPHLSALSARGASTPSRTGRESSQRRQDALPTVSPSPPRSRCATSVTRPYQSKQETPCS SRVFPGRASERPIASPSSPSIAANMDSVTPAAVTEDPQADGKQCAIMRTRGGRIRVVVRK RPLPPDENSCDCVSM DPPNVKAVRQVRDLTEYADVNDFTFDDAFGEDKHNEHVFNSSC KELLETTLQGSASCFAYGQGTGSGKTHTMLGNSGERGLYLAAAAIFSSLEKDQEVYASL YEIYCNSLFDLLNRSPPVVREDHNRMQITGLTWHAVTSAEELQLLINS GADQRSTGST TANERSRSHAVLTIQVRDREDNRF CGTLNLVDLAGSERAADTATNDRQTRQEGAEINKS LLALKECIRALDEKKHVFPFGSKLTEILRDSFIGNSRTVMIANI SASSQNYEHTLNTLR YAFRVKGLSIVNFEP SRARNAPRPLKPIVPDVNPAQGVPL MSGVPSRTPGRRRTASSNV TSHAAAGAAAPPAASHAKGYNSMVPVTTTRNVSSNNTPFNLRNAGSPFRGGAQGNVDS RADDEQVAEYVRLTREKVMNILPQTKLNEAREQPSPKNDYSLQDESCSFSFNHELMKEL EDRVVEEIKAE LTKAIKDVLLKRDKTFLRLRREKALLMRANTELEKRMADC PHCKGQAIR PVQQQPN
TbKif15	MPNIPLVAELGTKCAEFQRLNLTSEVPEVVKKLRPSMDPKELFTSQDSRIFVRCRPIIP FDQEDMNSKSIIRKVDGYRDPVMSPKISLAGQCTIEPHSVTLDGVF CGGDDTERVYME CAPLVHLSVEGASTCVLCYQGTGSGKTHTTLIGIVGLMSRDLAPYFASHNIFITVIEIQAN KNIDLLTGSEVQVEDISGELKIRGTDGFEC SNDEMLLAVFQEAASQRMTKATGRNEVSS RSHMVTCIQIICKNSTWVKPGE LFIVDLAGSENADSA THDKERQMEAKFINTSLM TKE CIRARAMAATSTSHLHIPFRSPLTLLLRDCFEI AVKRPTKTVVIACVSPLLRDSRHTIN TLRYASLLAVTVPARIVADD PDDPNGFDREQALAFICRCSRGRITNPEYILPEGDGRITLV HIPEAEFIRRIMESHAKISEKGAKQIYTSVWQKIVDARTKGRKVM TSSKKAPIAPRCATQ RR

Table S 5.4 (continued): The following are the protein sequences of the 6 Kinesin-13 family members studied in this report. The sequences highlighted in blue represent the region used in the production of polyclonal rabbit antibodies.

TbKif27	<p>MNNSRICVAVRKRPIVDVVDKDIVVAQSPHLVVNEPKVKYDLTPYTERHQFTYDCVLDENS NNALVYQHCCSKLIDTIFNQGNATCFAYGQTGSGKTHTMLGNDHEAGLYAIAAKEIFARS APLNSDVYVSFYEIYGRKIFDLLNNKEKLVAREADADKVINICGLTEHKVTDIQGLFDIIS RGSTYRAAGQTSANNESSRSHAVLQIEVRDPNNRRGKSIGRISFIDLAGNERGADTFDCD RKTRMEGAEINKSLLALKECIRALGMGKSHVPPFRGSILTEVLRDSFVGNRSRTTMIATISP TSTHCVNTLNTLRYTQRVKDLGGEAKAAPNEKAERRPVRRSKLFEAPPPLKARPEVDNF SANDEERGAEENEANSQADVSKAPPKPRANKMVGSGATGGGAPSAGGANRGRPPKREVVR DPKIATIVQNHISALDDSDETDEDEEEAPAAGAVLDALAKSEEKQVRKVHAHVVEEIAK AEEKLVALHRRHIDAKMTGIKDEIRAIQAFEESSVDEYVGRVRTLLVKQKQDVETILDL LNGITGMLREEEELSCTLNSSMKRRN</p>
TbKif45	<p>MAKWEKLVSLLEQHSGLHLAGKFMDSGITCEEFFVALQHEQYQYGVSSDEDTVNLYHAI KKLRGEPAVGSDSLQSEEESSLVPPILPSTSLPPPMEAAATATGAVGSDDDILDEKVKERQ YTTRGTTLLMRTDDSREVKRRKSRIVVAVRKRPI SQCEQQRGFTDVM'TTNDCELVLAET RQKVDLTRYTHAHRFFFDEVFETAENTDVYKRATAALIDTVFEGGYATCFAYGQTGSGK THTMLGTGGEPIYALAAKEMLARLDPTKQMFVSFYEIYSGKLYDLLNGRQPLRCLEDGK QNVNICGLTEHPQSNVKSIMRLIEEGTRIRSSGTTGANDTSSRSHAILEVKLRNRGDKEL FGKFTFIDLASERGADTMDCDRQTRIEGAQINKSLLALKECIRSLDLNHHKHPFRGSKL TEVLRDSFVGNCRVTMIGAVSPTSNSCEHTLNTLRYADRVKELKKSRSERKPLEENEQSE FIMEKKQTS PAARLS SHGRLS IS PQGSLNLGCVSTHQNTSNKGNSVNTSSPSLPKRRSGT MRPSGMLCGRSTEQFI SESTFKRSREDEDEGRSQSQSQSQSQGKEEAGRKSIDL DLGNRYDK VVDEIVQLERECVNTHRLYLDKDMALIKEEF SHIMSVEMPDSNIDTYVNNVLDILSVKLK AIHHFQGMRLRGLLDEEEKLQRLQNGI</p>

6 Appendix



Appendix 6.1: Western blot analysis of the whole cell lysate of wild type *T. brucei* 427 cells probed with pre-immunisation serum (1), ammonium sulfate precipitated total antibody (2) and affinity purified antibodies (3) for each of the respective kinesins. Western blot analysis revealed that the pre-immunisation serum (1) and unpurified antibodies (2) were cross-reacting with several additional protein bands as shown. The subsequent affinity purification described in chapter 3.3.3 resulted in the removal of these cross-reacting bands.